



NUREG/CR-7200

Influence of Coupling Erosion and Hydrology on the Long-Term Performance of Engineered Surface Barriers

Office of Nuclear Regulatory Research

AVAILABILITY OF REFERENCE MATERIALS IN NRC PUBLICATIONS

NRC Reference Material

As of November 1999, you may electronically access NUREG-series publications and other NRC records at NRC's Library at www.nrc.gov/reading-rm.html. Publicly released records include, to name a few, NUREG-series publications; *Federal Register* notices; applicant, licensee, and vendor documents and correspondence; NRC correspondence and internal memoranda; bulletins and information notices; inspection and investigative reports; licensee event reports; and Commission papers and their attachments.

NRC publications in the NUREG series, NRC regulations, and Title 10, "Energy," in the *Code of Federal Regulations* may also be purchased from one of these two sources.

1. The Superintendent of Documents

U.S. Government Publishing Office
Mail Stop IDCC
Washington, DC 20402-0001
Internet: bookstore.gpo.gov
Telephone: (202) 512-1800
Fax: (202) 512-2104

2. The National Technical Information Service

5301 Shawnee Rd., Alexandria, VA 22312-0002
www.ntis.gov
1-800-553-6847 or, locally, (703) 605-6000

A single copy of each NRC draft report for comment is available free, to the extent of supply, upon written request as follows:

Address: **U.S. Nuclear Regulatory Commission**
Office of Administration
Publications Branch
Washington, DC 20555-0001
E-mail: distribution.resource@nrc.gov
Facsimile: (301) 415-2289

Some publications in the NUREG series that are posted at NRC's Web site address www.nrc.gov/reading-rm/doc-collections/nuregs are updated periodically and may differ from the last printed version. Although references to material found on a Web site bear the date the material was accessed, the material available on the date cited may subsequently be removed from the site.

Non-NRC Reference Material

Documents available from public and special technical libraries include all open literature items, such as books, journal articles, transactions, *Federal Register* notices, Federal and State legislation, and congressional reports. Such documents as theses, dissertations, foreign reports and translations, and non-NRC conference proceedings may be purchased from their sponsoring organization.

Copies of industry codes and standards used in a substantive manner in the NRC regulatory process are maintained at—

The NRC Technical Library

Two White Flint North
11545 Rockville Pike
Rockville, MD 20852-2738

These standards are available in the library for reference use by the public. Codes and standards are usually copyrighted and may be purchased from the originating organization or, if they are American National Standards, from—

American National Standards Institute

11 West 42nd Street
New York, NY 10036-8002
www.ansi.org
(212) 642-4900

Legally binding regulatory requirements are stated only in laws; NRC regulations; licenses, including technical specifications; or orders, not in NUREG-series publications. The views expressed in contractor-prepared publications in this series are not necessarily those of the NRC.

The NUREG series comprises (1) technical and administrative reports and books prepared by the staff (NUREG-XXXX) or agency contractors (NUREG/CR-XXXX), (2) proceedings of conferences (NUREG/CP-XXXX), (3) reports resulting from international agreements (NUREG/IA-XXXX), (4) brochures (NUREG/BR-XXXX), and (5) compilations of legal decisions and orders of the Commission and Atomic and Safety Licensing Boards and of Directors' decisions under Section 2.206 of NRC's regulations (NUREG-0750).

DISCLAIMER: This report was prepared as an account of work sponsored by an agency of the U.S. Government. Neither the U.S. Government nor any agency thereof, nor any employee, makes any warranty, expressed or implied, or assumes any legal liability or responsibility for any third party's use, or the results of such use, of any information, apparatus, product, or process disclosed in this publication, or represents that its use by such third party would not infringe privately owned rights.

Influence of Coupling Erosion and Hydrology on the Long-Term Performance of Engineered Surface Barriers

Manuscript Completed: May 2016
Date Published: May 2016

Prepared by:
Crystal L. Smith and Craig H. Benson
Geological Engineering
University of Wisconsin-Madison
1415 Engineering Drive
Madison, WI 53706

Jacob Philip, NRC Project Manager

ABSTRACT

Design strategies were evaluated that couple erosion and hydrology for barriers over low level radioactive waste (LLW) disposal facilities by conducting long-term (1000 yr) parametric simulations with a landform evolution and hydrologic models. Topography of the Grand Junction Uranium Mill Tailings Disposal Site in Grand Junction, CO was used to define a realistic geometry. The most significant differences in maximum erosion depths were attributed to climate and vegetation. Approximately 4 m greater maximum erosion depth was estimated in semi-arid climates compared to humid climate for simulations with a rip-rap or gravel admixture surface. Vegetation decreased erosion in the semi-arid climate by 1.5 m, and by 4 m in the humid climate. Vegetation also increased the amount of evapotranspiration that occurred, decreasing percolation into the waste. Short slopes, slopes with a low grade, and slopes with small grade differences at the nickpoint decreased erosion. The humid climate had the least erosion when terraced slopes were utilized. Due to higher erosion rates in the semi-arid climate, natural and concave slopes that promote deposition produced the least erosion. Overall, a rip-rap surface layer prevented erosion most effectively for any type of topography, climate, or cover type. However, covers with a riprap surface had higher percolation rates. In contrast, a gravel admixture surface had slightly greater erosion, but was more effective in limited percolation.

CONTENTS

ABSTRACT	iii
CONTENTS	v
LIST OF FIGURES	vii
LIST OF TABLES	xiii
EXECUTIVE SUMMARY	xv
ACKNOWLEDGMENTS	xvii
1. INTRODUCTION	1-1
2. BACKGROUND	2-1
2.1 Factors Affecting Fluvial Erosion	2-1
2.2 Erosion Models.....	2-6
2.2.1 Empirical Erosion Models.....	2-6
2.2.2 Landform Evolution Models.....	2-14
3. METHODS	3-1
3.1 Reference Site – Grand Junction Uranium Mill Tailings Disposal Site.....	3-1
3.1.1 Engineered Barriers.....	3-1
3.1.2 Materials.....	3-1
3.2 Modeling Erosion with SIBERIA.....	3-4
3.2.1 Parameterization.....	3-7
3.2.2 DTM Formulation using SIBERIA.....	3-12
3.2.3 SIBERIA Inputs and Control Parameters.....	3-13
3.3 SVFLUX.....	3-13
4. RESULTS AND DISCUSSION	4-1
4.1 Effect of Type of Surface Layer on Erosion.....	4-1
4.1.1 Influence of Climate and Vegetation on Erosion.....	4-3
4.1.2 Influence of Barrier Type on Erosion.....	4-10
4.1.3 Hydrologic Comparison of Barrier Type and Surface Layer Type.....	4-10
4.2 Effect of Slope Length and Grade on Erosion.....	4-16
4.3 Effect of Slope Shape on Erosion.....	4-18
5. SUMMARY AND PRACTICAL IMPLICATIONS	5-1
6. REFERENCES	6-1
APPENDIX A: WEPP SENSITIVITY ANALYSIS TO INITIAL SOIL WATER CONTENT AND ALBEDO	A-1
APPENDIX B: SIBERIA PREDICTIONS FOR COVERS WITH WATER BALANCE BARRIERS	B-1
APPENDIX C: SVFLUX PREDICTIONS FOR RESISTIVE AND WATER BALANCE COVERS	C-1

APPENDIX D: SIBERIA PREDICTIONS FOR UNIFORM SIDE SLOPE TOPOGRAPHY	D-1
APPENDIX E: TOPOGRAPHIC MAPS USED IN SIBERIA	E-1
APPENDIX F: SIBERIA PREDICTIONS FOR SHALLOW AND DEEP CONCAVE SIDE SLOPES	F-1
APPENDIX G: SIBERIA PREDICTIONS FOR LEAST ERODED SURFACES	G-1
APPENDIX H: STEPS FOR RUNNING SIBERIA LANDFORM EVOLUTION MODEL USING A DIGITAL TERRAIN MODEL AND VIEWING MODEL OUTPUT	H-1
APPENDIX I: A SAMPLE LAYER.MODEL FILE USED IN SIBERIA.....	I-1
APPENDIX J: THE SIBERIA.SETUP FILE USED IN SIBERIA	J-1

LIST OF FIGURES

Fig. 2.1.	Slope shapes (a) uniform slope, (b) convex slope, and (c) concave slope	2-2
Fig. 2.2.	Interrill erosion area (a) and rill erosion area (b). Photo courtesy of USDA Natural Resource Conservation Service	2-4
Fig. 2.3.	Schematic of the armoring process: (a) original surface, (b) armored surface (adapted from Willgoose and Sharmeen, 2006).....	2-5
Fig. 2.4.	Conservation of mass for a segment along the overland flow path on a hillslope (adapted from http://www.ars.usda.gov/Research/docs.htm?docid=6014).....	2-9
Fig. 2.5.	Watershed and hillslope erosion processes evaluated by WEPP (adapted from USDA-ARS 1995).	2-12
Fig. 3.1.	Topography of Grand Junction Uranium Mill Tailings Disposal Site in Grand Junction, CO, the reference site for this study.	3-2
Fig. 3.2.	Resistive barrier profile (a) and water balance barrier profile (b).	3-3
Fig. 4.1.	Maximum erosion and average elevation predicted by SIBERIA for the reference site with a resistive barrier comparing rip-rap, topsoil, and gravel admixture surface layers: (a) semi-arid climate and (b) humid climate.	4-2
Fig. 4.2.	Elevation predicted for reference site with SIBERIA for a resistive barrier in a semi-arid climate: (a) rip-rap surface layer, (b) gravel admixture surface layer, and (c) topsoil surface layer. Elevation is shown in m and denoted by the color bar above.	4-4
Fig. 4.3.	Plan view of reference site with a resistive barrier in a semi-arid climate showing number of layers remaining intact across surface as predicted by SIBERIA: (a) rip-rap surface layer, (b) gravel admixture surface layer, and (c) topsoil surface layer. The color scale is layers of the barrier remaining intact ranging from one (tailings, red shading) to eight (deposition, blue shading). Green shading is all five layers of the cover plus the tailings layer remaining intact (six).	4-6
Fig. 4.4.	Elevation predicted for reference site predicted with SIBERIA for a resistive barrier in a humid climate: (a) rip-rap surface layer, (b) gravel admixture surface layer, and (c) topsoil surface layer. Elevation is shown in m and denoted by the color scale above.	4-7
Fig. 4.5.	Plan view of reference site predicted with SIBERIA for a resistive barrier in a humid climate: (a) rip-rap surface layer, (b) gravel admixture surface layer, and (c) topsoil surface layer. The color scale is layers of the barrier remaining intact ranging from one (tailings, red	

	shading) to eight (deposition, blue shading). Green shading is all five layers of the cover plus the tailings layer remaining intact (six).	4-8
Fig. 4.6.	Maximum erosion and average elevation predicted by SIBERIA for the reference site with a resistive barrier comparing gravel admixture surfaces with and without vegetation: (a) semi-arid climate and (b) humid climate.....	4-12
Fig. 4.7.	Maximum erosion and average elevation predicted by SIBERIA for resistive and water balance barriers with a rip-rap surface layer: (a) semi-arid climate and (b) humid climate.....	4-13
Fig. 4.8.	End-of-year cumulative flux above the tailings predicted by SVFLUX for the typical year and wettest year in a semi-arid climate: (a) resistive barrier and (b) water balance barrier. Negative flux indicates downward flow into the tailings.....	4-14
Fig. 4.9.	End-of-year cumulative flux above the tailings predicted by SVFLUX for the typical year and wettest year in a humid climate: (a) resistive barrier and (b) water balance barrier. Negative flux indicates downward flow into the tailings.....	4-15
Fig. 4.10.	Topography representing balanced side slopes with 20% maximum side slopes and 5.3% maximum top slope, referred to herein as the modified topography.	4-17
Fig. 4.11.	Maximum erosion and average elevation change predicted by SIBERIA for the reference site with rip-rap surface layer and a resistive barrier for various slope lengths: (a) semi-arid climate and (b) humid climate.....	4-20
Fig. 4.12.	Maximum erosion depth at 1000-yr for a 14.7% and 15.5% grade difference using a rip-rap surface over a resistive barrier in semi-arid and humid climates with slope length of 28 and 41 m.	4-21
Fig. 4.13.	Terraced (a), shallow concavity, 30% initial slope (b), deep concavity, 60% initial slope (c), and natural hillside slopes (d) used to evaluate influence of topography on erosion.	4-22
Fig. 4.14.	Maximum erosion, maximum deposition, and average elevation change predicted by SIBERIA for resistive barriers with a rip-rap surface and uniform, terraced, concave (semi-arid: deep concave, humid: shallow concave), or natural side slopes: (a) semi-arid climate and (b) humid climate.	4-23
Fig. 4.15.	Number of layers intact after 1000 years in a semi-arid climate predicted by SIBERIA for a resistive barrier with a rip-rap surface: (a) terraced side slopes, (b) concave side slopes (deep), and (c) natural side slopes.....	4-25

Fig. 4.16. Number of layers intact after 1000 years in a humid climate predicted by SIBERIA for a resistive barrier with a rip-rap surface: (a) terraced side slopes, (b) concave side slopes (shallow), and (c) natural side slopes.	4-26
Fig. 4.17. Maximum erosion, maximum deposition, and average elevation change predicted by SIBERIA for resistive barriers with a gravel admixture surface and uniform, terraced, concave (semi-arid: shallow, humid: deep), or natural side slopes: (a) semi-arid climate and (b) humid climate.....	4-27
Fig. 4.18. Number of layers intact after 1000 years in a semi-arid climate predicted by SIBERIA for a resistive barrier with a gravel admixture surface: (a) terraced side slopes, (b) concave side slopes (shallow), and (c) natural side slopes.	4-28
Fig. 4.19. Number of layers intact after 1000 years in a humid climate predicted by SIBERIA for a resistive barrier with a gravel admixture surface: (a) terraced side slopes, (b) concave side slopes (deep), and (c) natural side slopes.....	4-30
Fig. 4.20. Maximum erosion, maximum deposition, and average elevation change predicted by SIBERIA for resistive barriers with a topsoil surface and uniform, terraced, concave (semi-arid: shallow, humid: deep), or natural side slopes: (a) semi-arid climate and (b) humid climate.	4-31
Fig. 4.21. Number of layers intact after 1000 years in a semi-arid climate predicted by SIBERIA for a resistive barrier with a topsoil surface: (a) terraced side slopes, (b) concave side slopes (shallow), and (c) natural side slopes.....	4-32
Fig. 4.22. Number of layers intact after 1000 years in a humid climate predicted by SIBERIA for a resistive barrier with a topsoil surface: (a) terraced side slopes, (b) concave side slopes (deep), and (c) natural side slopes.	4-34
Fig. B.1. Maximum erosion, maximum deposition, and average elevation change predicted by SIBERIA for rip-rap, topsoil, and gravel admixture surface layer for a water balance barrier using the representative site topography: (a) semi-arid climate and (b) humid climate.	B-2
Fig. B.2. Erosion predicted by SIBERIA for a rip-rap surface with a water balance barrier in a semi-arid climate using the representative site topography: a) elevation predictions of the surface after 1000 years of erosion and, b) number of layers remaining intact after 1000 years of erosion, plan view.	B-3
Fig. B.3. Erosion predicted by SIBERIA for a gravel admixture surface with a water balance barrier in a semi-arid climate using the representative	

	site topography: a) elevation predictions of the surface after 1000 years of erosion and, b) number of layers remaining intact after 1000 years of erosion, plan view.....	B-4
Fig. B.4.	Erosion predicted by SIBERIA for a topsoil surface with a water balance barrier in a semi-arid climate using the representative site topography: a) elevation predictions of the surface after 1000 years of erosion and, b) number of layers remaining intact after 1000 years of erosion, plan view.	B-5
Fig. B.5.	Erosion predicted by SIBERIA for a rip-rap surface on a water balance barrier in a humid climate using the representative site topography: a) elevation predictions of the surface after 1000 years of erosion and b) number of layers remaining intact after 1000 years of erosion, plan view.	B-6
Fig. B.6.	Erosion predicted by SIBERIA for a gravel admixture surface on a water balance barrier in a humid climate using the representative site topography: a) elevation predictions of the surface after 1000 years of erosion and b) number of layers remaining intact after 1000 years of erosion, plan view.	B-7
Fig. B.7.	Erosion predicted by SIBERIA for a topsoil surface on a water balance barrier in a humid climate using the representative site topography: a) elevation predictions of the surface after 1000 years of erosion and b) number of layers remaining intact after 1000 years of erosion, plan view.	B-8
Fig. C.1.	Predictions from SVFLUX of precipitation, evapotranspiration, soil-water storage, and cumulative percolation for resistive and water balance barriers in a semi-arid climate. Some simulations required less years than others to stabilize. The last year of each simulation is the wettest year. Positive percolation is into the tailings, negative is out.	C-2
Fig. C.2.	Predictions from SVFLUX of precipitation, evapotranspiration, soil-water storage, and cumulative percolation for resistive and water balance barriers in a humid climate. Some simulations required less years than others to stabilize. The last year of each simulation is the wettest year. Positive percolation is into the tailings, negative is out.	C-3
Fig. D.1.	Maximum erosion, maximum deposition, and average elevation change predicted by SIBERIA for rip-rap, topsoil, and gravel admixture surfaces with 41 m side slopes and a resistive barrier: (a) semi-arid climate and (b) humid climate.....	D-2
Fig. D.2.	Maximum erosion, maximum deposition, and average elevation change in resistive and water balance barriers predicted by SIBERIA with 41 m side slopes and a rip-rap surface layer: (a) semi-arid climate and (b) humid climate.	D-3

Fig. D.3.	Elevation predicted for a rip-rap surface with various slope lengths and angles in a semi-arid climate: (a) 53 m side slopes, 15.3% side slopes, 2% top slope, (b) 28 m side slopes, 18.5% side slopes, 3% top slope, and (c) 41 m side slopes, 20% side slopes, 5.3% top slope. Elevation is shown in m and denoted by the color scale above.	D-4
Fig. D.4.	Plan view predicted for a rip-rap surface with various slope lengths and angles in a semi-arid climate: (a) 53 m side slopes, 15.3% side slopes, 2% top slope, (b) 28 m side slopes, 18.5% side slopes, 3% top slope, and (c) 41 m side slopes, 20% side slopes, 5.3% top slope.	D-5
Fig. D.5.	Elevation predicted for a rip-rap surface with various slope lengths and angles in a humid climate: (a) 53 m side slopes, 15.3% side slopes, 2% top slope, (b) 28 m side slopes, 18.5% side slopes, 3% top slope, and (c) 41 m side slopes, 20% side slopes, 5.3% top slope. Elevation is shown in m and denoted by the color scale above.	D-6
Fig. D.6.	Plan view predicted for a rip-rap surface with various slope lengths and angles in a humid climate: (a) 53 m side slopes, 15.3% side slopes, 2% top slope, (b) 28 m side slopes, 18.5% side slopes, 3% top slope, and (c) 41 m side slopes, 20% side slopes, 5.3% top slope.	D-7
Fig. E.1.	Topographic map of the representative site.	E-2
Fig. E.2.	Modified site topography used to create uniform, terraced, concave, and natural side slopes. See Fig. 4.13 for side slope views with top and side slope grades.	E-3
Fig. F.1.	Maximum erosion, maximum deposition, and average elevation change for resistive barrier in a semi-arid climate: a comparison of shallow and deep concavity for (a) a rip-rap surface, and (b) a topsoil surface.	F-3
Fig. F.2.	Maximum erosion, maximum deposition, and average elevation change for resistive barrier in a humid climate: a comparison of shallow and deep concavity for (a) a rip-rap surface, and (b) a gravel admixture surface.	F-4
Fig. G.1.	Elevation predictions from SIBERIA of the topography producing the least erosion with a resistive barrier in a semi-arid climate: (a) rip-rap surface layer with deep concavity and (b) gravel admixture surface layer with shallow concavity.	G-2
Fig. G.2.	Plan view SIBERIA predictions of the topography producing the least erosion with a resistive barrier in a semi-arid climate: (a) rip-rap surface layer with deep concavity and (b) gravel admixture surface layer with shallow concavity.	G-3

- Fig. G.3. Elevation predictions from SIBERIA of the topography producing the least erosion with a resistive barrier in a humid climate: (a) rip-rap surface layer with terraces and (b) gravel admixture surface layer with terraces..... G-4
- Fig. G.4. Plan view SIBERIA predictions of the topography producing the least erosion with a resistive barrier in a humid climate: (a) rip-rap surface layer with terraces and (b) gravel admixture surface layer with terraces..... G-5

LIST OF TABLES

Table 2.1.	Summary of key aspects of erosion codes evaluated for this study.	2-7
Table 3.1.	Material properties of surface layers, resistive barrier layers, water balance barrier layers, and waste (Benson et al. 2008 and 2010), Particle size fractions by Unified Soil Classification System. Organic matter by loss on ignition.	3-5
Table 3.2.	Hydraulic properties used in the hydraulic modeling portion of this study.....	3-6
Table 3.3.	Summary of parameterization and SIBERIA simulations in the literature.	3-8
Table 3.4.	Fluvial sediment transport parameters for resistive barriers used in the SIBERIA simulations.....	3-10
Table 3.5.	Fluvial sediment transport parameters for water balance barriers used in SIBERIA simulations.	3-11
Table 3.6.	SIBERIA input and control parameters for erosion, runoff and sediment transport.....	3-14
Table 3.7.	Vegetation parameter input to SVFLUX.....	3-16
Table 4.1.	Erosion process for fluvial erosion parameters m1 and n1 based on climate and surface layer type.	4-5
Table 4.2.	Side slope length, side slope grade, top slope grade, and grade difference compared with SIBERIA simulations to determine effects of slope length and grade.	4-19
Table A.1.	Effects of initial soil water content on discharge and sediment loss in WEPP. All other factors held constant.	A-2
Table A.2.	Effects of soil albedo on discharge and sediment loss in WEPP.....	A-3
Table F.1.	Best case scenario for concave side slopes based on climate and surface material.	F-2

EXECUTIVE SUMMARY

The objective of this study was to evaluate design strategies that couple erosion and hydrology for barriers of low level radioactive waste (LLRW) disposal facilities. This objective was met by conducting long-term (1000 yr) parametric simulations with the SIBERIA landform evolution model and the SVFLUX hydrologic model.

Landform evolution modeling considered four main factors affecting fluvial erosion: (1) climate, (2) soil, (3) vegetation, and (4) topography. Several scenarios were evaluated for semi-arid and humid sites. The topography of the Grand Junction Uranium Mill Tailings Disposal Site in Grand Junction, CO was used as a realistic starting point, and modifications were made to the topography, soil surface layer, cover type, and vegetation. The topographic changes included a modified cover with a central high point and more balanced slope lengths with uniform slopes, and modified cover with terraced, concave, and natural side slopes. Three types of surface layers were evaluated: rip-rap, topsoil, and topsoil mixed with gravel (gravel admixture). Conventional resistive barriers and water balance barriers with a capillary break were evaluated. Simulations were conducted with and without vegetation with native plants for each climate.

Hydraulic modeling was conducted using a one-dimensional profile for semi-arid and humid climates. Simulations were conducted using normal and wettest year precipitation data. Rip-rap, topsoil, and gravel admixture surface layers were used over resistive and water balance barriers in simulations to evaluate cumulative percolation into the waste.

Climate and use of vegetation produced significant differences in maximum erosion depths. The semi-arid climate had approximately 4 m greater maximum erosion depth than the humid climate for simulations with a rip-rap or gravel admixture surface. A topsoil surface in the semi-arid climate had approximately 2.5 m greater maximum erosion than the humid climate. Vegetation decreased the amount of erosion in the semi-arid climate by 1.5 m and 4 m in the humid climate. Vegetation also increased the amount of evapotranspiration that occurred, decreasing percolation into the waste.

The resistive barrier produced less erosion than the water balance barrier in the semi-arid climate. Neither allowed percolation into the waste. Percolation was high for the water balance cover in the humid climate and non-existent for the resistive cover. Both covers performed identically in the landform evolution predictions for the humid climate.

Short slopes, slopes with a low grade, and slopes with small grade differences at the nickpoint were found to decrease erosion. The humid climate had the least erosion when terraced slopes were utilized. Due to higher erosion rates in the semi-arid climate, natural and concave slopes that promote deposition produced the least erosion.

Overall, the rip-rap surface layer prevented the most erosion over any type of topography, climate, or cover type. However, covers with a riprap surface layer transmitted more percolation. In contrast, the gravel admixture surface had slightly greater erosion, but prevented percolation in typical year simulations for both climates.

ACKNOWLEDGMENTS

This study was supported by the US Nuclear Regulatory Commission via an Interagency Agreement with the US Geological Survey. Support was also provided by the US Department of Energy under Cooperative Agreement Number DE-FC01-06EW07053 entitled 'The Consortium for Risk Evaluation with Stakeholder Participation III. The opinions, findings, conclusions, or recommendations expressed herein are those of the author and do not necessarily represent the views of the US Nuclear Regulatory Commission, the US Geological Survey, or the US Department of Energy.

1 INTRODUCTION

Engineered barriers are used in waste containment facilities to limit human and animal contact with waste, to control ingress and egress of gases, and to limit exposure of waste to water sources by controlling percolation (Sackschewsky et al. 1995, Benson 2001, Walter and Dubreuilh 2007). Barriers for low-level radioactive waste (LLRW) and uranium mill tailings sites are designed to control percolation, radon emission, and erosion for a service life of at least 1000 yr (EPA 1983). Erosion can severely diminish the integrity of the barrier (Vaugh et al. 1994, Anderson and Stormont 1997, 2005, Stormont 2003) by exposing buried waste, or reduce the barrier thickness sufficiently to make the waste more susceptible to percolation (Richardson and Vaugh 1996).

The main objective of this study was to assess the coupling of erosion control strategies and hydrological performance of engineered barriers. Two models were chosen to evaluate how design strategies affect erosion and hydrology of barriers. Erosion was modeled using the SIBERIA landform evolution model, whereas hydrology was modeled using the variably saturated flow model SVFLUX. Climate, material used for the surface layer, barrier type (resistive vs. water balance), topography of the landform, erosion protection systems, and vegetation were varied systematically to assess how they influence erosion and percolation.

The SIBERIA landform evolution model was used to predict the long-term erosion of surface barriers for LLRW facilities. Multiple scenarios with different surface materials, barrier types, and topography were predicted with SIBERIA. The variably saturated flow code SVFLUX was used to predict the hydrology of barrier scenarios simulated in the SIBERIA model. The objective was to determine how modifications made to prevent erosion impact the hydrology of barriers. The SVFLUX predictions were used in conjunction with the SIBERIA predictions to evaluate the barrier system as a whole when comparing barrier scenarios designed to prevent erosion.

This report consists of the five sections. Section 2 of this report includes background information on erosion processes and erosion models. Section 3 includes a description of the reference site, materials used, and modeling methods. Results of the erosion and hydrologic modeling are presented and discussed in Section 4. Implications of coupling erosion and hydrologic barrier performance and best case scenarios are summarized in Section 5.

2 BACKGROUND

2.1 Factors Affecting Fluvial Erosion

Soil erodibility is the inherent susceptibility of the soil to erosive forces such as rainfall and overland flow. The USDA method to estimate erodibility is based on the particle size distribution, organic matter content, soil structure (e.g. granular, platy), and hydraulic conductivity (Wischmeier and Smith 1978, Toy et al. 2002). Soil erodibility depends on soil structure, texture, organic matter, water content, clay mineralogy, density, and chemical and biological characteristics of the soil (Foster et al. 1995). Larger particle sizes are easier to detach but more difficult to transport (i.e. clay soils are more difficult to detach but easier to transport than sandy soils) (Fangmeier et al. 2006). Fine-grained soils have attractive forces that must be overcome for erosion to occur (Toy et al. 2002). Granular soils do not have attractive forces, and are easier to detach (Fangmeier et al. 2006).

Vegetation can increase rainfall interception, retard erosion, increase plant residue on the surface, and restrain soil movement (Fangmeier et al. 2006). Land uses that incorporate vegetation have lower erosion than land uses with bare soil.

Topographic features that affect erosion include slope length, steepness, shape, and the size and shape of the watershed (Morgan 1995). Steep slopes can accelerate detachment and sediment transport by decreasing the stability of particles. Long slope lengths tend to concentrate flow, with sheet flow generally transitioning to concentrated flow within 30 m (Wischmeier and Smith 1978). Keeping slope lengths less than 30 m can significantly reduce development of rills and gullies (Wischmeier and Smith 1978).

Uniform, convex, and concave slopes are shown in Fig. 2.1. Concave slopes are flatter at the base of the slope and deliver less sediment to the base than convex slopes because most deposition occurs immediately following a section of steep slope (Toy et al. 2002). Variations in erosion due to shape are influenced by the location of overland flow processes on the hillslope in relation to the steepness of the slope. By placing the flatter slope towards the base, as with a concave slope, concentration is avoided and rills disperse over the flatter slope (Fangmeier et al. 2006).

There are two types of areas where overland flow causes erosion: interrill areas and rill areas (Toy et al. 2002), as shown in Fig. 2.2. Rill areas are small channels where flow concentrates. Rill location depends on the topography of the surface and can change with surface disruption (e.g., tilling). Overland flow causes detachment and erosion in rill areas, whereas raindrop impact and sheet flow cause detachment and erosion in interrill areas (USDA-ARS 2010b). Detachment in rills occurs when the sediment load in the overland flow is less than the transport capacity of the flow.

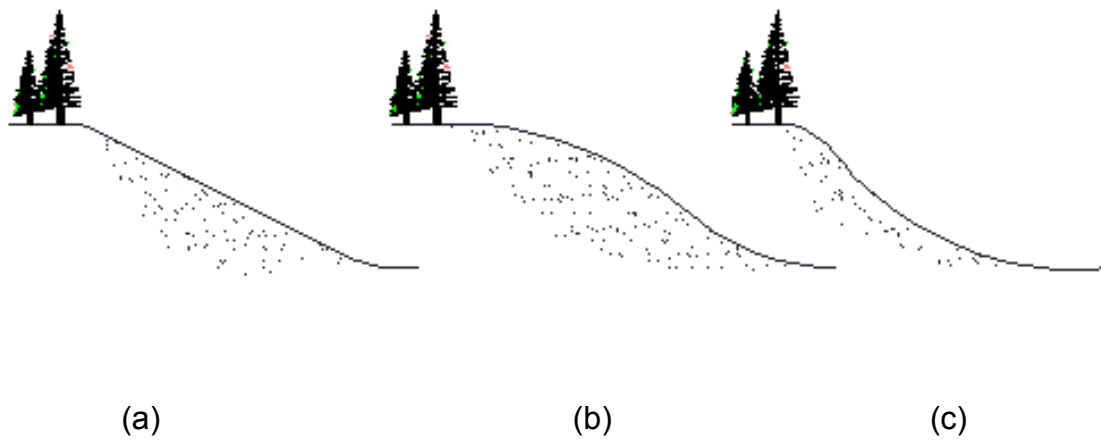


Fig. 2.1. Slope shapes (a) uniform slope, (b) convex slope, and (c) concave slope.

Thus, sediment load can also control detachment (Fangmeier et al. 2006).

Transport capacity is the amount of sediment that overland flow is capable of moving and is a function of the runoff rate, slope steepness, and hydraulic resistance (Toy et al. 2002). Deposition occurs when the sediment load in surface water is greater than the transport capacity of the flow. The largest particles are deposited first, and the smaller particles deposit further downstream (Willgoose and Sharmeen 2006).

Gully erosion is the most destructive form of erosion (Morgan 1995). Gullies are large channels that form in concentrated flows that have enough shear stress and carry enough abrasive sediment to cut into the surface by removing sediment. This first incision into the surface is called head-cutting and it begins downstream towards the channel outlet. Head-cutting moves upslope within the channel over time, incising the surface and creating the gully (Toy et al. 2002).

Erosion can be mitigated using several methods: (1) vegetating the surface layer, (2) decreasing slope steepness, (3) decreasing slope length, and (4) modifying the surface material. Vegetation reduces erosion by decreasing raindrop impact (i.e. by interception), decreasing interrill erosion, and if the plant stems are dense, limiting rill formation. Plant litter and biomass on the surface bind the surface soil so that it is less erodible, and surface biomass dissipates energy during water contact. Both of the factors are influenced by plant species and coverage.

Other surface materials such as rip-rap and gravel admixtures have been used successfully to control erosion on covers (Waugh et al. 1994). Rip-rap controls erosion by providing stability on the surface with a sufficiently large weight to resist movement by flow (Toy et al. 2002). Rip-rap has been successfully used on spillways and severely unstable slopes (Fangmeier et al. 2006). Gravel admixtures control erosion via natural surface armoring (Fig. 2.3). Over time, as overland flow events occur, the surface soil becomes more resistant to erosion than the underlying layer (Willgoose and Sharmeen 2006). Adding large particles expedites the armoring process by decreasing the amount of finer and more erodible soil (Willgoose and Sharmeen 2006). Reducing the steepness of the slope reduces velocity which slows channel development by head-cutting. Decreasing slope length decreases the size of the drainage area that a channel services. Long slopes tend to increase the accumulation of concentrated overland flow (Wischmeier and Smith 1978).

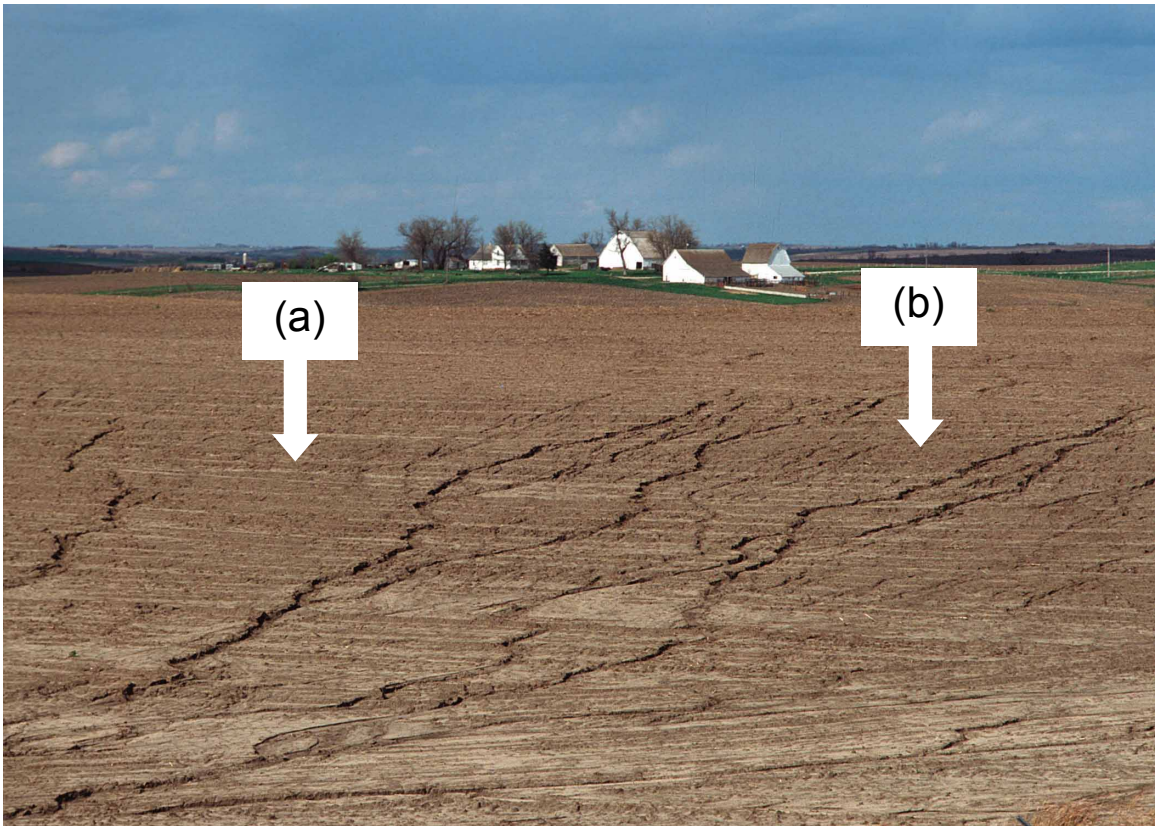


Fig. 2.2. Interrill erosion area (a) and rill erosion area (b). Photo courtesy of USDA Natural Resource Conservation Service

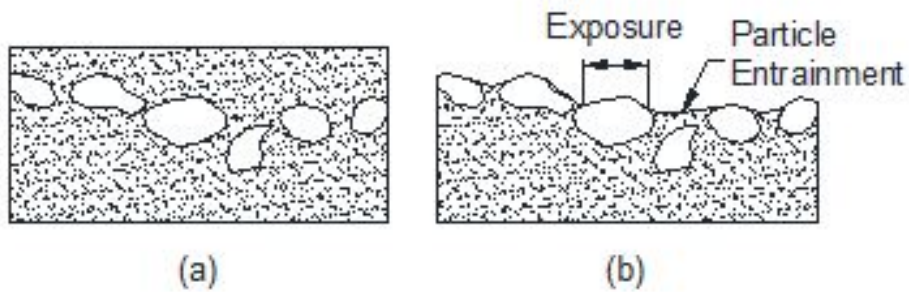


Fig. 2.3. Schematic of armoring process: (a) original surface and (b) armored surface (adapted from Willgoose and Sharmeen, 2006).

2.2 Erosion Models

Two empirical erosion models and six landform evolution models were evaluated when selecting an erosion model to use in this study. Key aspects of the erosion models that were considered are summarized in Table 2.1. Empirical erosion models provide an average soil loss per unit area, but provide no information on erosion patterns on the land surface. Landform evolution models are process-based representations of the mechanisms of erosion on a landform that couple hydrology, fluvial erosion, hillslope erosion processes, tectonic uplift, and climate (Coulthard 2001). Landform evolution models predict erosion patterns on the land surface, when erosion occurs, and where erosion starts.

2.2.1 Empirical Erosion Models

Empirical erosion models are used to compute an average soil loss per unit area. The most common are the Revised Universal Soil Loss Equation (RUSLE2) (USDA-ARS 2010a) and the Water Erosion Prediction Project (WEPP) model (USDA-ARS 1995). RUSLE2 and WEPP were developed for agricultural purposes by the United States Department of Agriculture - Agricultural Research Service (USDA-ARS) jointly with the Natural Resources Conservation Service (NRCS).

2.2.1.1 RUSLE2

The RUSLE2 model is used for conservation planning and erosion estimates in the United States (Walter and Dubreuilh 2007). RUSLE2 (USDA-ARS 2010a), and its predecessor, the Universal Soil Loss Equation (USLE) (Wischmeier and Smith 1978) use mechanistic and empirical equations to predict erosion. A schematic of the erosion processes in RUSLE2 is in Fig. 2. RUSLE2 is a modification of the original USLE model and is based on an updated evaluation of standard plot data (USDA-ARS 2008) and more recent field data (USDA-ARS 2010b) regarding erosion. USLE and RUSLE2 are based on Eq. 2.1 (USDA-ARS 2010b):

$$A=RKLSCP \quad (2.1)$$

where A is the average annual soil loss per unit area (tons/acre/yr), R is the average annual erosivity of rainfall and runoff [(ft-tonsf/ac)(in/hr)/yr = R-units], K is the soil erodibility factor (tons/ac/R-unit), LS is the length-slope factor (dimensionless), C is the barrier factor (dimensionless), and P is the conservation practice factor (dimensionless).

The R-factor is based on rainfall intensity and energy including the terminal velocity of raindrops. High intensity and energy are able to erode the surface with greater speed and depth (Walter and Dubreuilh 2007).

Table 2.1. Summary of key aspects of erosion codes evaluated for this study.

Variable/ Process	RUSLE2	WEPP	SIBERIA	ARMOUR	CAESAR	GOLEM	CASCADE	CHILD
Type of surface	General slope or watershed	General slope or watershed	DTM	DTM	DTM	DTM	DTM	DTM
Empirical or Mechanistic	Empirical	Mechanistic-Empirical	Mechanistic	Mechanistic	Mechanistic	Mechanistic	Mechanistic	Mechanistic
Grid type	Not applicable	Not applicable	Rectangular	Rectangular	Rectangular	Fixed Rectangular or 1km ² or 50m ²	TIN \geq 1 km ²	TIN with Voronoi diagrams
Relevant Site Size	Watershed	Hillslope or 640 acre field size	Watershed	Watershed	Watershed	Regional or Watershed	Regional Scale	Watershed
Relevant Time Scale	Annual	Up to 100 years	highly erodible < 1000 yr; hard surface <100,000 yr	highly erodible < 1000 yr; hard surface <100,000 yr	10 to 10,000 years	100,000 - 10,000,000 yr	Millions of years	Short Term
Erosion Calculations	Empirical	Shear stress	Conservation of mass and channel initiation function	Conservation of mass and shear stress	Multiple flow algorithm	Conservation of mass	Conservation of mass	Conservation of mass

Table 2.1. Summary of key aspects of erosion codes evaluated for this study (continued).

Variable/ Process	RUSLE2	WEPP	SIBERIA	ARMOUR	CAESAR	GOLEM	CASCADE	CHILD
Fluvial Erosion/ Diffusive Erosion	Fluvial and Diffusive Erosion	Fluvial and Diffusive Erosion	Fluvial and Diffusive Erosion	Fluvial Erosion	Fluvial and Diffusive Erosion	Fluvial and Diffusive Erosion	Fluvial Erosion	Fluvial and Diffusive Erosion
Vegetation Capabilities	Yes	Yes, many built in crops	Not directly, can be calibrated with model parameters	Not directly, can be calibrated with model parameters	Yes	Not directly, can be calibrated with model parameters	Not directly, can be calibrated with model parameters	Yes, including growth
Determination of Erosion	Average Annual Rates	Average Annual Rates	Average Annual Rates	Average Annual Rates	Event Based	Event Based	Average Annual Rates	Event Based
Unique Capabilities	Agriculture	Agriculture	Evolves catchment throughout simulation, layers, output at any time	Armoring of surface	Divergent flow (e.g. alluvial fans or braided rivers)	Landslides, weathering, sediment production	Graphical output of model evolution	Alluvial stratigraphy, layers
References	Wischmeier and Smith (1978), USDA-ARS (2010a), USDA-ARS (2010b)	Foster et al. (1995), USDA-ARS (1995), Flanigan and Nearing (1995)	Willgoose et al. (91 a, b, c; 1994), Willgoose (05a)	Sharmeen (2000), Willgoose and Sharmeen (2006)	Coulthard et al. (98, 99, 00), Coulthard and Macklin (2000)	Tucker and Slingerland (1994)	Braun and Sambridge (1997)	Tucker et al. (1997, 2001)

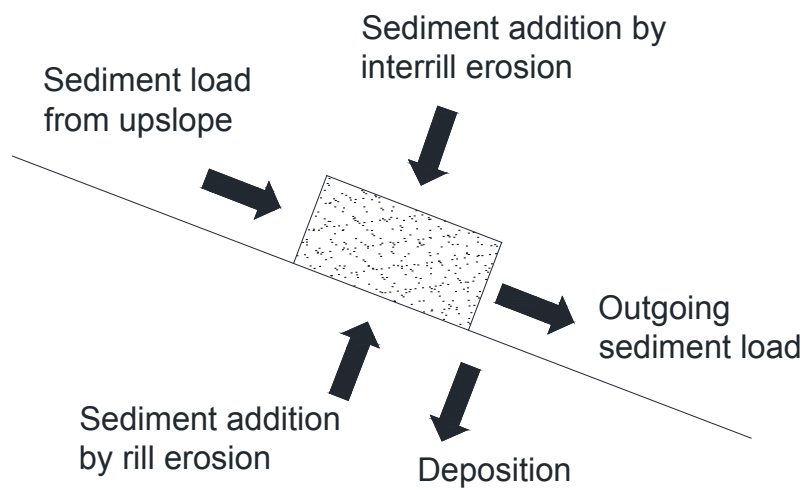


Fig. 2.4. Conservation of mass for a segment along the overland flow path on a hillslope (adapted from <http://www.ars.usda.gov/Research/docs.htm?docid=6014>).

The K-factor is based on the composition of the soil, namely the percentages of clay, silt, very fine sand, and organic matter (Wischmeier and Smith 1978). High organic matter decreases the erosion potential of soil, whereas erosion increases with clay and silt content (Walter and Dubreuilh 2007). Very fine sand is defined as particles greater than 0.050 mm and smaller than 0.10 mm. High very fine sand content also increases erosion because fine sand has little binding forces (USDA-ARS 2008). The K-factor also empirically accounts for perviousness of the soil (rapid to very slow) and soil structure (very fine granular to blocky, platy or massive) based on the texture and saturated hydraulic conductivity of the material (Wischmeier and Smith 1978).

The parameter LS is based on the slope length and slope percentage. Slope length is important because the drainage area increases, overland flow increases, and detachment and transport of soil increases as the slope length increases (Toy et al. 2002). High slopes increase the velocity of overland flow causing greater soil detachment and transport.

The surface cover factor, C, is the ratio of erosion for a type of barrier and practice to the erosion for two years of fallow conditions (the standard plot), and is used to compare the relative effect of management practices and cropping on erosion rates (Wischmeier and Smith 1978). Soil conservation practices affect the P-factor. They include contouring, strip cropping, and a combination of terracing and contouring. All reduce erosion and are reflected in a lower P.

The USLE and RUSLE2 equations were developed to compare any site to the standard plot using statistical relationships and produce an average annual soil loss for that site. The standard plot is 22.1 m long by 1.83 m wide at a 9% slope with tillage up and down the slope that has been fallow for a minimum of 2 yr. In several locations throughout the United States, standard plots were developed and monitored to gather statistical data regarding erosion. Data from these plots were used to develop USLE and RUSLE2. Most of the standard plots were developed in agricultural areas of the eastern United States where humid climates are prevalent, making RUSLE2 less useful for other land uses and climates (USDA-ARS 2010a).

The semi-empirical equations and statistical correlations employed by RUSLE2 can result in less accurate erosion estimations, and they are relevant specifically for conditions under which the expressions were derived. Walter and Dubreuilh (2007) reviewed previous studies on the accuracy of RUSLE2 and its predecessors, USLE and RUSLE, and found that soil loss generally is over predicted for rates less than 23 Mg/ha-yr, and under predicted soil loss for rates greater than 23 Mg/ha-yr.

2.2.1.2 WEPP

WEPP (Foster et al. 1995) has been used mainly by the United States Department of Agriculture for evaluating agricultural practices (Fig. 2.). WEPP uses mathematical descriptions of the physical processes of runoff, raindrop impact, and rain splash to

model detachment, erosion, and deposition on hillslopes rather than the statistical correlations of the standard plot as in RUSLE2. Interrill erosion is conceptualized as a process of sediment delivery to the rill. The sediment load is a function of the interrill erosion and the rill erosion. The sediment continuity equation (Eq. 2.2) is used to describe the movement of sediment to a rill (all equations in Section 2.2.1.2 are from USDA-ARS 1995):

$$\frac{dG}{dx} = D_f + D_i \quad (2.2)$$

where G is the sediment load ($\text{kg}/\text{m}\cdot\text{s}$), x is the distance downslope (m), D_i is the interrill sediment delivery to the rill ($\text{kg}/\text{m}^2\cdot\text{s}$), and D_f is the rill erosion rate ($\text{kg}/\text{m}^2\cdot\text{s}$).

The rill erosion rate is calculated when the hydraulic shear stress of the flow exceeds the critical shear stress of the soil. If the sediment transport capacity, T_c , has already been exceeded rill erosion does not occur.

Rill erosion is described by:

$$D_f = D_c \left(1 - \frac{G}{T_c} \right) \quad (2.3)$$

where D_c is the detachment capacity by rill flow ($\text{kg}/\text{m}^2\cdot\text{s}$) and T_c is the sediment transport capacity within the rill ($\text{kg}/\text{m}\cdot\text{s}$). The detachment capacity is calculated by Eq. 2.4 when the hydraulic shear stress of rill flow exceeds the critical shear stress of the soil:

$$D_c = K_r (\tau_f - \tau_c) \quad (2.4)$$

where K_r is the rill erodibility parameter (s/m), τ_f is the flow shear stress (Pa), and τ_c is the critical shear stress of the soil (Pa). Deposition of particles in a rill is calculated by Eq. 2.5 when the sediment load is greater than the sediment transport capacity ($G > T_c$):

$$D_f = \frac{\beta V_f}{q} (T_c - G) \quad (2.5)$$

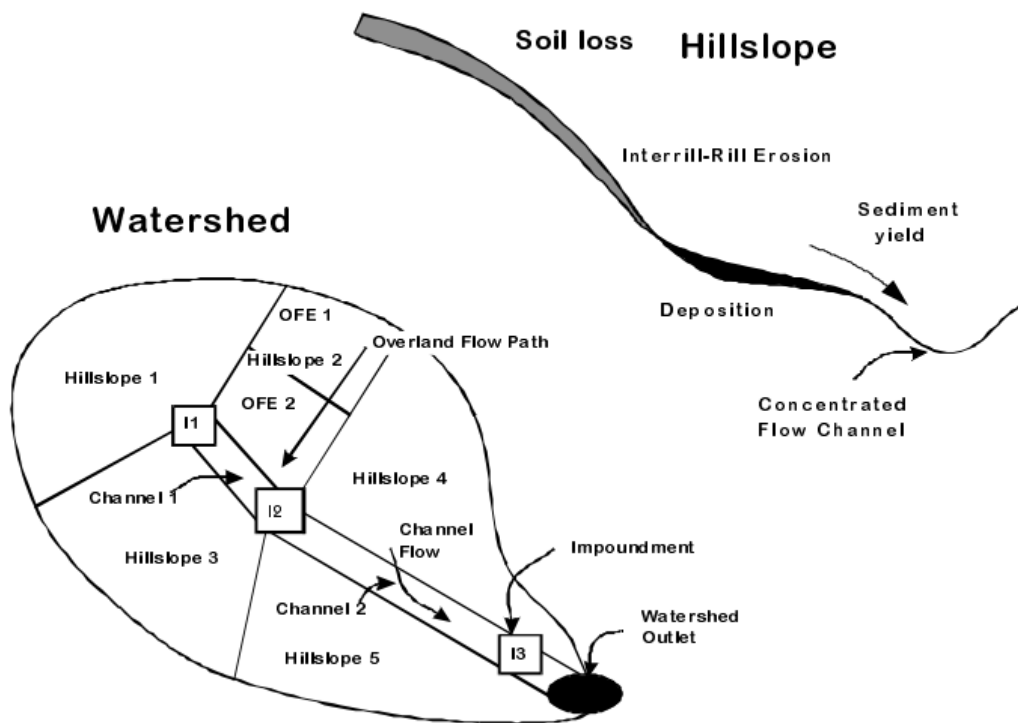


Fig. 2.5. Watershed and hillslope erosion processes evaluated by WEPP (adapted from USDA-ARS 1995).

where β is the raindrop-induced turbulence coefficient, V_f is the effective fall velocity for the sediment (m/s), and q is the flow discharge per unit width (m^2/s) (Foster et al. 1995).

WEPP can be used to model hillslopes and watersheds with or without existing channels and sub-watersheds. Watershed properties such as channel and impoundment characteristics as well as the outlet information are input variables (USDA-ARS 1995).

The water balance portion of WEPP is calculated using kinematic wave equations and infiltration is calculated using a modified Green–Ampt infiltration equation (USDA-ARS 1995). The plant growth component increases and decreases biomass above and below ground by calculating potential plant growth based on solar radiation, water availability, and temperature. Eq. 2.2 is the erosion component of WEPP that estimates the change in sediment load in the flow with the distance down slope using the shear stress of the material (Flanagan and Nearing 1995).

Climate, slope, soil, and management are the major input variables in WEPP. WEPP includes the stochastic weather generator, CLIGEN, which includes at least 25 years of precipitation and temperature data. CLIGEN has been parameterized by historical data from 1200 National Climatic Data Center weather stations in the United States. Each station has been collecting daily, hourly, and 15 minute precipitation and temperature data for at least 25 yr. By selecting the nearest weather station, precipitation, snowfall, storm duration, peak rainfall, time to peak, storm frequency, air temperature, dew point temperature, solar radiation, wind speed, and wind direction are all modeled within WEPP using the CLIGEN weather generator (Flanagan and Nearing 1995). Different climates can be modeled by simply selecting weather stations in the desired climates.

Slope inputs consist of steepness, length, width, and shape. Shapes that can be modeled include concave, convex, complex, and uniform. Soil characteristics include the soil depth, percent sand content, percent clay content, percent rock content, percent organic content, cation exchange capacity (CEC), soil albedo, and initial water content. Soil types can either be chosen from an extensive database within WEPP, or modified by input of soil characteristics (Flanagan and Nearing 1995). The user can specify or have the model calculate interrill erodibility, rill erodibility, critical shear, and effective hydraulic conductivity. Land use practices that describe different plants and tillage and management practices can be selected from the management section of WEPP (USDA-ARS 1995).

WEPP also determines the on-site and off-site effects of erosion and the particle size distribution for the sediment leaving the site. WEPP outputs can be adjusted by the user to obtain runoff and sediment loss on a storm-by-storm, monthly, annual, or average annual basis. Time sensitive estimates of runoff, erosion, sediment delivery, and sediment enrichment as well as spatial distribution of sediment loss on the hillslope are calculated and output in text files and on the interface. Predictions from

WEPP have been validated against 12 sites for approximately 1000 plot years of natural runoff and erosion data (Flanagan and Meyer 2010).

2.2.2 Landform Evolution Models

Landform evolution models predict the geometry of a watershed over time by routing water across a grid network and representing erosion by changing the grid elevations to reflect the evolving geomorphic characteristics of the site (Willgoose 2005a, Coulthard et al. 2007). Some landform evolution models (e.g. ARMOUR, CHILD) use a short-term event-based time scale, whereas others calculate long-term average annual erosion (e.g. SIBERIA, CAESAR, GOLEM, and CASCADE) for intervals of tens to thousands of years. The following landform evolution models were evaluated in this study: SIBERIA, ARMOUR, CAESAR, GOLEM, CASCADE, and CHILD. These models were included because they have been used in practice and tested and verified. Other landform evolution models were available but were not considered because they have not been verified or used in practice.

2.2.2.1 SIBERIA

The SIBERIA (Willgoose et al. 1991c, 1994) landform evolution model is a mechanistic model that predicts fluvial and diffusive sediment transport for a watershed-sized area (Willgoose et al. 1991a, 1991b, and Willgoose 2005a) and has been used for mine site rehabilitation (Evans and Willgoose 2000, Hancock et al. 2000, Hancock et al. 2003, Hancock and Turley 2006, Hancock et al. 2010). SIBERIA is unique because (1) it uses digital terrain maps (DTMs) to determine watershed size and drainage areas and (2) efficiently adjusts the landform with time as erosion occurs (Willgoose 2005a).

SIBERIA models fluvial and diffusive sediment transport, channel network development, runoff, and tectonic uplift processes and predicts the evolving landform using two partial differential equations: (1) a continuity equation for sediment transport and elevation change and (2) a channel indicator equation to identify whether a point is a channel or hill slope. SIBERIA uses the finite-difference method on a DTM with rectangular grid spacing to move water and sediment in the direction of the steepest slope using the continuity equation (Eq. 2.6).

$$\frac{\partial z}{\partial t} = c_0(x, y) + \frac{1}{\rho_s(1-n)} \left(\frac{\partial q_{sx}}{\partial x} + \frac{\partial q_{sy}}{\partial y} \right) + D_z \left(\frac{\partial^2 z}{\partial x^2} + \frac{\partial^2 z}{\partial y^2} \right) \quad (2.6)$$

where z is elevation, t is time, $c_0(x, y)$ is the rate of tectonic uplift, ρ_s is the density of the solids, n is the porosity of material before erosion and after deposition, q is the

discharge per unit width, x and y are horizontal coordinates, D_z is the erosive diffusivity (Willgoose et al. 1991a).

Channel growth is a function of hillslope form, discharge from upstream to the channel head, and the resistance of the hillslope to channel formation. The channel indicator equation (Eq. 2.7) is used to describe the transition point between a hillslope and a channel (Willgoose 2005a).

$$\frac{\partial Y}{\partial t} = d_t \left[0.0025 \frac{a}{a_t} + \left(-0.1Y \frac{Y^2}{1+9Y^2} \right) \right] \quad (2.7)$$

where t is time, d_t is the rate constant for channel growth, a is the channel initiation function, a_t is the channel initiation threshold, and Y is the indicator variable for channelization ($Y=0$, hillslope mode; $Y=1$, channel mode) (Willgoose et al. 1991a). The channel indicator equation is based on the channel initiation threshold which is dependent on the resistance of the watershed to channelization.

In SIBERIA, erosion is modeled by combining fluvial and diffusive sediment transport processes. The fluvial processes depend on the discharge and slope in the steepest downhill direction. Diffusive processes, which include soil creep, rain splash, and rockslides, are modeled using a spatially constant Fickian diffusion term. The sediment transport constitutive equations are used to calculate the sediment transport rate (Hancock et al. 2003). Eq. 2.8 quantifies sediment transport in SIBERIA:

$$q_s = q_{sf} + q_{sd} \quad (2.8)$$

where q_s is the sediment transport rate per unit width, q_{sf} is the fluvial sediment transport term, and q_{sd} is the diffusive transport term. Eq. 2.9 quantifies rill and channel erosion:

$$q_{sf} = \beta_1 q^{m_1} S^{n_1} \quad (2.9)$$

where q is the discharge per unit width, S is the slope in the steepest downslope direction, β_1 , m_1 , and n_1 are fluvial sediment transport parameters, and q_{sf} is defined above. Eq. 2.10 quantifies soil creep, rain splash, and other diffusive processes:

$$q_{sd} = DS \quad (2.10)$$

where D is diffusivity and q_{sd} and S are described above.

Runoff, sediment transport, and channel characteristics can be modeled in SIBERIA with multiple options (Willgoose 2005a). SIBERIA only simulates Hortonian runoff (points on the watershed that are saturated cause runoff). Thus, fluvial erosion and sediment transport occurs at saturated points. Sediment transport is either transport limited or source limited. Transport-limited flow assumes an unlimited amount of sediment can be removed from the surface. Source-limited processes recognize a finite sediment amount exists and can only transport that amount of sediment. Two types of channel characteristics can be modeled: the fixed channel model fixes the channel in place forever once it is created; the stochastic channel model allows channels to advance and retreat in response to climate fluctuations.

Tectonic uplift processes are also modeled in SIBERIA. There are three options for incorporating tectonic uplift: (1) continuous spatially uniform uplift over a specified time, (2) continuous, tilting uplift over a specified time, (3) spatially uniform, cyclic uplift with either a sinusoidal uplift, square wave uplift, or pulse uplift over the whole simulation time (Willgoose 2005a). Uplift is added to the change in elevation over time over each grid space.

Hancock and Willgoose (2001) and Dinwiddie and Walter (2008) have conducted validation studies for SIBERIA. Hancock and Willgoose (2001) performed a laboratory validation study using a landscape simulator box equipped with a rainfall simulator to erode the sediment and stereo digital photogrammetry to analyze the results. The photogrammetry was compared with 3D erosion predictions from SIBERIA. They found that "...the landscapes produced by SIBERIA are visually representative of what would occur for field scale watersheds."

Dinwiddie and Walter (2008) evaluated the predictions of three SIBERIA simulations for physically realistic and expected landscape evolution. Physical characteristics of slope angle, surface roughness, and magnitude of the coefficient of fluvial sediment transport (β_1) were evaluated relative to expected behavior, (1) more erosion should occur on steeper slopes than shallower slopes, (2) multidirectional, branching channelized erosion should occur on a rough slope, whereas unidirectional erosion should occur on a smooth slope, and (3) as the magnitude of the coefficient of fluvial sediment transport increases, erosion should also increase. Each expected result

was validated by comparing each to the 3D SIBERIA predictions. The erosion predictions indicated that SIBERIA adequately predicted erosion to the set expectations.

2.2.2.2 ARMOUR

The ARMOUR model (Sharmeen 2000) was developed for modeling surface armoring of the soil, erosion of the surface, and deposition of the eroded sediment (Willgoose and Sharmeen 2006). ARMOUR is driven by precipitation events and can model single events or multiple events over time allowing for time varying runoff and erosion.

The main part of the ARMOUR model, surface armoring, depends on the shear stress of flow moving over the surface. A schematic of the armoring process is shown in Fig. 2.3. Over time, as overland flow events occur, the surface soil layer becomes coarser than the underlying layer, a process called armoring (Willgoose and Sharmeen 2006). As flow passes over the surface, selective erosion of fine particles occurs, making the remaining fine particles more difficult to remove. Coarse particles within the soil help bind the remaining fines and form a desert pavement. Desert pavements are natural formations consisting of a surface layer comprised of closely packed gravel and fines that is one to two particles thick (McFadden et al. 1987).

The ARMOUR model extends this theory to unsteady flow conditions creating a surface armor that changes with time and varying runoff conditions (Sharmeen 2000). At any point in time, the concentration of particles in each size class constant over the depth of overland flow, but varies spatially. Simultaneous erosion and deposition cannot occur. Sediment flux is determined by the median diameter (d_{50}) of the sediment and both cohesive and non-cohesive sediment can be modeled.

Erosion, deposition, time varying runoff, and surface armor development in ARMOUR are calculated using shear stress mechanisms and a mass balance equation (Willgoose and Sharmeen 2006). The differential equations used in ARMOUR include a mass balance equation to determine the change in elevation over time and an equation to determine the potential rate of erosion or deposition for each size class of the surface material (Sharmeen 2000, Willgoose and Sharmeen 2006). ARMOUR is one-dimensional and uses the finite-difference method to solve the partial differential equations.

The mass balance equation in ARMOUR is:

$$\frac{\partial z}{\partial t} = \frac{\partial q_s}{\partial x} = \sum_k^M \frac{\partial q_{s, k}}{\partial x} \quad (2.11)$$

where z is the elevation, t is time, q_s is the sediment flux, M is the number of different size classes in the sediment mixture, k is the size class, and x is the position on the hillslope. The erosion or deposition potential is based on the size class and the availability of particles of that size class on the surface, and is defined by:

$$\frac{\partial P_k}{\partial x} = \left[\frac{\partial R_k}{\partial t} / \sum_j^M \frac{\partial R_j}{\partial t} \right] \frac{\partial q_s}{\partial x} \quad (2.12)$$

where P_k is the potential depth of material entrained/deposited in each size class, R_k is the rate of sediment entrainment or deposition for each size class, j is the node, and R_j is the rate of sediment entrainment or deposition at node j . Sediment transport is based on a size threshold of sediment entrainment based on the shear stress at the bottom of the flow (Willgoose and Sharmeen 2006).

Like SIBERIA, ARMOUR can simulate transport-limited and source-limited sediment transport processes. However, ARMOUR can track many different fractions of sediment trapped in overland flow, whereas SIBERIA can only track one sediment fraction (Willgoose 2005b).

Willgoose and Sharmeen (2006) used predictions from ARMOUR, field runoff and erosion data, concentration peaks of runoff events, and depletion of fines on the surface, to compare to results from rainfall simulator trials. ARMOUR was able to adequately replicate the rainfall simulator experiments after calibration.

2.2.2.3 CAESAR

The CAESAR landform evolution model (Coulthard et al. 1998, 1999, 2000) predicts fluvial erosion processes using a high-resolution rectangular grid (1 to 50 m). CAESAR has been applied to land use and climate change (Coulthard et al. 2000), sediment waves and alluvial fan evolution (Coulthard et al. 1999), large watersheds with large scale grids (400 km² watershed with 50 m grid spacing) (Coulthard and Macklin 2000), and time spans ranging from 10 to 10,000 years.

CAESAR is simplified by limiting overland flow to channels using the Chezy-Manning equation. Because interrill erosion is not modeled, Coulthard et al. (2000) recommend that CAESAR predictions be used qualitatively rather than quantitatively. Overland flow routing is performed cell-to-cell requiring any channel to be the width of the cell, making channel sizes unrealistic and either eliminating or making small rills very large.

Spatial variation in surface materials is not available, but multiple particle sizes may be routed through the watershed. The overland flow routing equation is:

$$Q=UA=\frac{1}{n}h^{2/3}\sqrt{SA} \quad (2.13)$$

where Q is the discharge, U is the flow velocity, A is the cross sectional area of the flow, n is Manning's coefficient, h is the flow depth, and S is the average downstream slope (Coulthard et al. 2002, Van De Wiel et al. 2007).

Sediment transport is determined by:

$$q_i = \frac{F_i U_*^3 W_i^*}{(s-1)g} \quad (2.14)$$

where q_i is the sediment transport rate for the i^{th} sediment fraction, F_i is the fractional volume of sediment in the active layer, U_* is the shear velocity, W_i^* is a function relating the fractional transport rate to the total transport rate, s is the ratio of sediment to water density, and g is gravimetric acceleration (Van De Wiel et al. 2007).

Unlike the other landform evolution models, CAESAR allows for divergent flow (e.g. alluvial fans, braided rivers). CAESAR also performs a grain-size sorting for deposition layers for up to nine grain sizes, along with soil creep and mass movement processes. Although some interrill erosion processes are modeled in CAESAR, Welsh et al. (2009) suggest that CAESAR should increase the level of slope process representation, especially for studies where hillslope processes are an essential and important part of the fluvial system. At small time scales, CAESAR is ineffective as it fails to incorporate long-term rock weathering, soil generation, and tectonic uplift processes (Coulthard 2001). Long run times are a major drawback to the high-resolution capabilities of CAESAR (Coulthard 2000).

Welsh et al. (2009) performed a validation study on CAESAR using two sub-watersheds in the French Alps from 1826 to 2005. The site has a long history of research focused on historical documentation of the geomorphology, land use, and environmental changes. The uncertainty of the records was ± 10 yr. Comparing CAESAR modeling and the decadal DTM patterns in two watersheds produced a broad similarity in the overall patterns of erosion, deposition, and sediment

discharge. Realistic simulations of the behavior of larger flood and sediment events at the decadal time scale were also found in the study by Welsh et al. (2009).

2.2.2.4 GOLEM

The GOLEM model (Tucker and Slingerland 1994) was developed for regional scale landform evolution processes and geologic time frames (100,000 to 10,000,000 years). GOLEM includes the erosion processes of overland flow, bedrock weathering, sediment transport, stream incision, slope failure, diffusive hillslope transport, and uplift (Tucker and Slingerland 1994). Two modes of operation are available for modeling erosion: watershed mode is used when hillslope-scale processes of weathering, soil creep, landslides, and channel initiation are desired; regional-scale mode operates for large-scale studies where channel evolution, but not individual hillslope processes are required. In either mode, GOLEM tracks the thickness of a surficial sediment layer and can handle multiple soil and rock types with varying resistance to erosion in either layers or regions.

GOLEM routes water over a rectangular grid. Spacing of the DTM is fixed to 1 km² for regional-scale mode and 50 m² for watershed mode. Water and sediment flow from each grid cell in the direction of the steepest slope to one of the eight surrounding cells. Sediment transport by overland flow is transport-limited, supply-limited, or a third case that uses transport and supply-limited sediment transport (e.g., channel incision and weathering). The continuity of mass equation that describes the changing elevation of the landform in GOLEM is:

$$\frac{\Delta h}{\Delta t} = \frac{Q_s^{(in)} - Q_s^{(out)}}{\Delta x^2} \quad (2.15)$$

where Δh is the change in the elevation of a cell, Δt is the change in time, Q_s is volumetric sediment flux in and out of the cell, and Δx^2 is the surface area of the cell.

The GOLEM model is different from SIBERIA and ARMOUR because GOLEM quantifies sediment production in terms of bedrock erosion. GOLEM also is limited to a single output time and a single grain size with sediment transport and deposition modeling. No validation studies on GOLEM were identified.

2.2.2.5 CASCADE

The CASCADE model (Braun and Sambridge 1997) was created for mountain-range scale and geological time scales (millions of years) with spatial resolution on the order of 1 km. CASCADE runs on fixed 100-yr time steps and uses a “bucket” algorithm to route water through the system using the finite-element method. The

“bucket” algorithm gives each node on the grid a set amount of water (a bucket) to convey along to the next lowest neighbor (i.e. the next node with the lowest elevation). Water is transferred until all nodes are connected by the flow paths. This simplified fluvial process should only be used for the low-resolution, large-scale, long-term simulations because CASCADE lacks the spatial resolution in SIBERIA, CAESAR, and CHILD.

CASCADE uses an irregular grid rather than the rectangular grid used in SIBERIA, ARMOUR, CAESAR, and GOLEM. Irregular grid spacing eliminates the directional bias that creates artificial symmetry invoked by rectangular grids (Braun and Sambridge 1997). Irregular grid spacing can also easily incorporate irregular watershed boundaries and spatial variability in resolution size, for instance a watershed with both flat and steep areas could have wide grid spacing in the flat land and dense grid spacing in the steep areas.

No validation studies for CASCADE were identified.

2.2.2.6 CHILD

The CHILD model (Tucker et al. 1997) is based on a short-term and event-based time scale (Coulthard 2001). Events are based on rainfall intensity and duration and drive the unsaturated flow model selected (four available). Storm events have been enlarged for larger time scales to incorporate several years of erosion and deposition into a single storm event. Enlarging a storm event consists of calibrating the event to the amount of erosion and deposition for a set time period. In this manner, an event can be many years in a simulation. The sediment transport rules, a meandering model, and overbank deposition are driven by the calculation of channel width and depth within each node.

The continuity of mass equation that drives sediment transport is:

$$\frac{dV_i}{dt} = \sum_{j=1}^{N_i} Q_{ji} \quad (2.16)$$

where i and j are nodes, V_i is the volume or mass stored at node i , t is time, N_i is the number of nodes connected to node i , and Q_{ji} is the total flux from node j to i (Tucker et al. 2001). The equation for changes in surface elevation due to erosion or deposition is:

$$\frac{dz_i}{dt} = \frac{(\sum_{j=1}^n Q_{sj}) - Q_{si}}{(1-v)A_i} \quad (2.17)$$

where z_i is the elevation at node i , t is time, n is the number of nodes flowing directly into i , Q_s is the sediment flux, v is the sediment porosity, and A_i is the Voronoi area of node i (Tucker et al. 1997). The equations for fluvial sediment transport (Eq. 2.16) and elevation change (Eq. 2.17) are solved using the finite-difference method across the irregular grid network.

CHILD can account for vegetative growth and allows user-specified grain sizes and can record the age of deposits to develop an alluvial stratigraphy within the model using the irregular grid network (Tucker et al. 1997). This elaborate fluvial system is more suited for shorter time periods because of its higher resolution; however CHILD has been used for simulations over millions of years.

The disadvantages of the CHILD model are the complexity of the grid which uses an irregular network with a Voronoi diagram and overall complexity of the code (Tucker et al. 2001). No validation studies for CHILD were identified.

3 METHODS

3.1 Reference Site – Grand Junction Uranium Mill Tailings Disposal Site

The Grand Junction Uranium Mill Tailings Disposal Site in Grand Junction, Colorado was used as a reference site for this study (DOE Office of Legacy Management 2009). The topographic map of the reference site is shown below in Fig. 3.1. The surface area of the disposal cell is approximately 390,000 m², the side slopes are 20% and range from 15 to 60 m long, and the top slope is 2% and ranges from 450 m to 770 m long. The depth of the tailings is approximately 22 m and the disposal cell is approximately 12 m above the original ground surface. The barrier slopes to the south and west. The existing topography was used as a base scenario. The footprint of the site and the total elevation change were held constant in all simulations. Modifications to the topography during modeling included changes to the slope and slope length.

3.1.1 Engineered Barriers

Two types of barriers were evaluated, a resistive barrier and a water balance barrier. The barrier profiles are shown in Fig. 3.2. The resistive barrier includes a compacted fine-textured soil barrier to control water and gas flow and is based on the barrier system employed in Grand Junction, CO (Benson et al. 2010). The water balance barrier stores water during wetter periods and then releases stored water through evaporation and transpiration (Benson et al. 2008), and is based on the final cover employed in Monticello, UT.

3.1.2 Materials

The surface layers were assumed to be topsoil, rip-rap, and topsoil blended with gravel (40% by weight), referred to herein as a gravel admixture.

The resistive barrier consisted of a surface layer, a bedding layer (only if rip-rap was used as the top layer), a frost protection layer, a radon barrier, and a transition layer. The bedding layer and transition layer were classified as poorly graded gravel. The frost protection layer and radon barrier were classified as clayey sand. A summary of the particle size characteristics assumed for the barrier materials is shown in Table 3.1. Material properties of surface layers, resistive barrier layers, water balance barrier layers, and waste (Benson et al. 2008 and 2010), Particle size fractions by Unified Soil Classification System. Organic matter by loss on ignition..

The water balance barrier consists of the top layer, a bedding layer (only if rip-rap is used), a water storage and frost protection layer, a biointrusion layer, and a sand layer (capillary break). The water storage and frost protection layers were assumed to be sandy silt, the animal intrusion layer was assumed to be poorly graded gravel with silt and sand, and the sand layer was assumed to be poorly graded sand.

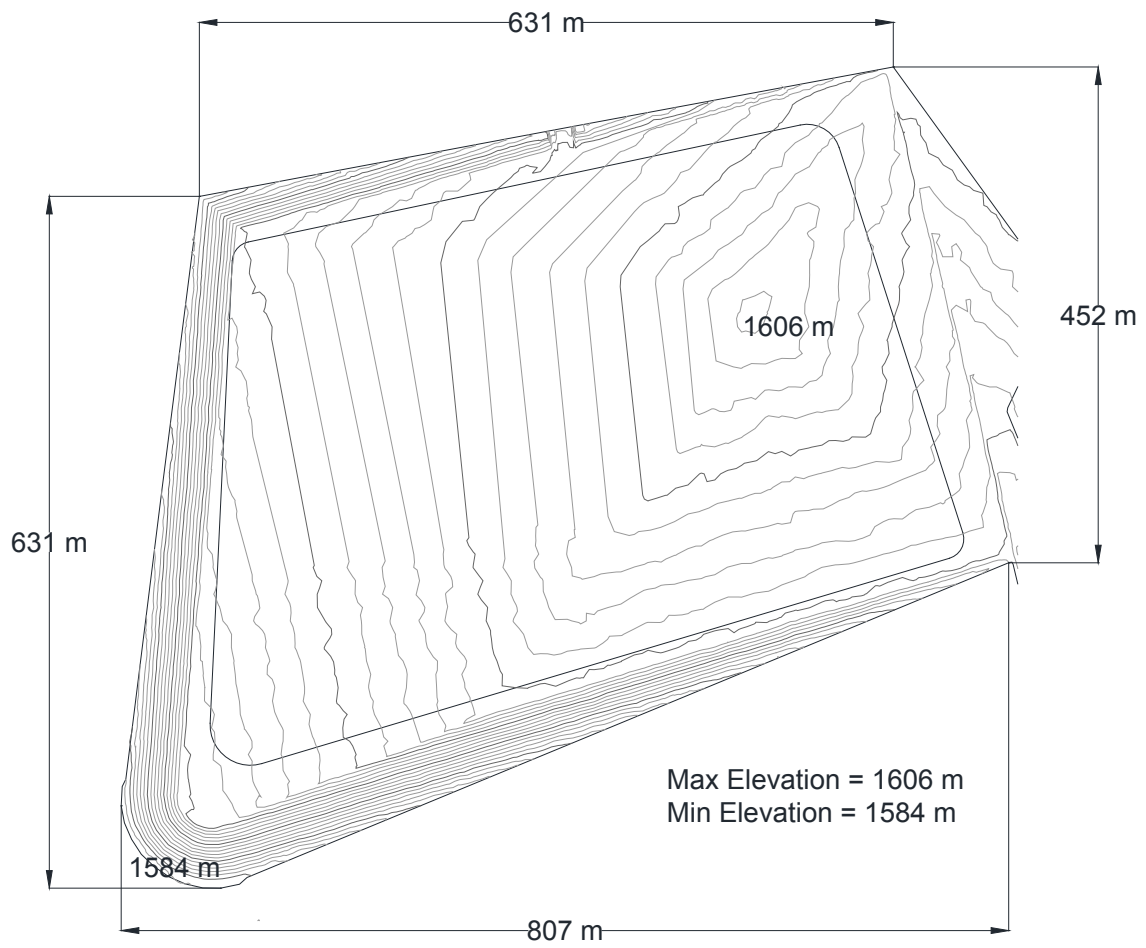


Fig. 3.1. Topography of Grand Junction Uranium Mill Tailings Disposal Site in Grand Junction, CO, the reference site for this study.

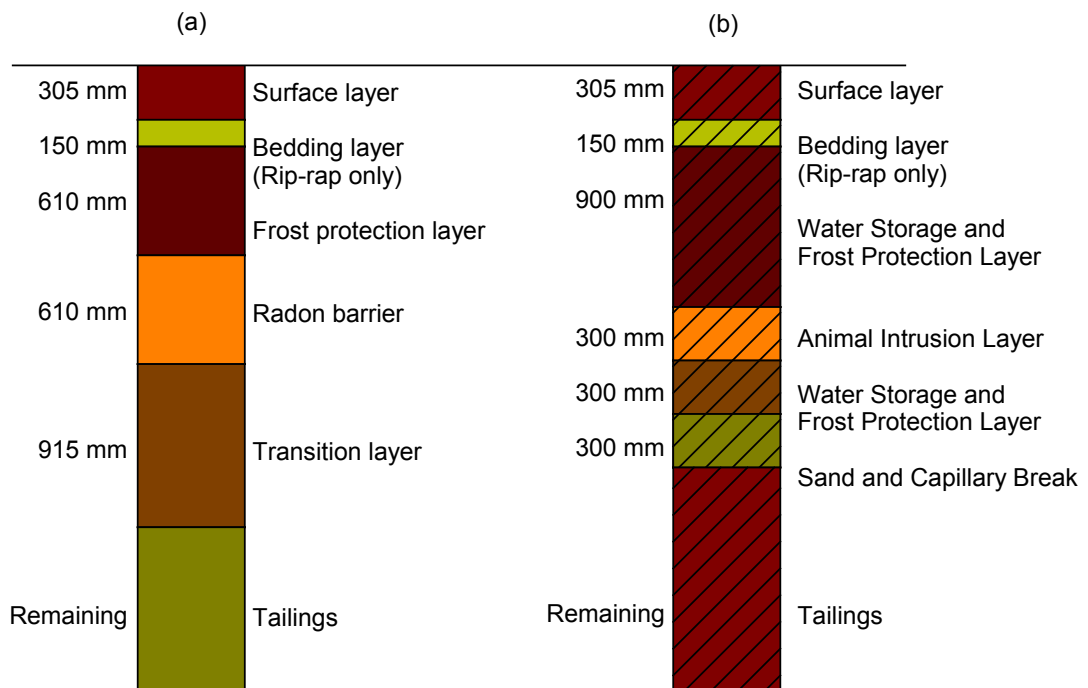


Fig. 3.2. Resistive barrier profile (a) and water balance barrier profile (b).

Particle size distributions assumed for the water balance barrier materials are summarized in Table 3.1.

The tailings were assumed to behave similar to silt and were assigned properties of Boardman silt (Boardman, OR) from the University of Wisconsin-Madison soil bank (Gurdal et al. 2003, Benson and Gurdal 2013).

Saturated and unsaturated hydraulic properties of the soils are summarized in Table 3.. Hydraulic conductivity and soil water characteristic curves (SWCC) of each soil were obtained from Benson et al. (2008, 2010). Methods described in Benson et al. (2007, 2011) were used to account for pedogenesis.

Van Genuchten's equation (1980) was used to describe the SWCC:

$$\theta = \theta_r + (\theta_s - \theta_r) \left[\frac{1}{[1 + (\alpha\psi)^n]^m} \right] \quad (3.1)$$

where θ is the volumetric water content at suction (ψ), θ_r is the residual volumetric water content, θ_s is the saturated volumetric water content, α and n are the van Genuchten parameters, and $m = 1 - 1/n$.

3.2 Modeling Erosion with SIBERIA

SIBERIA has high spatial resolution, the ability to model layers of different materials, and has been validation with field and laboratory experiments. Because of these characteristics, SIBERIA was used for predicting erosion.

The fluvial sediment transport equation is:

$$q_s = \beta_1 q^{m_1} S^{n_1} \quad (3.2)$$

where q_s is the sediment flux per unit width ($m^3/year/width$), q is the discharge per unit width ($m^3/year/width$), S is the slope in the steepest downhill direction (m/m), β_1 is the rate constant for sediment transport (dimensionless), and m_1 and n_1 are parameters of the model (dimensionless) (Willgoose et al. 1991a).

Table 3.1. Material properties of surface layers, resistive barrier layers, water balance barrier layers, and waste (Benson et al. 2008 and 2010). Particle size fractions by Unified Soil Classification System. Organic matter by loss on ignition.

Cover Section	Material Description	Particle Size Characteristics	Thickness (mm)	Dry Density (kg/m ³)	Particle Size Fractions (%)			Organic Matter (%)	
					Sand	Silt	Clay		
Surface Layers	Rip-rap	Poorly graded gravel with silt and sand	305	2700	20	10	0	70	0.01
	Gravel Admixture	Silty gravel with sand	305	2510	24	24	12	40	0.01
	Topsoil	Silty sand	305	1553	40	40	20	0	0.1
Resistive Cover Layers	Bedding Layer (Rip-rap surface only)	Poorly graded gravel	150	2338	3.3	0.1	3.3	93.3	0.01
	Frost Protection Layer	Clayey sand	610	2028	47.8	12.4	39.8	0	0.01
	Radon Barrier	Clayey sand	610	1865	45	11.6	43.4	0	0.01
	Transition Layer	Poorly graded gravel	915	1234	3.3	0.1	3.3	93.3	0.01
Water Balance Cover Layers Waste	Bedding Layer (Rip-rap surface only)	Poorly graded gravel	150	2338	3.3	0.1	3.3	93.3	0.01
	Water Storage and Frost Protection Layer	Sandy elastic silt	900	1443	22.3	49	25.8	2.9	1.5
	Animal Intrusion Layer	Poorly graded gravel with silt and sand	300	2510	20	10	0	70	0.01
	Water Storage and Frost Protection Layer	Sandy elastic silt	300	1443	22.3	49	25.8	2.9	1.5
	Sand Layer and Capillary Break	Poorly graded sand	300	1551	85	5	0	10	0.01
Tailings	Silt	Remaining	1404	10	85	5	0	0.01	

Table 3.2. Hydraulic properties used in the hydraulic modeling portion of this study.

Cover Section	Material Description	Saturated hydraulic conductivity, K_s (m/d)	SWCC van Genuchten Parameters				
			θ_r	θ_s	α (kPa ⁻¹)	n	
Surface Layers	Rip-rap	10800	0.04	0.40	0.60	1.40	
	Gravel Admixture	0.86	0.04	0.40	0.03	1.26	
	Topsoil	0.86	0.04	0.40	0.02	1.27	
Resistive Cover Layers	Bedding Layer	130	0.05	0.25	0.44	1.36	
	Frost Protection Layer	0.055	0.00	0.38	0.04	1.30	
	Radon Barrier	0.055	0.00	0.38	0.04	1.30	
	Transition Layer	108	0.06	0.25	0.57	1.36	
	Bedding Layer	130	0.05	0.25	0.44	1.36	
Water Balance Cover Layers	Water Storage and Frost Protection Layer	0.13	0.00	0.41	0.03	1.27	
	Animal Intrusion Layer	0.13	0.00	0.41	0.03	1.27	
	Sand Layer and Capillary Break	130	0.05	0.25	0.44	1.36	
Waste	Tailings	0.043	0.00	0.99	0.02	1.30	

The fluvial sediment transport equation can be parameterized using field data or a validated computational erosion model. Field calibration consists of fitting the parameters β_1 , m_1 , and n_1 to site-specific and soil-specific sediment transport and hydrology data from natural rainfall events or a rainfall simulator. This method is data intensive and is described in detail by Willgoose and Riley (1998) and Hancock et al. (2000). SIBERIA can also be calibrated using another erosion model to determine a target erosion rate for the site. A previously validated model such as RUSLE2, CREAMS, or WEPP can be used for this method (Willgoose, personal communication, 2010).

3.2.1 Parameterization

SIBERIA has been successfully parameterized and run for many sites in Australia and Argentina. Table 3.3 summarizes parameterization methods, the fluvial erosion parameters, and erosion depths from several from several sites simulated with SIBERIA, and input and control parameters used in SIBERIA.

The fluvial sediment transport parameters in SIBERIA (Eq. 2.9) were obtained by matching erosion rates predicted by SIBERIA to average erosion rates predicted by WEPP. WEPP was used in this study to calibrate SIBERIA because it is mechanistic and input parameters for WEPP are readily available. Multiple slope lengths with the slope width equal to the grid spacing (10 m) used in SIBERIA were simulated with WEPP to determine the average annual soil loss and average annual runoff for the site. Slope lengths were varied in the WEPP simulations to represent the different slope lengths of the top (450 m to 770 m) and side slopes (15 m to 60 m).

When multiple layers are modeled in SIBERIA, each layer is assigned a unique β_1 , whereas the same m_1 and n_1 are used to represent the entire barrier. SIBERIA parameters m_1 and n_1 were calibrated to the surface layer. The fluvial sediment transport parameters are summarized in Table 3.4 (resistive barrier) and Table 3.5 (water balance barrier).

The following steps were followed to obtain the fluvial erosion parameters m_1 and n_1 : (1) WEPP was run for an individual soil layer, (2) the predicted average annual runoff rate and sediment loss were recorded for 2% and 20% slopes with varying slope lengths found on the reference site (15 to 770 m), (3) the erosion rate was computed from eroded depth over the slope, the bulk density of the soil, and the area, and (4) the m_1 and n_1 parameters were obtained by fitting the \log_{10} transform of Eq. 3.2 to WEPP predictions of q and q_s using linear regression:

$$\log q_s = \log \beta_1 \cdot m_1 \log q \cdot n_1 \log S \quad (3.3)$$

Table 3.3. Summary of parameterization and SIBERIA simulations in the literature.

Site	Site Characteristics	Soil Characteristics	Calibration/Parameter selection	Parameter Values			Grid Spacing	Watershed Size	Years Simulated	Erosion Rate	Source/Citation
				β_1	m_1	n_1					
Waste rock dump and pit, Nabarlek uranium mine, Northern Territory, Australia	Short, high intensity storms. Wet-dry tropical environment. Annual rainfall of 1400 mm.	Armour of coarse material with negligible vegetation cover.	Used the ERA Ranger Mine and the Jabliuka project sediment loss and runoff data from rainfall simulator experiments.	24463	2.52	0.69	12 m	36 km ²	1000	0.281 mm/yr maximum erosion depth	Hancock et al. (2008)
Airstrip, Nabarlek uranium mine, Northern Territory, Australia	Annual rainfall of 1400 mm.	All-weather bitumen surface surrounded by bare, compacted soil, no vegetative cover.	rainfall simulator experiments.	22899	2.24	0.69	12 m	36 km ²	1000	0.145 mm/yr maximum erosion depth	Hancock et al. (2008)
Tin Camp Creek Catchment 1 (C1), western Arnhem Land, Northern Territory, Australia	Representation of the pre-mined Ranger Mine site. Short, high intensity storms. Average annual rainfall is 1400 mm.	Red, loamy material and shallow gravely lam with some micaceous silty yellow earths.	Sediment loss, rainfall, and runoff field data for discrete rainfall events were used to calibrate the erosion and hydrology models.	1067	1.7	0.69	10 m	2032 m ²	10,000	0.16 mm/yr maximum erosion depth	Hancock et al. (2010)
Tin Camp Creek Catchment 2 (C2), western Arnhem Land, Northern Territory, Australia	Slopes are generally 15 to 50%. Vegetation is annual grasses in the wet	Minor solodic soils on alluvial flats. Gravely cobble quartz lag on slope surfaces and hill crests.	the erosion and hydrology models.	384	1.69	0.69	10 m	2947 m ²	10,000	0.064 mm/yr maximum erosion depth	Hancock et al. (2010)
Section 6, Tom Price mine, NW Western Australia	No vegetation. Average annual rainfall of 281 mm.	Rocky spoil mainly comprised of hematite. Different particle size distributions due to mechanical processes of blasting, handling,	Sediment concentration data from rainfall simulator experiments was used to calibrate the sediment discharge equation.	0.0007	2.53	2.67	10 m	1 km ²	100	20 tonnes/ha/yr	Hancock et al. (2003)
Section 10 East, Parraburdo, NW Western Australia	Average annual rainfall of 281 mm.			0.075	1.11	1.5		0.94 km ²		20 tonnes/ha/yr	Hancock et al. (2003)

Table 3.3. Summary of parameterization and SIBERIA simulations in the literature (continued).

Site	Site Characteristics	Soil Characteristics	Calibration/Parameter selection	Parameter Values			Grid Spacing	Watershed Size	Years Simulated	Erosion Rate	Source/Citation
				β_1	m_1	n_1					
Xstrata Alumbreira copper mine, Argentina	High rainfall (400 mm/year). Arid climate. Evaporation rate = 1385 mm/year. Intense storms. Low Rainfall/Low Incision (160 mm/year) Low Rainfall/High Incision (160 mm/year)	Benign waste rock dumped to create a rough humpy surface. Humps range in height from 2 to 3m.	Data from Sheridan et. al. using the particle size distributions of the soil and spoil materials were used in calibration to provide a range of values for β_1 , m_1 , and n_1 .	0.00225	1.5	2.1	2 m	0.25 km ²	1000	8.09 m maximum erosion depth	Hancock and Turley (2006)
				0.00075	1.5	2.1				Not available	
				0.00075	2.0	2.1				3.28 m maximum erosion depth	
ERA Ranger Mine, Northern Territory, Australia	Waste rock dump cover, unvegetated, unrippled. High intensity storms (973-1480 mm/year). Average slope of 2.8%. Waste rock dump cover, vegetated, ripped. High intensity storms (973-1480 mm/year). Vegetated with low shrubs and grasses. Average slope of 1.2%.	Fine material overlying a hard pan-like surface which developed cracks during the prolonged dry season. Top-soiled, surface ripped and revegetated area.	Data from natural storm events was used in the DISTFW rainfall-runoff model to determine long term average parameters for SIBERIA.	0.00027	1.59	0.69	30 m	1.6 km ²	1000	7.6 m maximum erosion depth	Evans and Willgoose (2000)
				0.000005	1.59	0.69				2.4 m maximum erosion depth	
Scinto 6 mine, ERA Ranger Mine, Northern Territory, Australia	High intensity storms (973-1480 mm/year). 52-58% batter slope. Vegetation had little effect on hydrology.	Dumped, precambrian volcanic waste rock.	Rainfall, runoff, and sediment data were measured from 9 actual rainfall events on site. This data was used to parameterize the DISTFW rainfall-runoff model which was used to derive long-term average parameters for SIBERIA.	0.003	1.68	0.69	0.5 m	1600 m ²	50	0.45 mm maximum erosion depth	Hancock et al. (2000)

Table 3.4. Fluvial sediment transport parameters for resistive barriers used in the SIBERIA simulations.

Resistive Covers		Semi Arid - Big Mountain			Humid - Bluestem Prairie		
Surface Layer	Material	β_1	m_1	n_1	β_1	m_1	n_1
Rip-rap	Vegetated Rip-rap	0.00200	1.201	4.166	0.00014	1.114	0.698
	Bedding Layer	2.10000			0.0299		
	Frost Protection Layer	1.84000			0.0223		
	Radon Barrier	7.30000			0.0620		
	Transition Layer	2.10000			0.0299		
	Tailings	1.05000			0.0175		
Gravel Admixture	Vegetated Gravel Admixture	0.0050	1.205	4.586	0.00008	1.265	0.789
	Frost Protection Layer	4.29000			0.00984		
	Radon Barrier	17.5000			0.02400		
	Transition Layer	4.90000			0.01345		
	Tailings	2.42000			0.00763		
Topsoil	Vegetated Topsoil	6.000E-11	4.651	3.925	5.70E-05	1.416	1.045
	Frost Protection Layer	2.170E-09			0.00403		
	Radon Barrier	2.980E-09			0.00828		
	Transition Layer	2.390E-09			0.0055		
	Tailings	1.220E-09			0.00313		

Table 3.5. Fluvial sediment transport parameters for water balance barriers used in SIBERIA simulations.

Water Balance Covers		Semi Arid - Big Mountain			Humid - Bluestem Prairie		
Surface Layer	Material	β_1	m_1	n_1	β_1	m_1	n_1
Rip-rap	Vegetated Rip-rap	0.002	1.201	4.166	0.00014	1.114	0.698
	Bedding Layer	2.1			0.0299		
	Water Storage/Frost Protection	1.59			0.0176		
	Animal Intrusion	0.91			0.0178		
	Water Storage/Frost Protection	1.59			0.0176		
Gravel Admixture	Sand and Capillary Break	0.14			0.00385		
	Tailings	1.05			0.0175		
	Vegetated Gravel Admixture	0.005	1.205	4.586	0.00008	1.265	0.789
	Water Storage/Frost Protection	3.7			0.00771		
	Animal Intrusion	2.1			0.00778		
Topsoil	Water Storage/Frost Protection	3.7			0.00771		
	Sand and Capillary Break	0.32			0.0019		
	Tailings	2.42			0.00763		
	Vegetated Topsoil	6.000E-10	4.651	3.925	5.70E-05	1.416	1.045
	Water Storage/Frost Protection	1.88E-09			0.00316		
Topsoil	Animal Intrusion	1.05E-09			0.00319		
	Water Storage/Frost Protection	1.88E-09			0.00316		
	Sand and Capillary Break	1.57E-10			0.00089		
	Tailings	1.220E-09			0.00313		

Multiple linear regressions were conducted using SYSTAT12 (Systat Software, Inc., Chicago, IL) to obtain unique m_1 and n_1 parameters for each soil type and climate.

To calibrate the β_1 parameter, WEPP and SIBERIA need to produce the same average erosion rate for a simple slope. The average slope from the reference site was used with the width equal to the grid spacing of the DTM (11% slope, 10 m wide). WEPP was run using 60 yr simulations, the minimum required to quantify erosional response to $\pm 10\%$ (Nearing 2004). The average erosion rate was compiled as the product of the average sediment loss and time divided by the bulk density. SIBERIA was then run with the same simple slope. The β_1 fluvial erosion parameter was systematically modified so that the SIBERIA average erosion rate was equal to the WEPP average erosion rate. This process was used to obtain the fluvial sediment transport parameters for the 12 soil types for both semi-arid and humid climates.

Soil types were defined in WEPP using percent sand, percent clay, percent rock, organic content, and depth of each layer to represent all soils used in the barrier scenarios. The soil properties used in WEPP are in Table 3.1. Cation exchange capacity (CEC) can also be input to WEPP, but was not available for the various soil types in this study. Thus, CEC was held constant at 8.0 meq/100 g to represent soil with a high sand content and low water holding capacity (Holtz and Kovacs 1981).

A sensitivity analysis on the soil albedo and initial water content showed that neither had a significant effect on predicted discharge or sediment flux, so both were held constant for each soil type (Appendix A). Albedo was set at the mean albedo of the earth, 0.36. Initial water content was set at 17%, the average water content of each soil layer, measured previously by Benson et al. (2008, 2010). The sites include the reference site and another disposal facility in Monticello, UT that employs the water balance barrier used in this study. The interrill erodibility, rill erodibility, critical shear, and effective hydraulic conductivity WEPP input parameters were estimated by WEPP based on the particle size distribution for use in the calculations for discharge and sediment flux.

Weather data for two sites were generated by the CLIGEN weather generator in WEPP (Flanagan and Nearing 1995) for use in the WEPP simulations. These sites were calibrated using meteorological data from the Grand Junction WB AP CO (Grand Junction, CO) and the Pittsburgh WB AP 2 PA (Pittsburgh, PA) stations in the National Climatic Data Center. The sites were chosen because of nearby existing disposal sites for uranium mill tailings and their representation of semi-arid (Grand Junction, CO) and humid (Pittsburgh, PA) climates.

3.2.2 DTM Formulation using SIBERIA

A digital terrain model (DTM) was created for SIBERIA by (1) saving an AutoCAD drawing (.dwg) that includes site topographic information as a .dxf file, (2) using the EAMS MOSCOW interface to select the .dxf file to turn into a DTM, (3) enter the coordinates to be gridded, and (4) enter the desired spacing between nodes. This process outputs a DTM in the form of a grid.raw file for using site topography in SIBERIA.

3.2.3 SIBERIA Inputs and Control Parameters

The SIBERIA inputs include the topography in the form of a DTM, soil types with their unique β_1 parameters and layer depths, the m_1 and n_1 parameters of the surface layer, the bulk density of the surface layer, and the USLE barrier factor. The barrier factor from USLE was used to account for varying particle sizes on the surface (i.e. rip-rap, gravel admixture, and topsoil). The barrier factor was calculated by:

$$C = \exp(-bf_g) \quad (3.4)$$

where C is the barrier factor (USLE), b is the coefficient that describes the relative effectiveness of the ground barrier, and f_g is the percent ground barrier (Toy et al. 1998, USDA-ARS 2008). Vegetation was accounted for when calibrating the fluvial sediment transport parameters β_1 , m_1 , and n_1 , using WEPP.

SIBERIA also requires control parameters to define the duration of the simulation, time period between outputs, erosion file output, time step, and mode for running the erosion, runoff, and sediment transport models. The duration of the simulation was set to 1000 yr to be consistent with the design life for disposal facilities for low-level radioactive waste (US EPA 1983). Output was selected for 1, 5, 10, 30, 60, 100, 500, and 1000 yr to obtain estimates of when and where erosion occurs. The modes used for erosion, runoff, and sediment transport are in Table 3. and account for the layered system defined in the layer.model file. Steps for running SIBERIA are outlined in Appendix H, the layer.model file is described in Appendix I, and the sample siberia.setup file is in Appendix J.

3.3 SVFLUX

Hydraulic modeling was conducted with the variably saturated flow model SVFLUX, which Bohnhoff et al. (2009) provides reliable hydrological predictions for covers when parameterized realistically. The resistive and water balance barriers described in Section 3.1.1 were used as the base profiles. The surface layer was changed for each simulation to evaluate how the differences between surface layer materials affect hydrology. SVFLUX simulations were run for both semi-arid (Grand Junction, CO) and humid (Pittsburgh, PA) climates. SVFLUX input includes climate, vegetation, and soil data.

Table 3.6. SIBERIA input and control parameters for erosion, runoff and sediment transport.

Parameter Type	SIBERIA Description	Parameter Description	Value
Run Parameters	Duration of simulation (years)	Years of simulation from beginning to end	1000
	Time step (years)	The resolution used within SIBERIA	0.01
	Period between output of diagnostic statistics (years)	Time period between output of summary statistics to the DOS window	100
	Times of erosion output	Time in years of when erosion files are output	1, 5, 10, 30, 60, 100, 500, and 1000
Erosion Parameters	Mode for Sediment Transport Model	The default fluvial erosion model where parameters β_1 , m_1 , and n_1 are spatially constant and the layer.model file is used	4
	Input File: Sediment Transport Model	The input file for the layer β_1 and depth specifications	File: layer.model
	Coefficient of the fluvial transport relationship	β_1 for the soil layer	Varies by material
	Exponent on discharge in the fluvial transport relationship	m_1 for the surface layer	Varies by material
	Exponent on slope in the fluvial transport relationship	n_1 for the surface layer	Varies by material
	Bulk density of the soil	Bulk density of the surface layer (tonnes/m ³)	Varies by material
	Cover factor	USLE's Cover factor used to differentiate between particle sizes	Varies by material
Hydrology Parameters	Mode for Runoff Model	Spatially constant fluvial erosion	0
Advanced Parameters #2	Mode for Sediment Transport Solver	Solution method of the physical transport equation where the layer.model file is used	8

SVFLUX solves Richards' equation, the governing partial differential equation for unsaturated flow:

$$\frac{\partial \theta}{\partial t} = \frac{-\partial}{\partial z} \left[K_{\psi z} \frac{\partial \Psi}{\partial z} \right] + \frac{\partial K_{c\psi}}{\partial z} + \frac{\partial}{\partial z} \left[-K_v \frac{\partial \Psi}{\partial z} \right] \quad (3.5)$$

where θ is volumetric water content, t is time, $K_{\psi z}$ is hydraulic conductivity, Ψ is matric suction, z is the vertical component, K_v is the diffusive conductivity, and $K_{c\psi}$ is the total water conductivity (hydraulic conductivity + diffusive conductivity).

SVFLUX simulations were conducted using a typical precipitation year and the maximum precipitation year for each climate. The typical precipitation year was defined as the year having annual precipitation as close as possible to the average annual precipitation (1969 in Grand Junction, 231 mm; 2010 in Pittsburgh, 961 mm). The maximum precipitation year was defined as the year with the maximum annual precipitation (1965 in Grand Junction, 382 mm; 2004 in Pittsburgh, 1458 mm). Daily data were obtained for precipitation, temperature, and wind speed from the High Plains Regional Climate Center and the Northeast Regional Climate Center (HPRCC and NRCC 2011).

Precipitation was assumed to begin at 12 hr and end at 19.2 hr on days with rainfall events. Daily average solar radiation, wind speed, relative humidity, and temperature were used in conjunction with the Penman method (Penman 1948) to define potential evaporation. Actual evaporation was defined by the Wilson-Penman equation (Wilson et al. 1994).

Mountain Big Sagebrush was assumed to be the prominent vegetation in the semi-arid climate and Bluestem Prairie Grass was assumed to be the prominent vegetation in the humid climate. The vegetation parameters input into SVFLUX are in Table 3.. The leaf area index (LAI), plant limiting factor, and potential root uptake were specified for both vegetation types (Table 3.) (Kirkham 2005, Klett et al. 2010, White 2010, USDA-Bureau of Reclamation 2011). In SVFLUX, the LAI was generated using the dates for the start of germination and the date when plants cease to transpire. The LAI was set to excellent growth giving a maximum LAI of 3 during the peak of the growing season. The plant limiting factor was generated using the moisture wilting point and the moisture limiting point for the plant based on the climate (Benson 2011). The potential root uptake (depth where roots can extract water) was specified as 2 m.

The saturated hydraulic conductivity, residual and saturated volumetric water content, and van Genuchten's α , n , and m parameters input to SVFLUX are in Table 3..

Table 3.7. Vegetation parameter input to SVFLUX.

SVFLUX Vegetation Parameter	Units	Mountain Big Sagebrush	Bluestem Prairie	Source
Growing season start date	day	120	114	Allen (2010), Klett et al. (2010), Grand Valley Project (2011)
Growing season end date	day	310	280	
Wilting point	kPa	-4000	-1500	Benson (2011), Kirkham (2005)
Limiting point	kPa	-1000	-800	
Max. root depth	m	2	2	
Max Leaf Area Index (LAI)	--	3	3	Foster et al. (1995)

A one-dimensional simulation was conducted for each case using the profile shown in Fig. 3.2. To minimize the impact of the unit gradient boundary at the lower boundary, the tailings layer was assumed to be 5 m thick. Sensitivity analysis indicated that a thicker tailings layer had no impact on the solution. The upper boundary was assigned as a climatic flux boundary. The typical year climate data were applied each year for the first 3 to 5 yr until a steady condition was reached (i.e. initial conditions no longer affected predictions). The maximum precipitation year was then applied for one year.

4 RESULTS AND DISCUSSION

4.1 Effect of Type of Surface Layer on Erosion

Vegetated rip-rap, topsoil, and gravel admixture surfaces were simulated to determine how type of surface layer affects erosion. Each surface was simulated in semi-arid and humid climates using resistive and water balance barriers. Topography representative of the Grand Junction, CO site was used for all simulations as a base topography so that surface layer effects could be compared while keeping site topography constant.

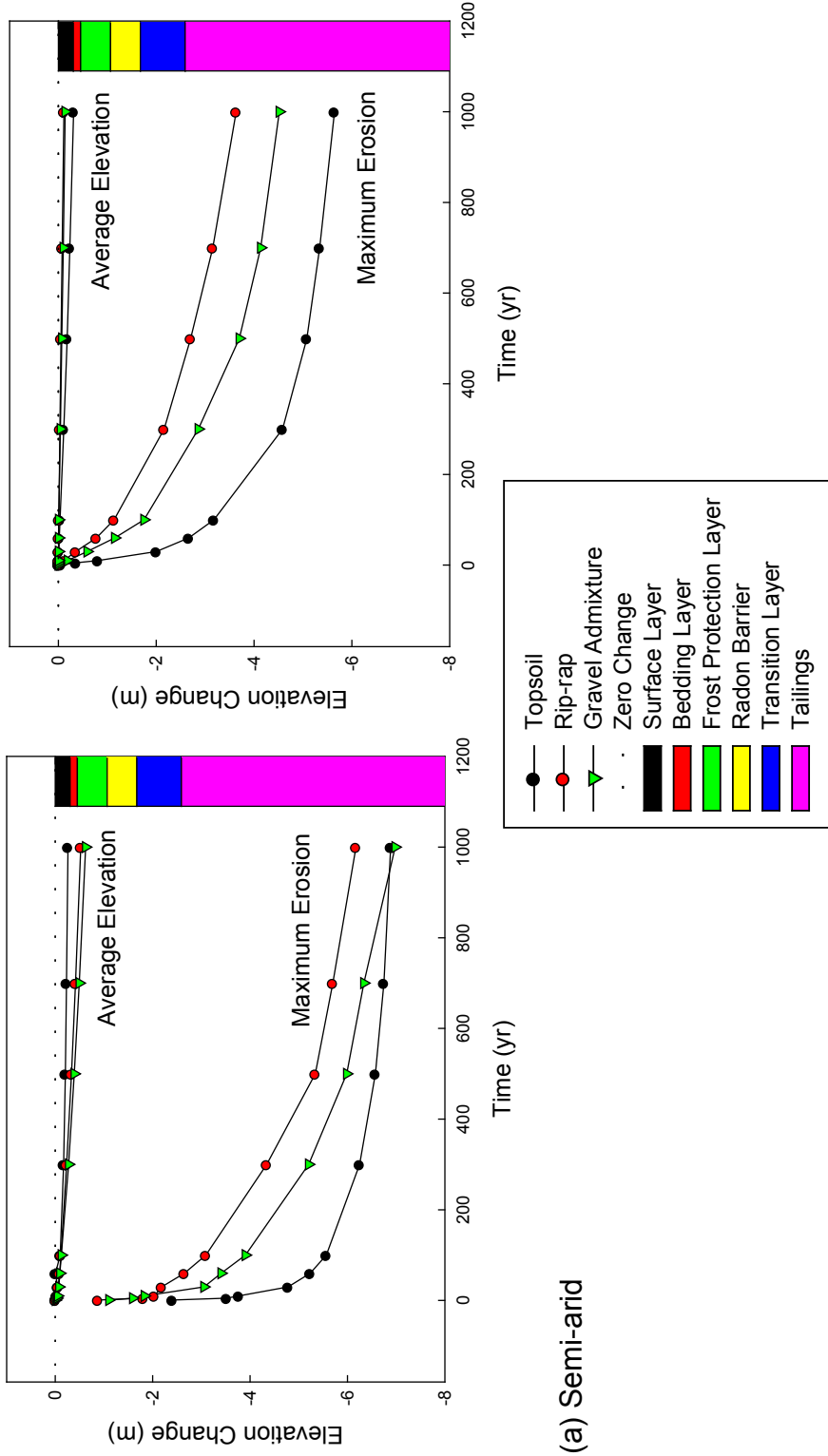
Predictions of maximum erosion and average elevation for a resistive barrier with rip-rap, topsoil, and gravel admixture surface layers are shown in Fig. 4.1. Predictions for semi-arid and humid climates are shown in Fig. 4.1 (a) and (b), respectively. The following nomenclature is defined as follows:

- Maximum erosion corresponds to the maximum depth of erosion for any node over the DTM. Maximum erosion can occur at one node or at multiple nodes. Maximum erosion indicates the greatest depth of erosion predicted for the site.
- Average elevation is the average elevation for each node on the DTM. Average elevation is a good indication of the average amount of erosion that is occurring over the site.

These definitions of maximum erosion and average elevation are used throughout this report. Predictions are shown for up to 1000 yr, which is the minimum design life for LLRW disposal facilities.

The relative magnitudes of maximum erosion between the surface layer types in Fig. 4.1 indicate that a rip-rap surface layer produces less maximum erosion over a 1000-yr period than the topsoil and gravel admixture surface layers in either climate. In both semi-arid and humid climates, all surfaces had a similar average elevation. However, maximum erosion evolved more rapidly with the topsoil surface, less rapidly for the gravel admixture surface, and slowest for the rip-rap surface.

Once the erosion level is below the surface layer (the only layer varied between simulations) erosion should occur at the same rate. However, Fig. 4.1 shows that erosion occurs at different rates for the same layers beneath the surface. This difference is due to the calibrated fluvial erosion parameters, m_1 and n_1 . Although a unique β_1 parameter is used for each layer, the same m_1 and n_1 must be applied to each layer. This is a limitation of the SIBERIA model when evaluating layered soil systems. Thus the layers below the surface are eroded by the same processes as the surface layer regardless of their own soil properties.



(a) Semi-arid

Fig. 4.1. Maximum erosion and average elevation predicted by SIBERIA for the reference site with a resistive barrier comparing rip-rap, topsoil, and gravel admixture surface layers: (a) semi-arid climate and (b) humid climate.

A 3D depiction of surface elevation at 1000 yr of erosion is shown in Fig. 4.2 for (a) rip-rap, (b) gravel admixture, and (c) topsoil surface layers. The gravel admixture surface and the rip-rap surface show no gullies and little visible erosion. Erosion of the topsoil surface shows gully formation as the primary source of erosion. The scale is exaggerated to 20V:1H to magnify the elevation change, which causes the base of the slope to have vertical yellow or black streaks. These streaks are an artifact of the graphics software used to prepare the images and should be ignored.

A plan view of the (a) rip-rap, (b) gravel admixture, and (c) topsoil surfaces is shown in Fig. 4.3 in terms of the number of layers remaining intact on the barrier. There are eight layers shown, with five layers for the barrier, one for the tailings, and two deposition layers. One layer remaining intact (red on the scale) means that the tailings layer has been partially eroded. Six layers remaining intact (green on the scale) indicates that none of the layers in the barrier has been fully penetrated. Eight layers intact (blue on the scale) indicates deposits of eroded material above the original surface of the cover.

The processes that drive erosion are determined by the calibrated fluvial erosion parameters, m_1 and n_1 (Kirkby 1971 and Hancock 2004). Table 4.1 shows the m_1 and n_1 input to the model and the erosion processes predicted for each climate and surface layer type. The erosion predictions from Fig. 4.2 and Fig. 4.3 follow the erosion process outlined from Kirkby (1971), with rip-rap and gravel admixture surfaces having soil wash erosion and deep gully formation in the topsoil surface. For the rip-rap and gravel admixture surface layers, erosion occurs only in the side slopes and over the entire side slope as soil wash (not in defined gullies). The plan view of the gravel admixture surface, Fig. 4.3 (b), shows a similar erosion pattern as the rip-rap surface, but erosion occurs over a slightly larger in area. The plan view of the topsoil surface, Fig. 4.3 (c), shows that gully erosion occurs rather than soil wash. The maximum erosion depth for the topsoil surface is the same as the maximum erosion depth for the gravel admixture surface.

The surface layers with larger particle sizes have the least maximum erosion. As particles sizes get smaller with the gravel admixture (40% gravel and 60% topsoil) and topsoil surfaces, the erosion depth increases, with the greatest depth in the cover with a topsoil surface.

4.1.1 Influence of Climate and Vegetation on Erosion

Predictions of surface elevation for the rip-rap and gravel admixture surface layers in a humid climate are shown in Fig. 4.4. In contrast to the soil wash erosion in the semi-arid climate (Fig. 4.3, Fig. 4.4), rip-rap and gravel admixture surfaces erode in gullies. Erosion occurs in similar locations, on the side slopes and across the nickpoint into the top slope, but the erosion depth is greater in the gravel admixture surface (Fig. 4.1).

Semi-Arid Climate

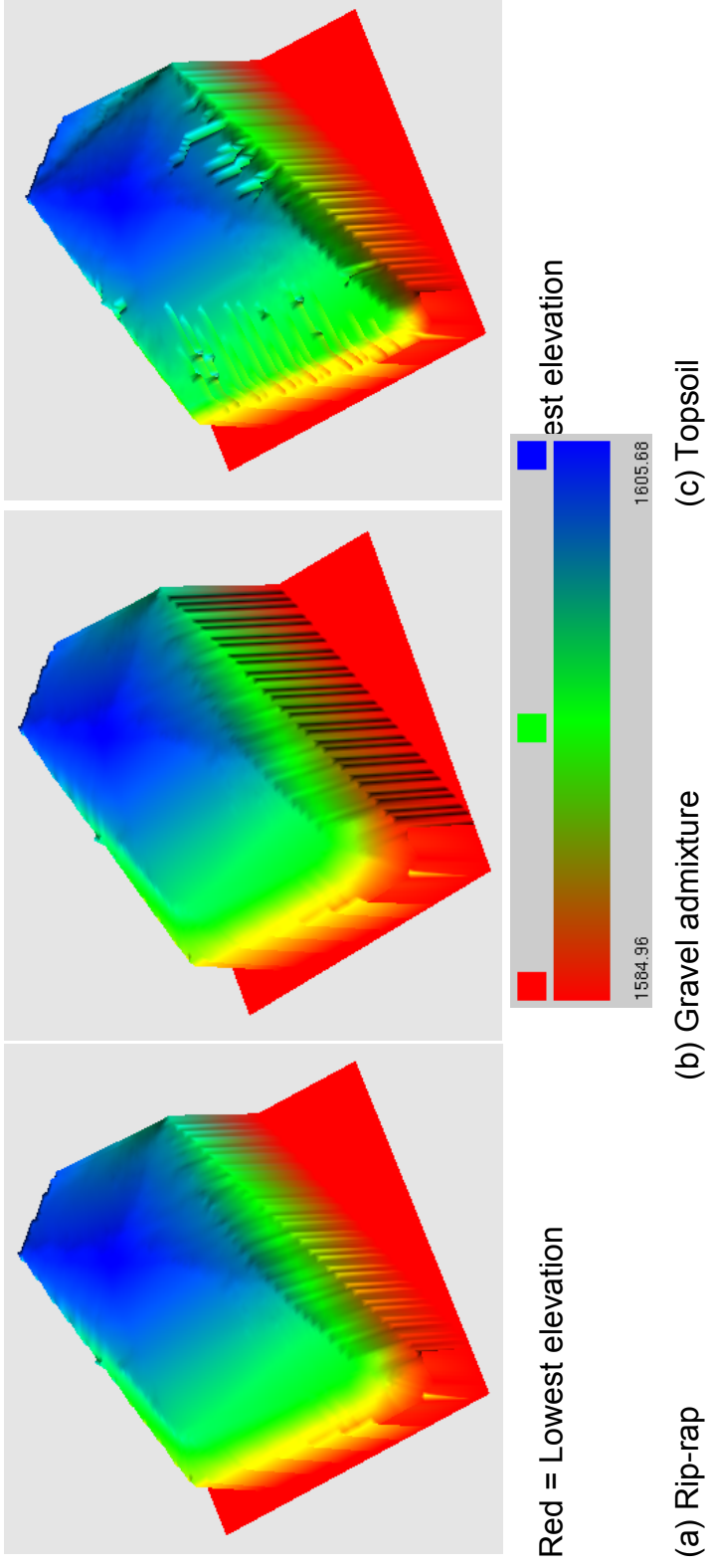


Fig. 4.2. Elevation predicted for reference site with SIBERIA for a resistive barrier in a semi-arid climate: (a) rip-rap surface layer, (b) gravel admixture surface layer, and (c) topsoil surface layer. Elevation is shown in m and denoted by the color bar above.

Table 4.1. Erosion process for fluvial erosion parameters m_1 and n_1 based on climate and surface layer type.

Climate	Surface Layer	m_1	n_1	Erosion Process (Kirkby 1971)
Semi-Arid Climate	Rip-rap	1.201	4.166	Soil wash with gullyng
	Gravel Admixture	1.205	4.586	Soil wash with gullyng
	Topsoil	4.651	3.925	Gullyng
Humid Climate	Rip-rap	1.114	0.698	Soil wash on an armored surface
	Gravel Admixture	1.265	0.789	Soil wash on an armored surface
	Topsoil	1.416	1.045	Soil wash

Semi-Arid Climate

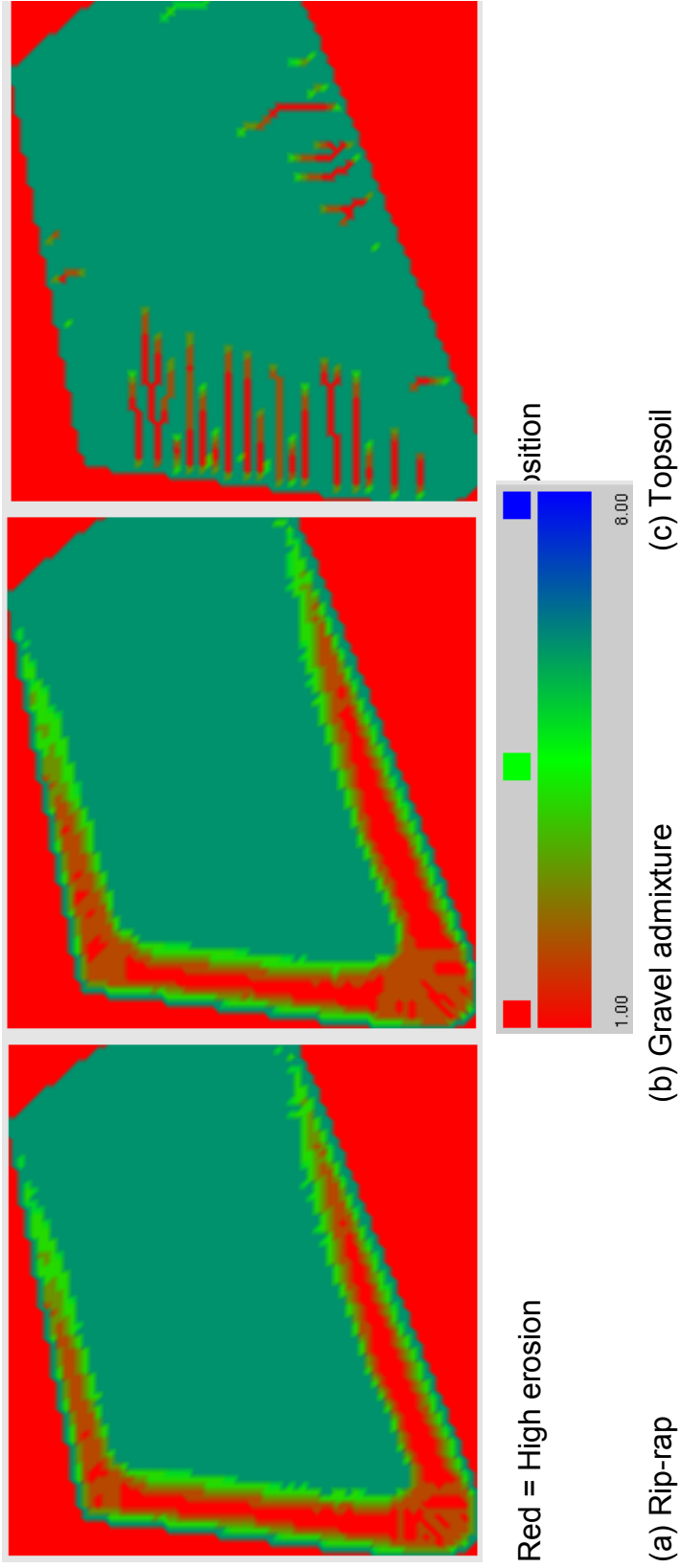


Fig. 4.3. Plan view of reference site with a resistive barrier in a semi-arid climate showing number of layers remaining intact across surface as predicted by SIBERIA: (a) rip-rap surface layer, (b) gravel admixture surface layer, and (c) topsoil surface layer. The color scale is layers of the barrier remaining intact ranging from one (tailings, red shading) to eight (deposition, blue shading). Green shading is all five layers of the cover plus the tailings layer remaining intact (six).

Humid Climate

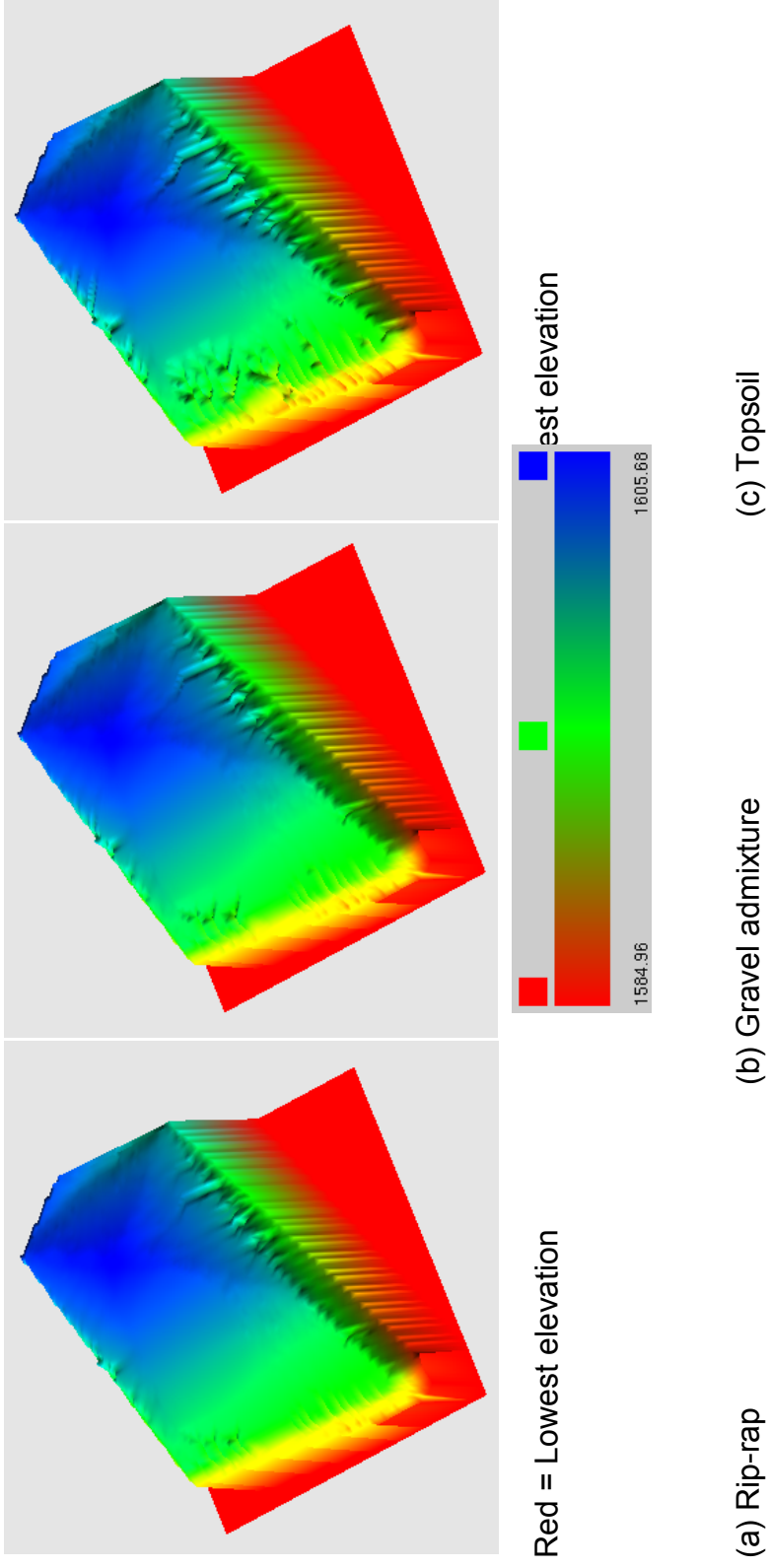


Fig. 4.4. Elevation predicted for reference site predicted with SIBERIA for a resistive barrier in a humid climate: (a) rip-rap surface layer, (b) gravel admixture surface layer, and (c) topsoil surface layer. Elevation is shown in m and denoted by the color scale above.

Humid Climate

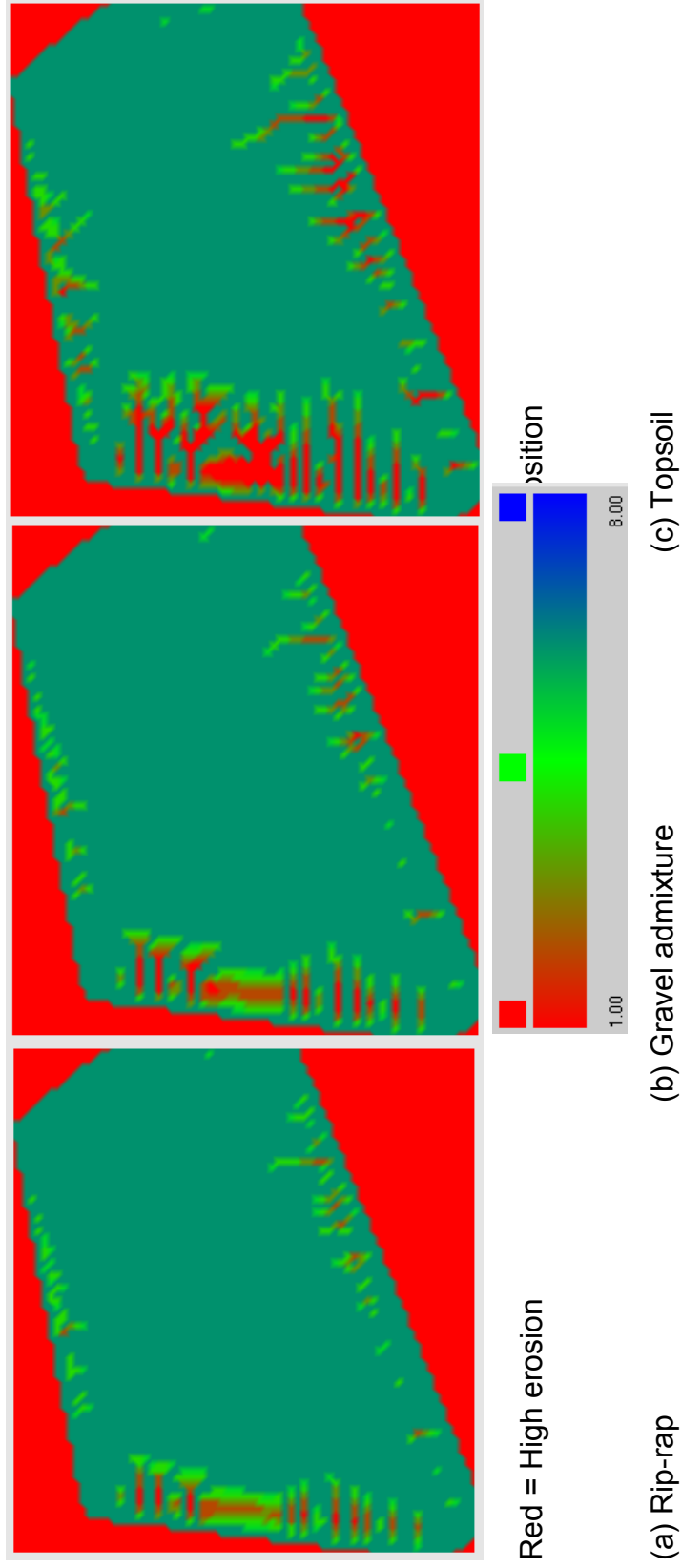


Fig. 4.5. Plan view of reference site predicted with SIBERIA for a resistive barrier in a humid climate: (a) rip-rap surface layer, (b) gravel admixture surface layer, and (c) topsoil surface layer. The color scale is layers of the barrier remaining intact ranging from one (tailings, red shading) to eight (deposition, blue shading). Green shading is all five layers of the cover plus the tailings layer remaining intact (six).

The plan view (Fig. 4.5) shows that erosion occurs in the same location in the rip-rap and gravel admixture layers, by the same mechanism (gully formation), and that erosion is deeper in the gravel admixture than in the rip-rap. In contrast, more extensive gullying occurs with the topsoil surface, with longer and deeper gullies.

Maximum erosion in the semi-arid climate is much greater than maximum erosion in the humid climate for all three surface layer types (Fig. 4.1). All surface layers in the semi-arid climate had a maximum erosion of 6 to 7 m and the humid climate had a maximum erosion of 3.5 to 5.5 m, despite greater rainfall in the humid climate. For example, consider the plan views of the rip-rap surface layers in the semi-arid climate (Fig. 4.3 a) and the humid climate (Fig. 4.5 a). Erosion occurs across the side slopes as soil wash in the semi-arid climate, whereas erosion is in defined gullies in the humid climate. Semi-arid climates have less rainfall compared to humid climates (average annual rainfall is 230 mm in Grand Junction, CO compared to 961 mm in Pittsburgh, PA), but often have more fluvial erosion than humid climates because of sparse vegetative cover (Hudson 1987). These effects can be exacerbated when the surface is modified due to other factors, such as fire.

Monthly average precipitation data were analyzed for potential causes of greater erosion in the semi-arid climate. Precipitation data from the normal annual precipitation cycle for the three consecutive months with the greatest precipitation for both Grand Junction, CO and Pittsburgh, PA were explored for connections with the growing cycle for each climate. The three consecutive months with greatest rainfall for Grand Junction occur in March, April, and May, with 31.6% of the annual rainfall (NRCC 2009). Much of the rainfall occurs prior to the start of the growing season (April 30 to November 6) (Grand Valley Project 2011). In contrast, 31.4% of the annual rainfall for Pittsburgh occurs in May through July (NRCC 2009); i.e. after the growing season begins (April 24 to October 6) (Allen 2010 and Klett et al. 2010). Significant rainfall prior to the start of the growing season may be the cause of greater erosion seen in the semi-arid climate. The opportunity to establish vegetation prior to the period of greatest rainfall may significantly reduce erosion in the humid climate. Precipitation and growing season data are included in the WEPP calibrations of the fluvial erosion parameter β using the built-in climate and plant databases.

The calibrated n_1 fluvial erosion parameter also corresponds to erosion mechanisms, and controls the type of erosion over the landscape (Kirkby 1971 and Hancock 2004). Descriptions of erosion processes corresponding to the fluvial erosion parameters are in Table 4.1. An n_1 of 1 to 2 corresponds to soil wash without gullying and $n_1 = 0.7$ is reasonable for an armored surface. An n_1 of > 2 represents gullying. For the semi-arid climate, n_1 ranged from 3.9 to 4.6, indicating gullying occurs. For the humid climate, n_1 ranged from 0.7 to 1.0, indicating surface armoring occurs. These erosion mechanisms are consistent with erosion rates associated with areas of higher rainfall intensity (semi-arid climate) and lower rainfall intensity (humid climate).

Vegetative cover for this study was the average cover established by the USDA (Foster et al. 1995) for each type of vegetation (Big Mountain Sagebrush for a semi-arid climate and Bluestem Prairie Grass for a humid climate): 30% for the semi-arid climate and 56% for the humid climate. Vegetative cover for the humid climate was reduced to 30% for a resistive barrier with a gravel admixture surface to test if the differences in percent vegetative cover between climates affected erosion predicted by the model. The fluvial erosion parameters had no change after lowering the vegetative cover percentages, meaning that a change in percentage vegetative cover of this magnitude did not impact the model predictions.

Erosion of vegetated gravel admixture and un-vegetated gravel admixture surface layers for a resistive barrier is compared in Fig. 4.6. In the semi-arid climate, the vegetated gravel admixture has less maximum erosion and a higher average elevation than un-vegetated gravel admixture (Fig. 4.6 (a)). With vegetation, the average elevation depth is in the bedding layer (layer 2) rather than the much deeper transition layer (layer 5) with an un-vegetated surface. For the humid climate, the vegetated gravel admixture had 6 m less maximum erosion and the average elevation was 4 m higher than the un-vegetated gravel admixture over the 1000-yr design life of the cover. Vegetation has the same decreasing effect on erosion of the topsoil and rip-rap surface layers. Vegetation was also found to have the same decreasing effect on erosion for water balance barriers. All subsequent erosion simulations were performed using vegetated surface layers.

4.1.2 Influence of Barrier Type on Erosion

Maximum erosion and average elevation for water balance and resistive barriers in (a) semi-arid and (b) humid climates are shown in Fig. 4.7. In a semi-arid climate, the maximum erosion and average elevation for a water balance barrier fall slightly deeper than the maximum erosion and average elevation for a resistive barrier. There is no difference between maximum or average erosion in the water balance and resistive barriers in a humid climate. Additional figures showing predictions are in Appendix A for resistive barriers and Appendix B for water balance barriers.

The difference in average erosion depth between water balance and resistive barriers in a semi-arid climate appears to begin in the third layer of the water balance barrier. The difference between the two barriers is due to the higher silt content for the water storage layer (third layer of the water balance barrier) compared to the frost protection layer (third layer of the resistive barrier) (49% silt in the water storage layer, 12% silt in the frost protection layer), as erodibility increases with silt content (Fangmeier et al. 2006).

4.1.3 Hydrologic Comparison of Barrier Type and Surface Layer Type

Cumulative percolation from the barrier was predicted using SVFLUX for water balance and resistive barriers with rip-rap, gravel admixture, and topsoil surface

layers. Simulations were conducted for semi-arid and humid sites. Predictions are shown in Fig. 4.8 for the semi-arid climate and in Fig. 4.9 for the humid climate.

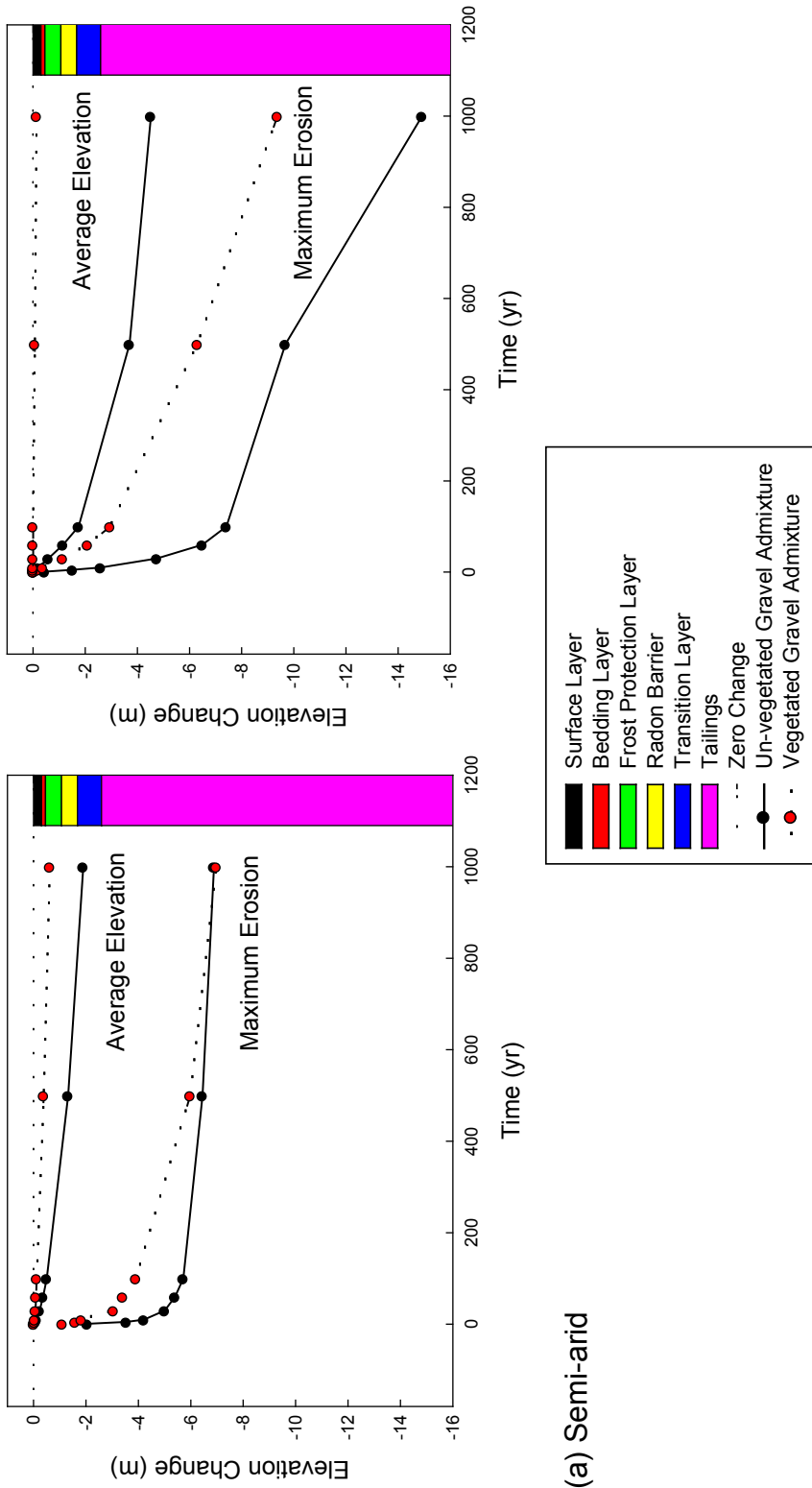
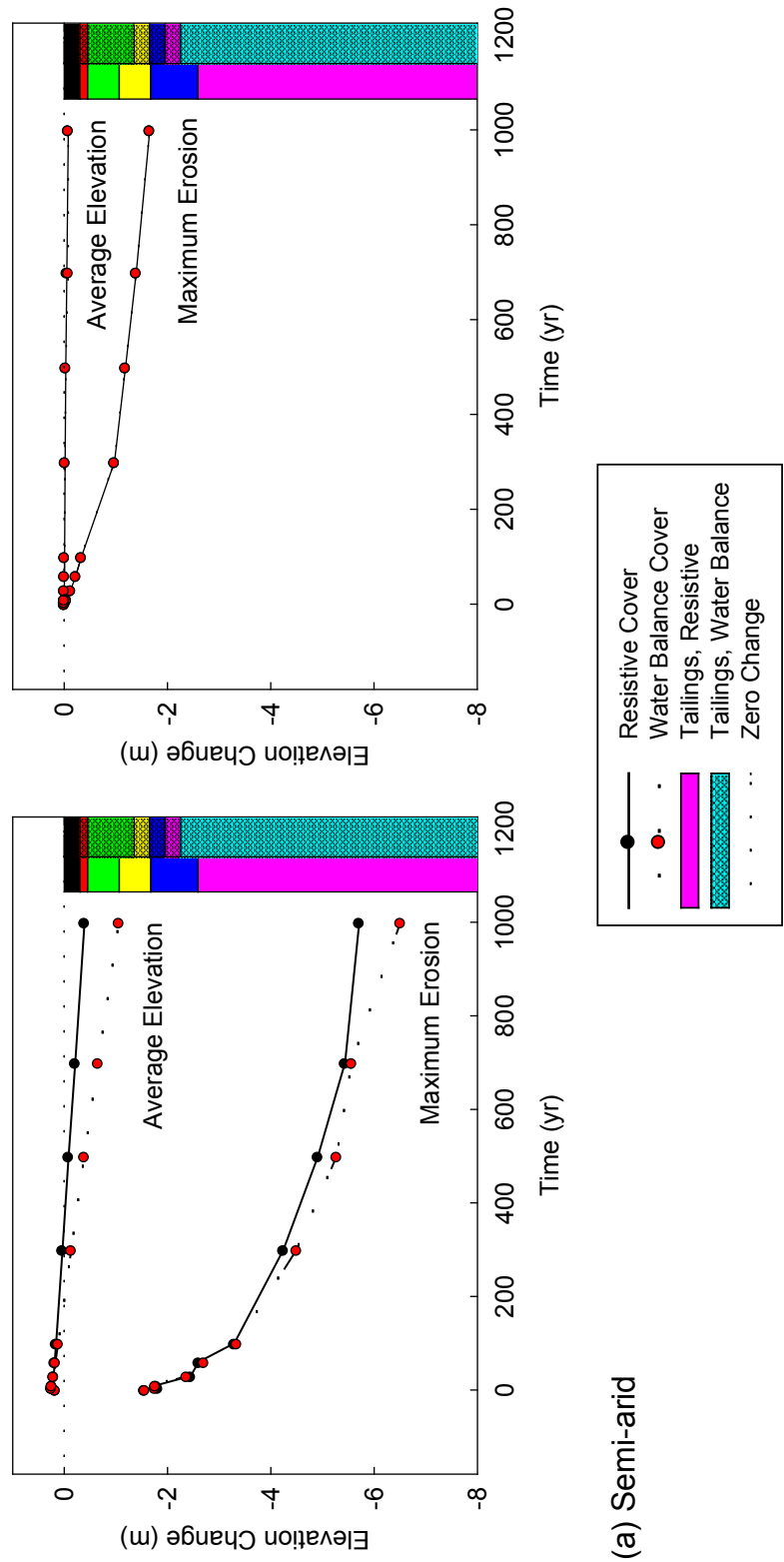


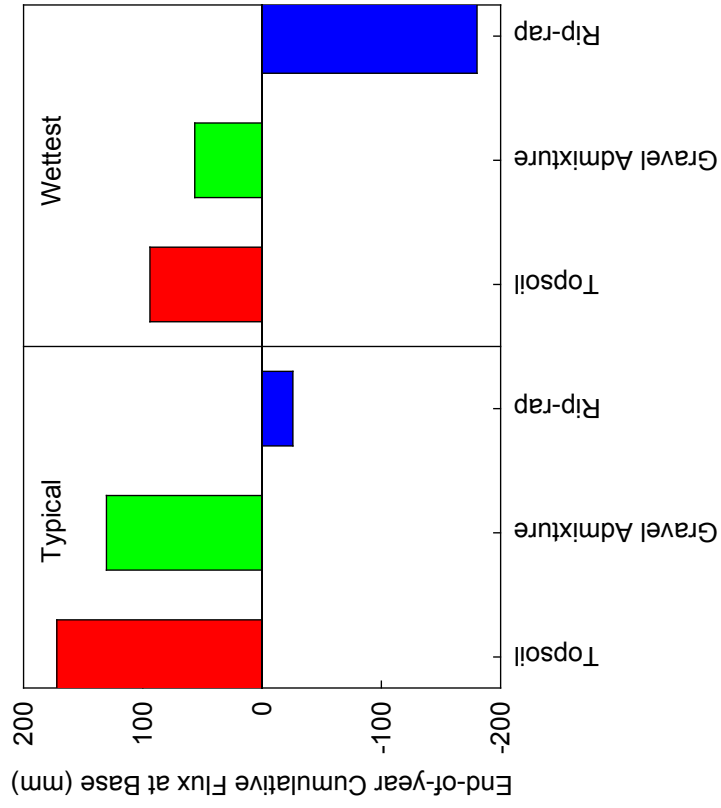
Fig. 4.6. Maximum erosion and average elevation predicted by SIBERIA for the reference site with a resistive barrier comparing gravel admixture surfaces with and without vegetation: (a) semi-arid climate and (b) humid climate.



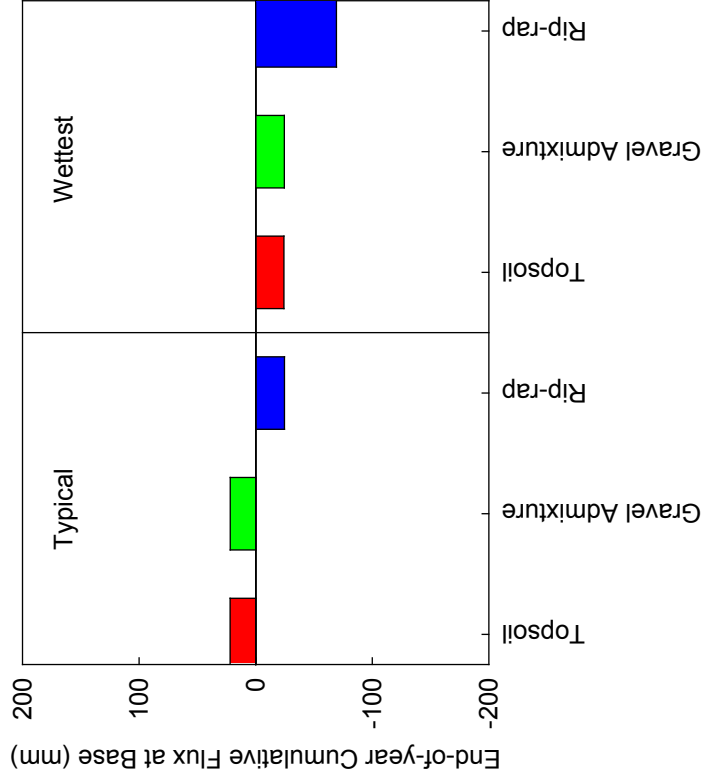
(a) Semi-arid

Fig. 4.7. Maximum erosion and average elevation predicted by SIBERIA for resistive and water balance barriers with a rip-rap surface layer: (a) semi-arid climate and (b) humid climate.

Semi-Arid Climate



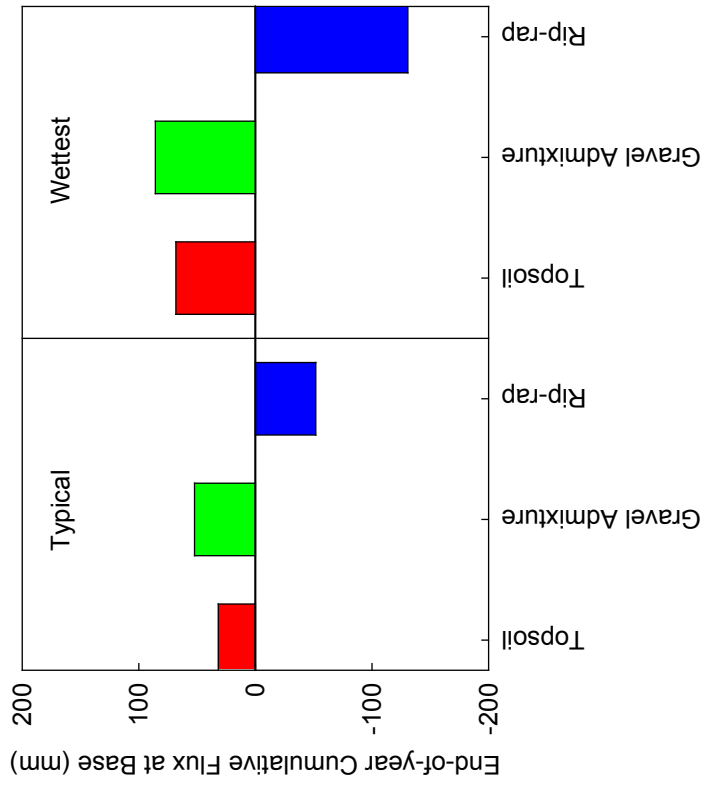
(a) Resistive barrier



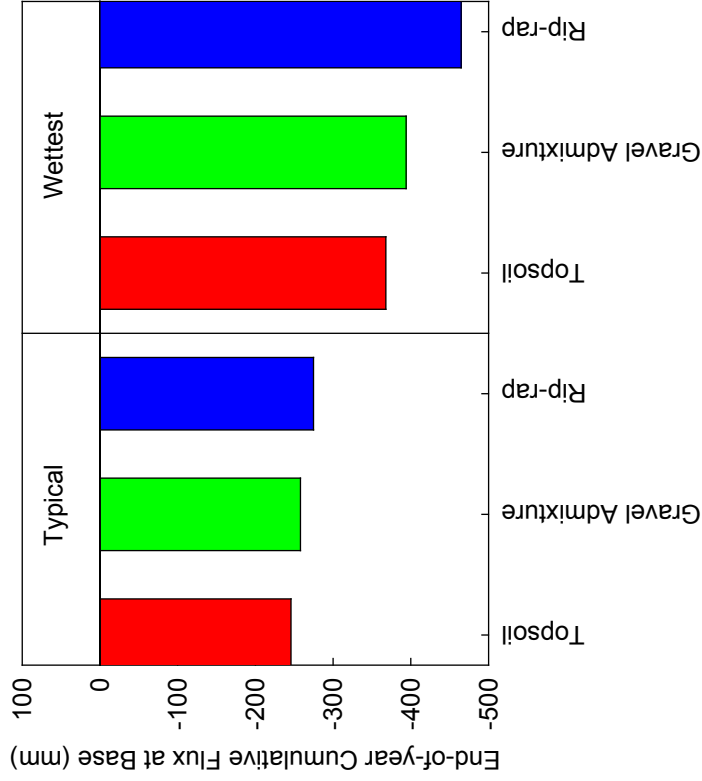
(b) Water balance barrier

Fig. 4.8. End-of-year cumulative flux above the tailings predicted by SVFLUX for the typical year and wettest year in a semi-arid climate: (a) resistive barrier and (b) water balance barrier. Negative flux indicates downward flow into the tailings.

Humid Climate



(a) Resistive barrier



(b) Water balance barrier

Fig. 4.9. End-of-year cumulative flux above the tailings predicted by SVFLUX for the typical year and wettest year in a humid climate: (a) resistive barrier and (b) water balance barrier. Negative flux indicates downward flow into the tailings.

Negative percolation in Fig. 4.8 and Fig. 4.9 is downward flow (i.e. into the tailings). Additional figures showing SVFLUX predictions for precipitation, evapotranspiration, soil-water storage, and cumulative percolation are in Appendix C.

In the semi-arid climate (Fig. 4.8), the barriers with a rip-rap surface transmit percolation into the tailings (negative flux) regardless of barrier type or typical or wettest year simulations. The resistive barrier with topsoil and gravel admixture surface layers had upward flow out of the tailings (positive flux) for typical and wettest year simulations (Fig. 4.8 (a)). In contrast, percolation into the tailings occurred in the wettest year for all surface layer types with a water balance barrier, and only with the rip-rap surface for the typical year (Fig. 4.8 (b)). Topsoil and gravel admixture surfaces with water balance barriers had upward flux (out of the tailings) for the typical year simulation.

In the humid climate (Fig. 4.9), both barrier types with a rip-rap surface had percolation into the tailings (negative flux) for the typical and wettest year simulations. Resistive barriers with topsoil and gravel admixture surfaces had upward flow for both the typical and wettest year simulations (Fig. 4.9 (a)) due to evapotranspiration of water stored in finer-textured soil layers.

Barriers with a gravel admixture surface layer were most effective in controlling both erosion and percolation. Although percolation was slightly lower in some cases when topsoil was used for the surface layer, the gravel admixture layer was much more effective in controlling erosion than the topsoil layer. In contrast, the rip-rap surface layer was most effective in controlling erosion, but barriers with a rip-rap surface layer consistently transmitted the most percolation.

A gravel admixture surface includes both fine and coarse soil within a single surface layer. This combination of particle sizes provides the surface with a high interlock of soil particles, helping prevent erosion (Toy et al 1998), and higher soil water storage, with the finer soil allowing the barrier to store water until evapotranspiration can occur (Kirkham 2005). The fine-textured soil in the gravel admixture surface also allows water to move upward to the surface for evaporation. In contrast, the permeable rip-rap layer promotes infiltration during precipitation events, and the capillary break formed between the coarse rip-rap and finer underlying layers traps water within the cover, reducing evapotranspiration and increasing percolation.

4.2 Effect of Slope Length and Grade on Erosion

Slope length and grade difference at the nickpoint (i.e. the location of the change in grade between the top and side slopes) both affect erosion. To evaluate the effect of slope length and slope grade, the topography was modified to be symmetrical in both base and peak (Fig. 4.10). This new topography had one base elevation representing a disposal site on a level surface and with a mound shape.

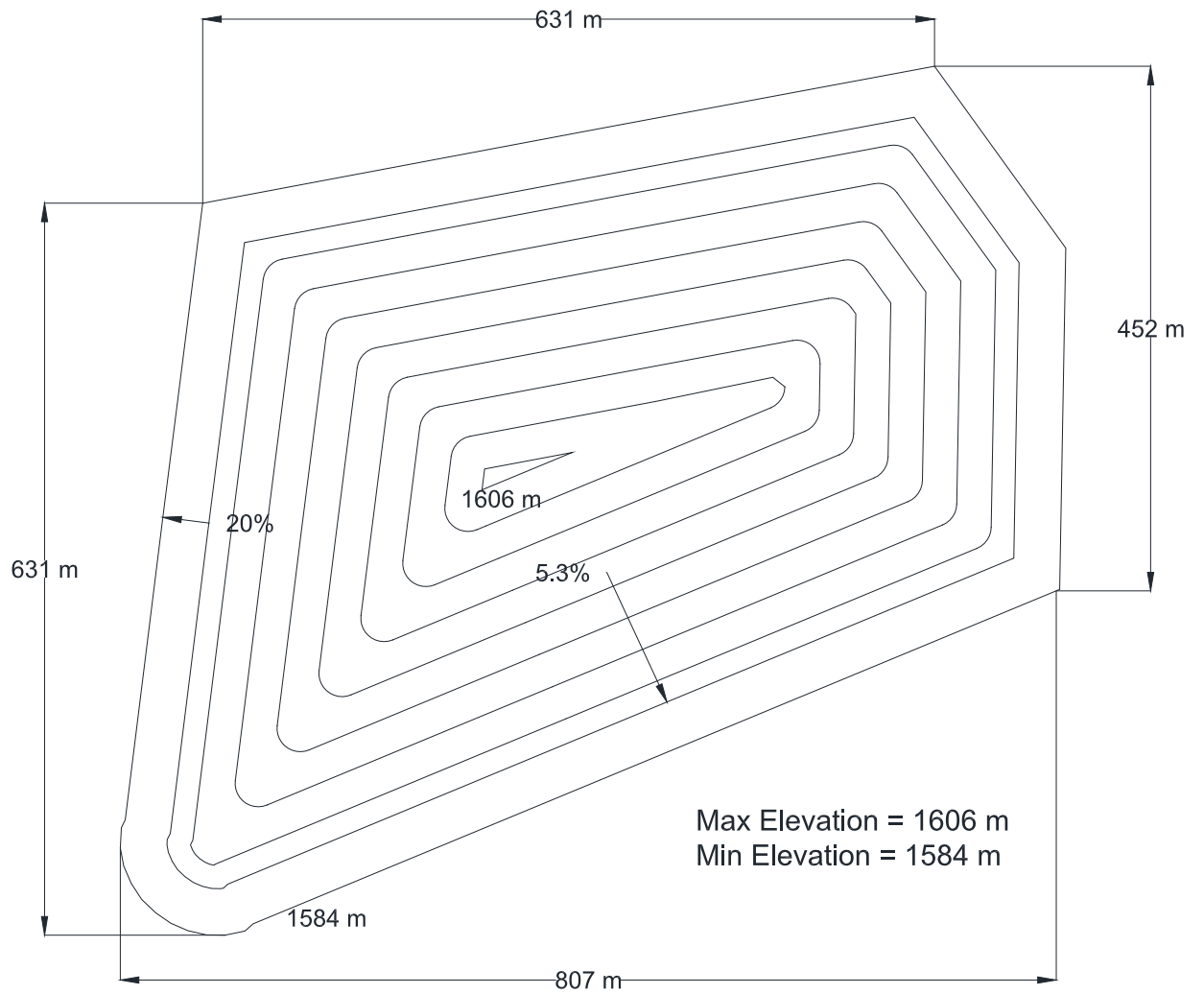


Fig. 4.10. Topography representing balanced side slopes with 20% maximum side slopes and 5.3% maximum top slope, referred to herein as the modified topography.

When changing the topography, the same lowest base elevation and highest peak elevation were maintained so that the storage volume of the new topography would remain similar to the storage volume of the reference site described in Section 4.1. Three cases with different side slope length (distance between top and bottom of the side slope) were evaluated to compare how different slope lengths and angles influence erosion. The side slope lengths were 53 m, 41 m, and 28 m, with corresponding side slope grades of 15.3, 20.0, and 18.5% (Table 4.2).

Maximum erosion and average elevation are shown in Fig. 4.11 for a rip-rap cover with 53-m, 28-m, and 41-m side slope lengths in the (a) semi-arid and (b) humid climates. For both climates (Fig. 4.11), the 41-m long slope has less maximum erosion and a higher average elevation than the 53-m and 28-m slopes. The 41-m slope has approximately 5 m less maximum erosion than the 28-m long slope in the semi-arid climate, and approximately 4 m less maximum erosion than the 28-m long slope in the humid climate.

When the slope angle is held constant, an increase in slope length increases the amount and depth of erosion for both climates. For example, the 53-m slope has deeper maximum erosion than the 41-m slopes; 7 m deeper in the semi-arid climate and 5 m deeper in the humid climate. Slope grade also has an effect, with larger slope grades producing more erosion (e.g. the 28-m slopes have greater maximum erosion than the 41-m slopes because slope grade difference at the nickpoint is larger; the nickpoint is where erosion begins to occur, and is typically where the deepest erosion occurs). Fig. 4.12 shows the effect of grade difference on erosion for semi-arid and humid climates; the larger maximum erosion associated with the 28-m slope is concomitant with the larger grade difference associated with the 28-m slope (15.5%). Additional figures showing different slope lengths and angles are Appendix D.

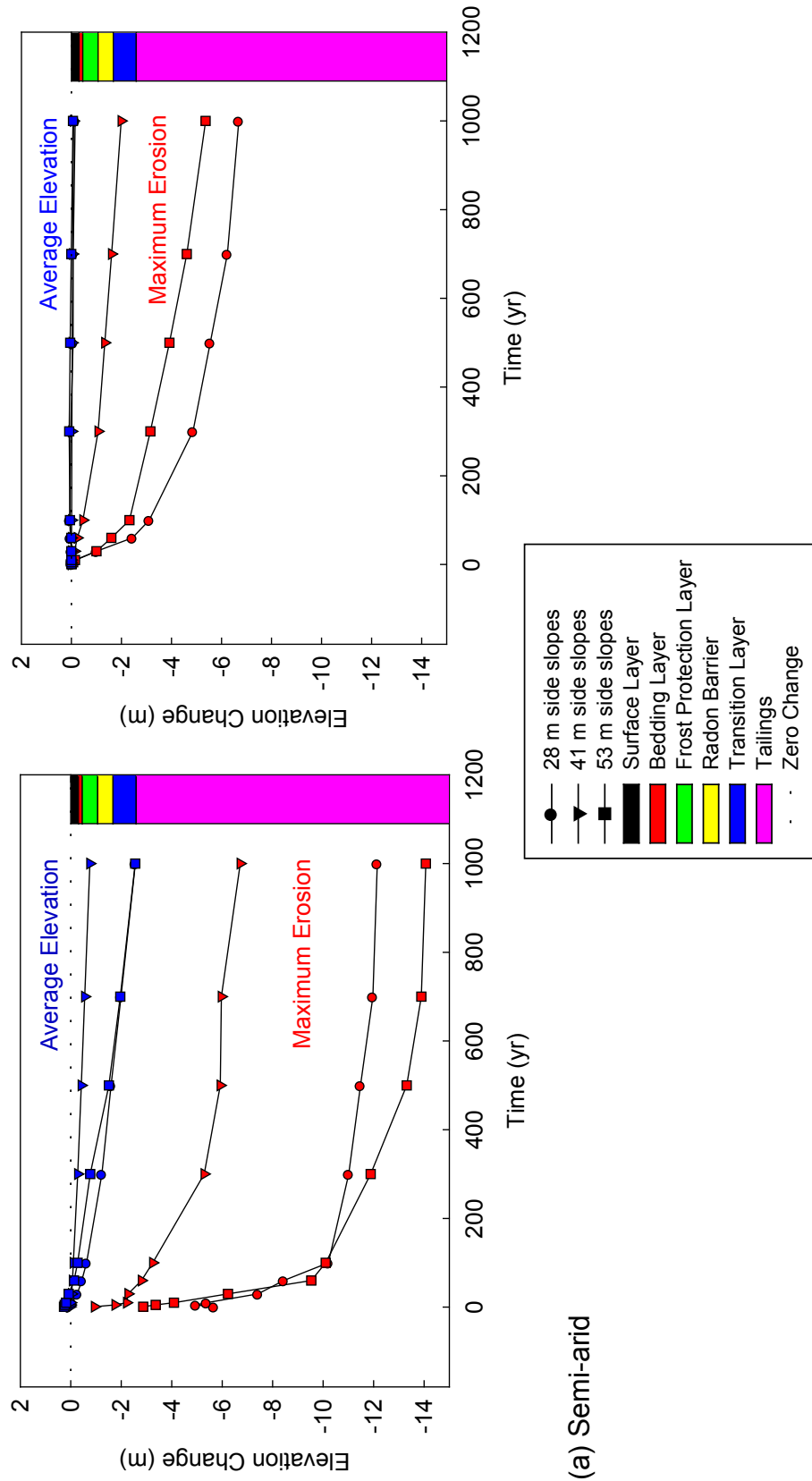
4.3 Effect of Slope Shape on Erosion

Terraced, concave, natural, and uniform slopes (Fig. 4.13) were simulated with SIBERIA to compare the effect of slope shape on erosion. Shallow and deep concave side slopes were evaluated to compare differences between a shallow (30%) initial slope and a deep (60%) initial slope. The uniform side slope shape is the modified mound shape from Section 4.2. Rip-rap, gravel admixture, and topsoil surface layers were used for the simulations. Topographic views of the four slope shapes are in Appendix E.

Predictions of maximum erosion, maximum deposition, and average elevation change for the various slope shapes with a rip-rap surface are shown in Fig. 4.14 for barriers in (a) semi-arid and (b) humid climates. Predictions labeled concave correspond to the shallow or deep concave slope that produced the least maximum erosion and least average elevation change for that surface type. In Fig. 4.14, the

Table 4.2. Side slope length, side slope grade, top slope grade, and grade difference compared with SIBERIA simulations to determine effects of slope length and grade.

Side Slope Length	Side Slope Grade	Top Slope Grade	Grade Difference
53 m	15.3%	2.0%	13.3%
41 m	20.0%	5.3%	14.7%
28 m	18.5%	3.0%	15.5%



(a) Semi-arid

Fig. 4.11. Maximum erosion and average elevation change predicted by SIBERIA for the reference site with rip-rap surface layer and a resistive barrier for various slope lengths: (a) semi-arid climate and (b) humid climate.

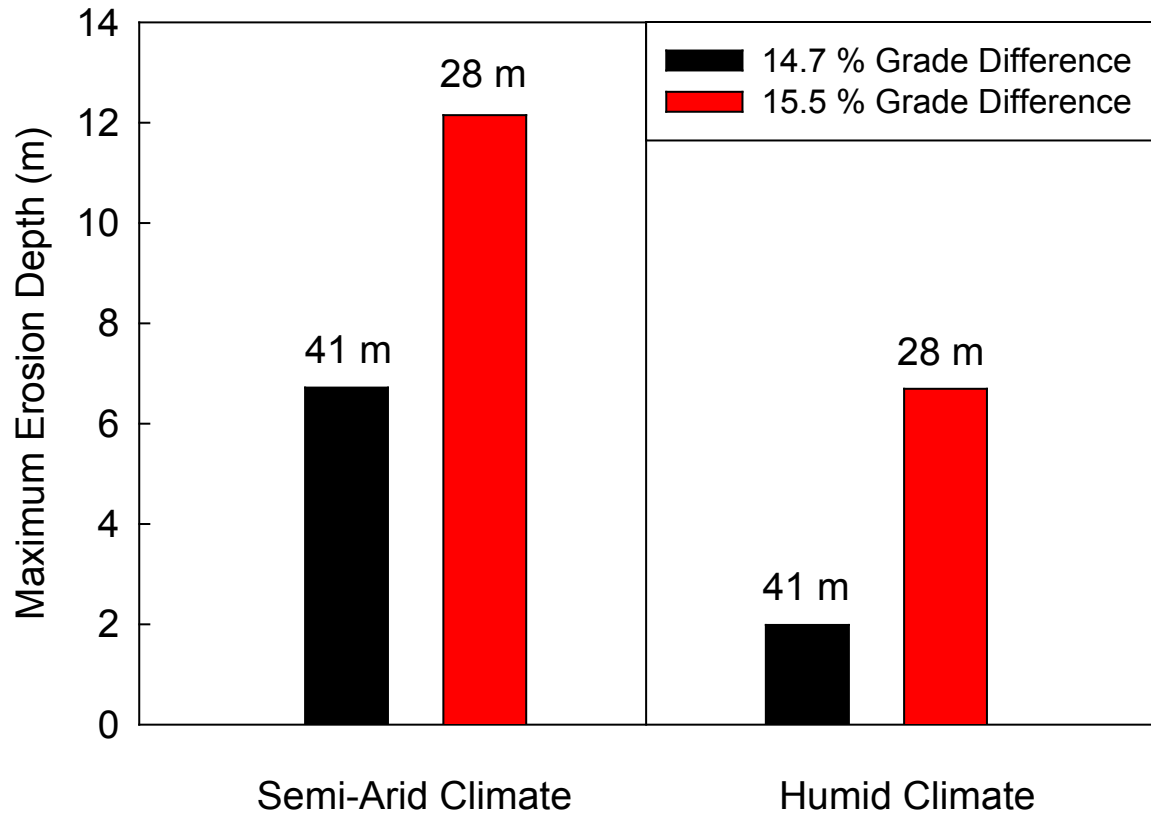
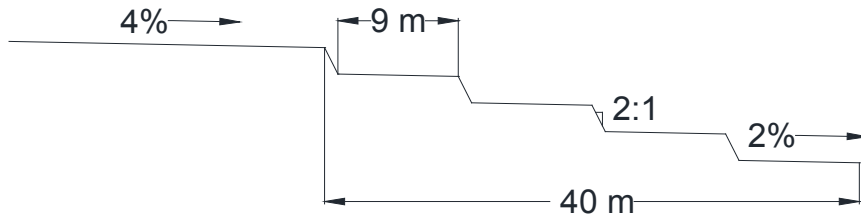
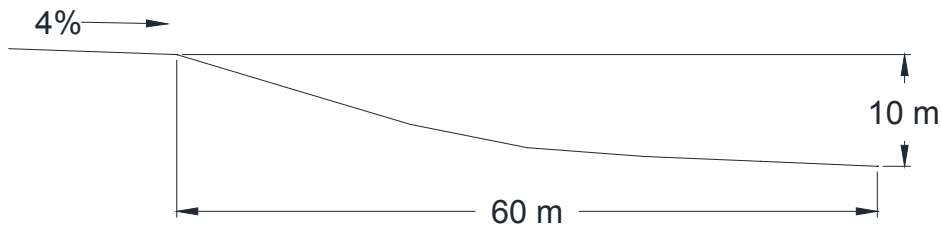


Fig. 4.12. Maximum erosion depth at 1000-yr for a 14.7% and 15.5% grade difference using a rip-rap surface over a resistive barrier in semi-arid and humid climates with slope lengths of 28 and 41 m.

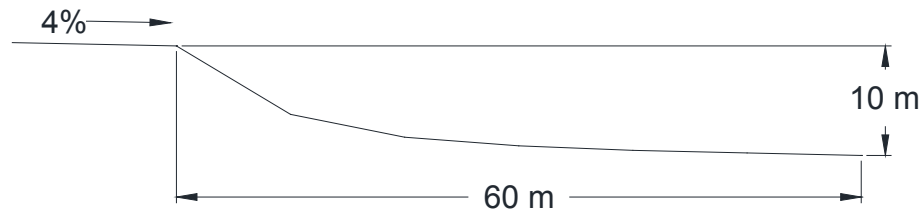
(a) Terraced



(b) Shallow Concavity



(c) Deep Concavity



(d) Natural Hillside

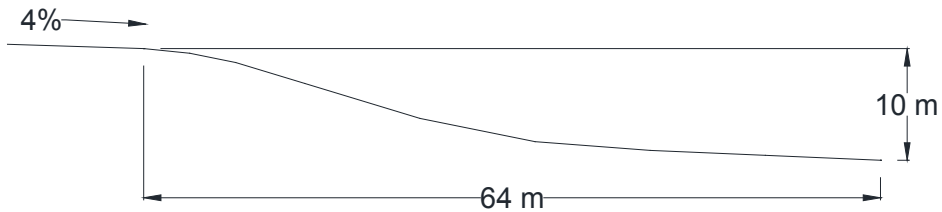


Fig. 4.13. Terraced (a), shallow concavity, 30% initial slope (b), deep concavity, 60% initial slope (c), and natural hillside slopes (d) used to evaluate influence of topography on erosion.

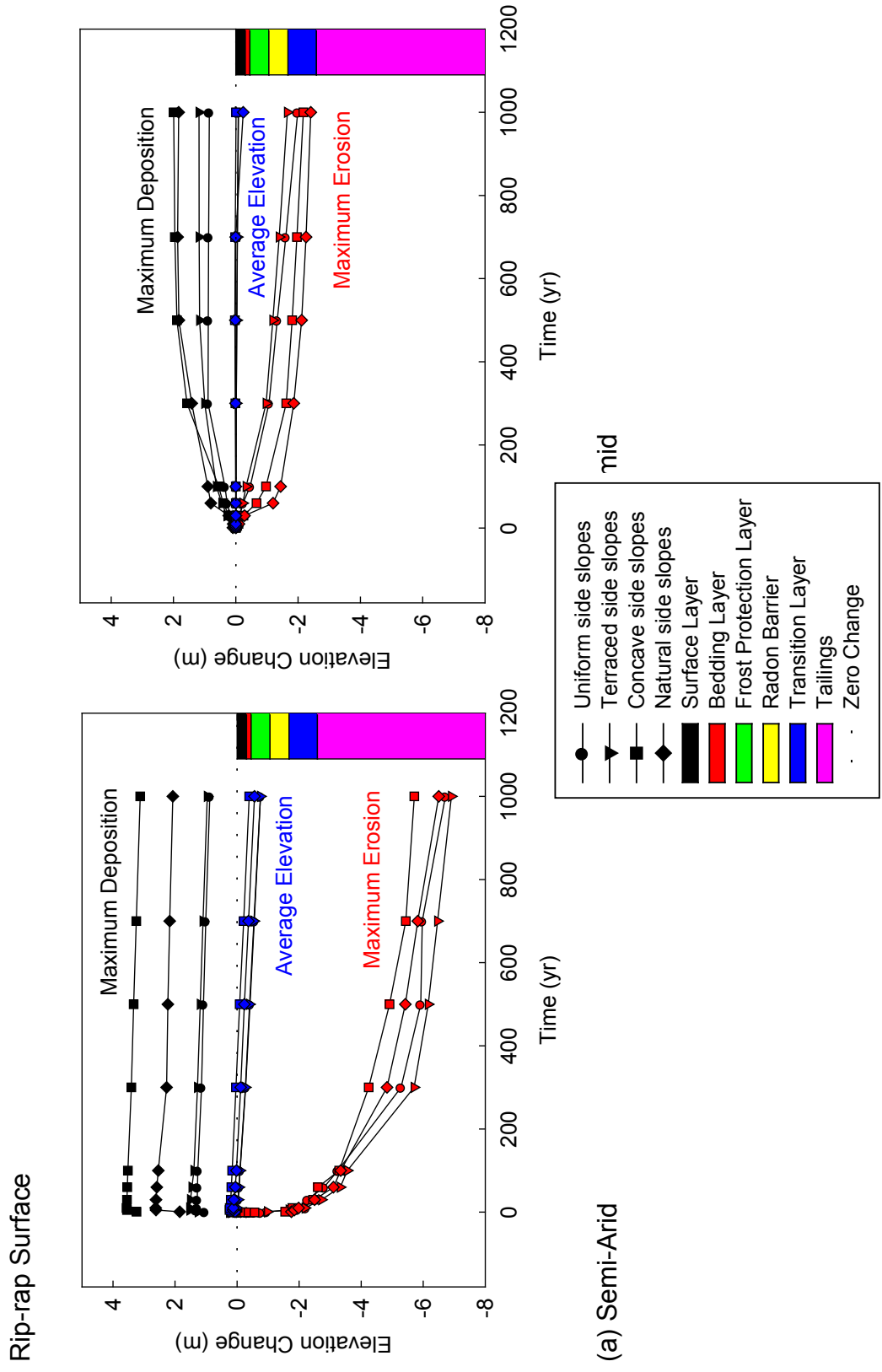


Fig. 4.14. Maximum erosion, maximum deposition, and average elevation change predicted by SIBERIA for resistive barriers with a rip-rap surface and uniform, terraced, concave (semi-arid: deep concave, humid: shallow concave), or natural side slopes: (a) semi-arid climate and (b) humid climate.

semi-arid climate has deep concave slopes and the humid climate has shallow concave slopes. In semi-arid environments, the deep concave slope has the least maximum erosion, whereas the terraced slope has the greatest maximum erosion. In contrast, in humid climates, terraced side slopes had the least maximum erosion and natural side slopes had the greatest maximum erosion. Additional figures comparing shallow and deep concave slopes are in Appendix F.

Images showing the number of intact layers for a rip-rap surface in a semi-arid climate are shown in Fig. 4.15 for (a) terraced, (b) concave, and (c) natural side slopes. Concave side slopes have approximately 2 m more maximum deposition and 1 m less maximum erosion than terraced side slopes. On-site deposition plays a part in keeping the cover intact for concave side slopes (Fig. 4.15, blue shading). Sediment is deposited at the base of the steepest slope section in a concave slope, allowing more layers to build up at the base. Deposition is shown by the number of layers remaining intact over 6 (blue shading). Deposition at the toe of the slope also occurs on natural slope shapes, whereas terraced side slopes do not show deposition (Fig. 4.15 (a)).

The effect of slope shape on erosion predictions for a rip-rap surface was significantly different in the humid climate. At least 3 layers (no evident red or deep red shading) remained intact over the 1000-year simulation for terraced slopes (Fig. 4.16). As observed for the semi-arid simulation, deposition was not significant for terraced slopes in the humid climate (blue shading not evident). Natural and concave slopes had more erosion at the top of the slope (red shading), indicating that the head-cut progression was more advanced than with terraced side slopes. Deposition was approximately 2 m at the base of both natural and concave slopes. This deposition limits erosion depth at the base of the slopes, but the advanced head-cutting created deeper erosion further up slope.

The steepness of the slope immediately at the transition point between the top slope and side slope is a reason for the advance head-cutting on the natural and concave slopes in the humid climate. The side slope for the natural and concave slopes has a steeper slope for a longer length, causing erosion to easily move upwards. Terraced slopes limit head-cutting by having short lengths of steep slope sections and several small “step” grade changes, rather than one large grade change. Shorter slopes prevent large quantities of overland flow (Toy et al. 2002, Fangmeier et al. 2006), and shallow slopes slow the movement of the rill head-cut by reducing the velocity of the flow (Willgoose and Sharmeen 2006); both limit erosion.

The predictions for a gravel admixture surface with the four slope shapes in both climates are shown in Fig. 4.17. At 1000 yr, there is no observable difference in either maximum erosion or average elevation change between the slope shapes for the semi-arid climate. Concave and natural slopes have about 1.5 m more deposition (blue shading) at the base of the slope than uniform and terraced slopes (Fig. 4.18).

Rip-rap Surface (Semi-Arid Climate)

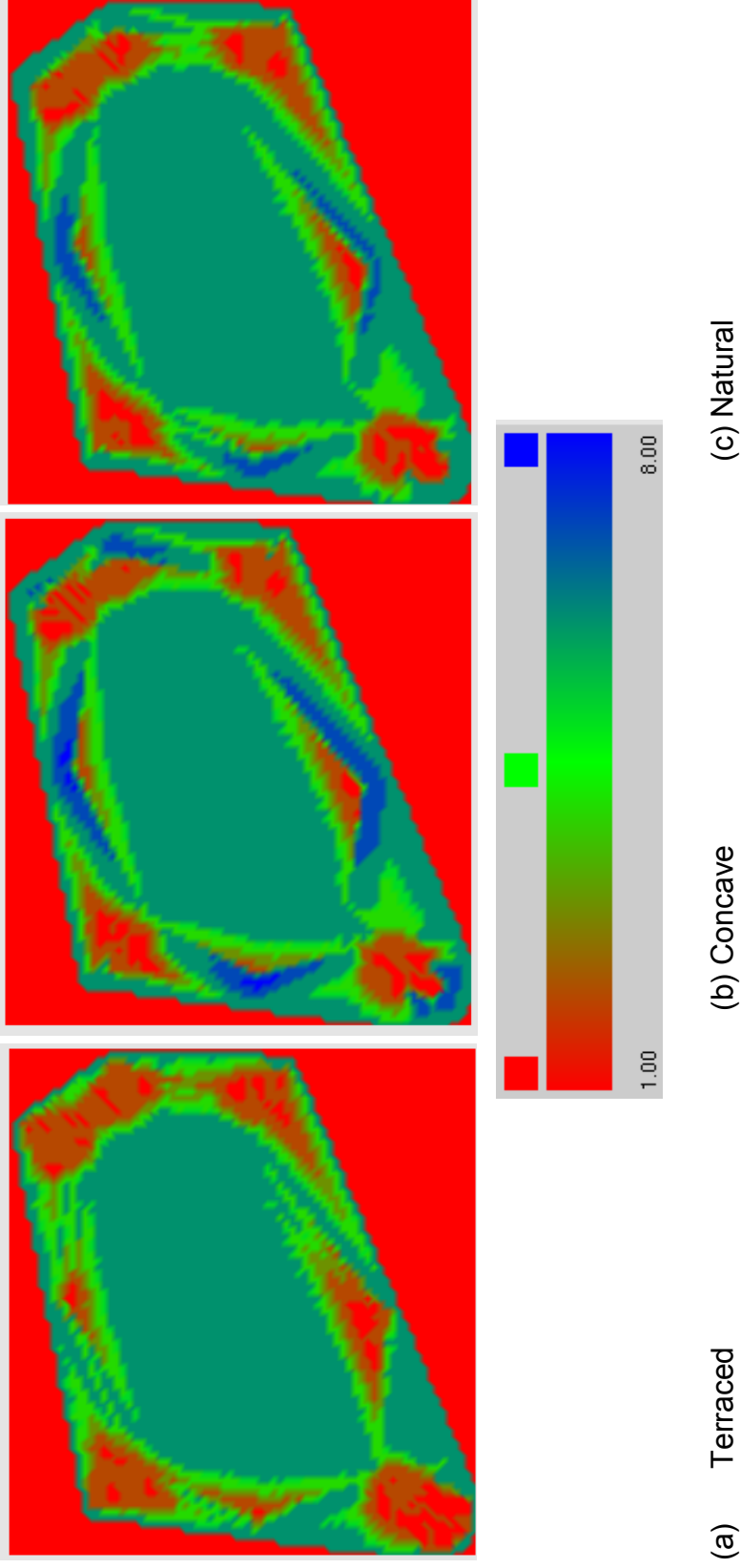


Fig. 4.15. Number of layers intact after 1000 years in a semi-arid climate predicted by SIBERIA for a resistive barrier with a rip-rap surface: (a) terraced side slopes, (b) concave side slopes (deep), and (c) natural side slopes.

Rip-rap Surface (Humid Climate)

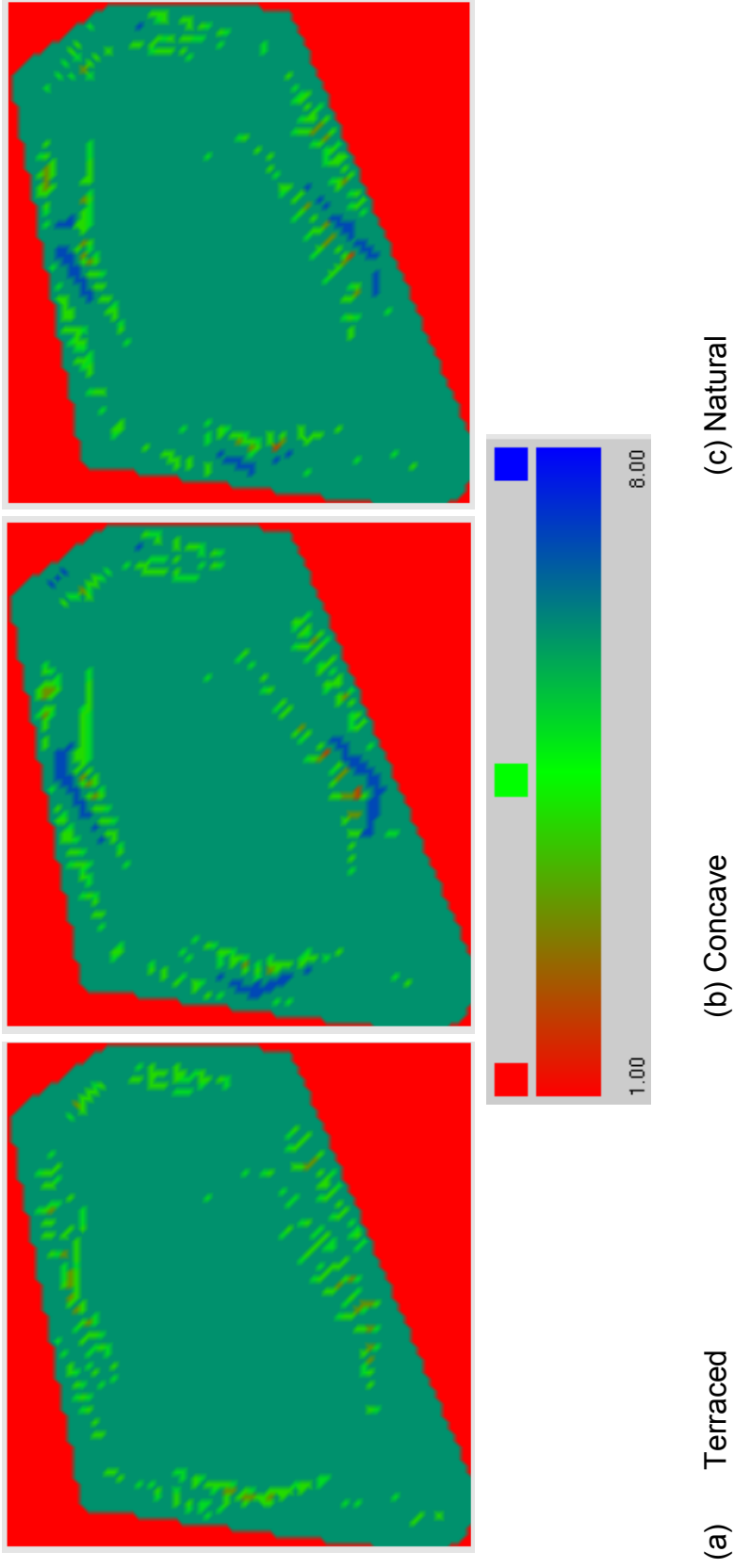


Fig. 4.16. Number of layers intact after 1000 years in a humid climate predicted by SIBERIA for a resistive barrier with a rip-rap surface: (a) terraced side slopes, (b) concave side slopes (shallow), and (c) natural side slopes.

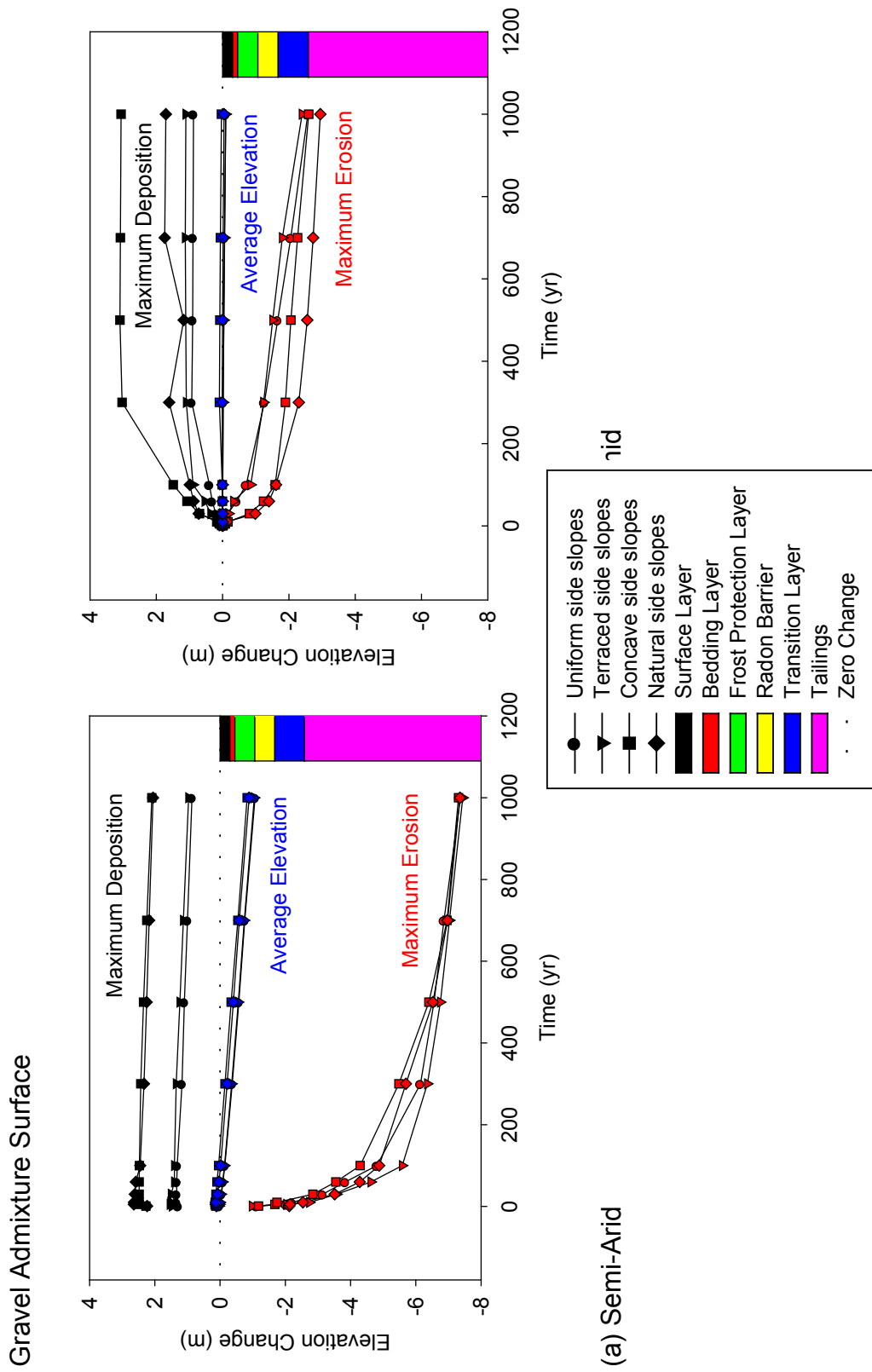


Fig. 4.17. Maximum erosion, maximum deposition, and average elevation change predicted by SIBERIA for resistive barriers with a gravel admixture surface and uniform, terraced, concave (semi-arid: shallow, humid: deep), or natural side slopes: (a) semi-arid climate and (b) humid climate.

Gravel Admixture Surface (Semi-Arid Climate)

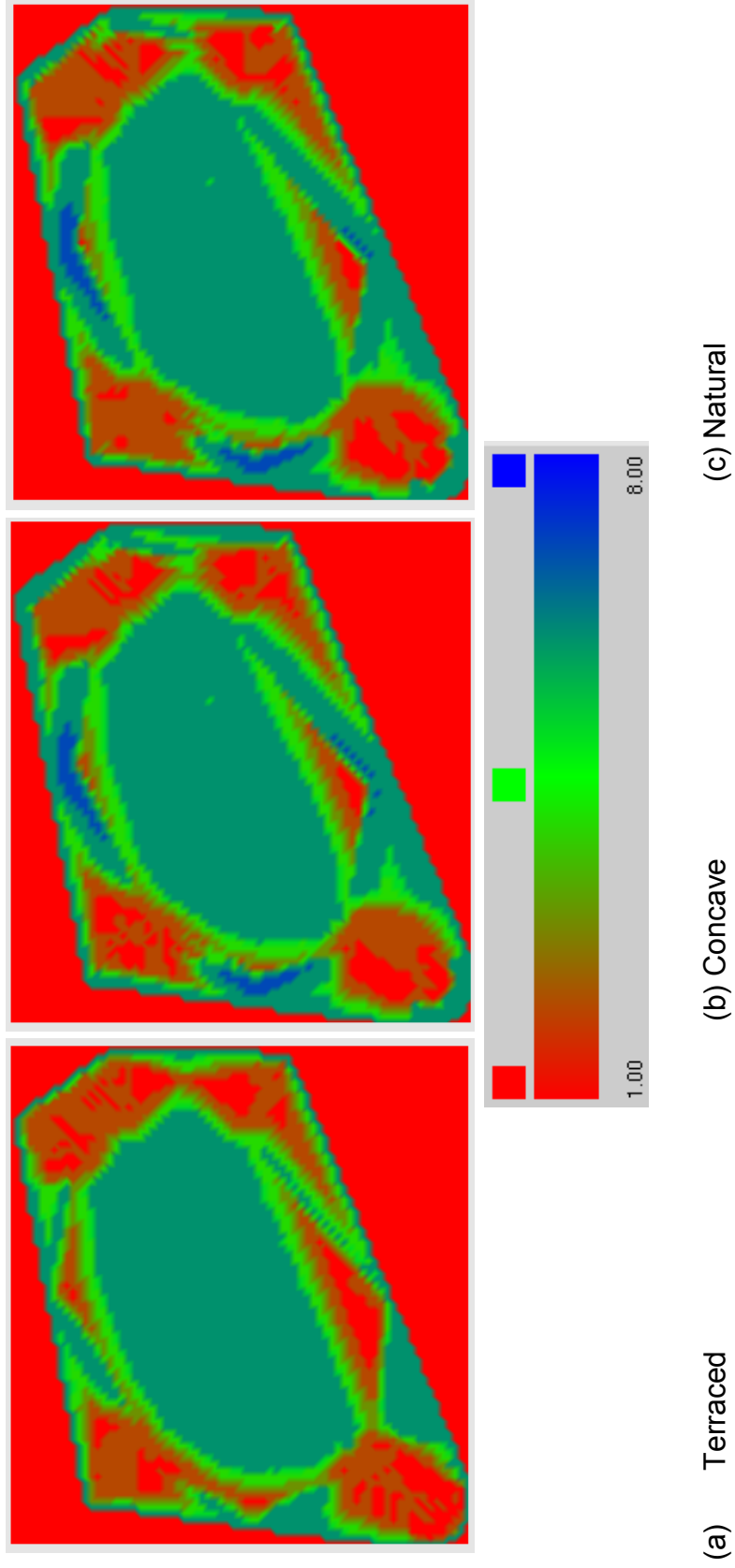


Fig. 4.18. Number of layers intact after 1000 years in a semi-arid climate predicted by SIBERIA for a resistive barrier with a gravel admixture surface: (a) terraced side slopes, (b) concave side slopes (shallow), and (c) natural side slopes.

Erosion is significant on the side slopes for all four slope shapes, but the deep erosion on the side slopes occurs over a smaller area for concave and natural slopes.

Gravel admixture surfaces on terraced side slopes in a humid climate have the least maximum erosion (Fig. 4.17 (b)), with the 1000-yr maximum erosion in the transition layer. The average elevation change for all slope shapes is in the surface layer. Natural and concave slopes have the greatest amount of maximum erosion, and have a maximum deposition of approximately 2 m and 3 m, respectively.

Erosion on natural and concave slopes progresses further up slope than erosion on terraced slopes (Fig. 4.19, red shading), as was found in the simulations for the rip-rap surface in a humid climate (Fig. 4.16).

The differences between erosion for the four slope shapes in semi-arid and humid climates for the rip-rap and gravel admixture surfaces can be explained by the maximum amount of erosion (Fig. 4.14 and Fig. 4.17). For all slopes in the semi-arid climate, the rip-rap surface had approximately 4 m greater maximum erosion, creating more sediment movement than in a humid climate. A similar situation occurred for the gravel admixture surface in the semi-arid climate; all slope shapes had approximately 4 m greater maximum erosion depth than slope shapes in the humid climate with the same gravel admixture surface. Concave and natural slope shapes have a flatter grade at the base of the slope, which creates a sediment trap that promotes deposition.

Deposition is important in the more eroded semi-arid climate because sediment fills eroded regions near the base, keeping sediment on the slope (blue shading; Fig. 4.15b, c) and Fig. 4.18b, c), rather than migrating off site (no blue shading evident, Fig. 4.15a, Fig. 4.18a). Terraced slopes produce the least maximum erosion for rip-rap and gravel admixture surfaces in a humid climate (Fig. 4.14b and Fig. 4.17b). Terraces have many short slopes whereas concave and natural slope shapes have long slope lengths. Sediment deposition is not significant on the terraced slopes because less erosion occurs on the short slopes.

Predictions are shown in Fig. 4.20 for resistive barriers with topsoil surfaces in (a) semi-arid and (b) humid climates. The deepest rills and greatest deposition in the semi-arid climate occur in the concave side slope. Terraced and natural slopes have the least maximum erosion. Terraced slopes have shorter slope lengths and natural slopes have less abrupt changes in grade than slopes with a concave shape. The concave slope also has more branches within its rill system, indicating the rills on the concave slope began much earlier than the straighter rills on the terraced and natural slopes (Fig. 4.21).

Gravel Admixture Surface (Humid Climate)

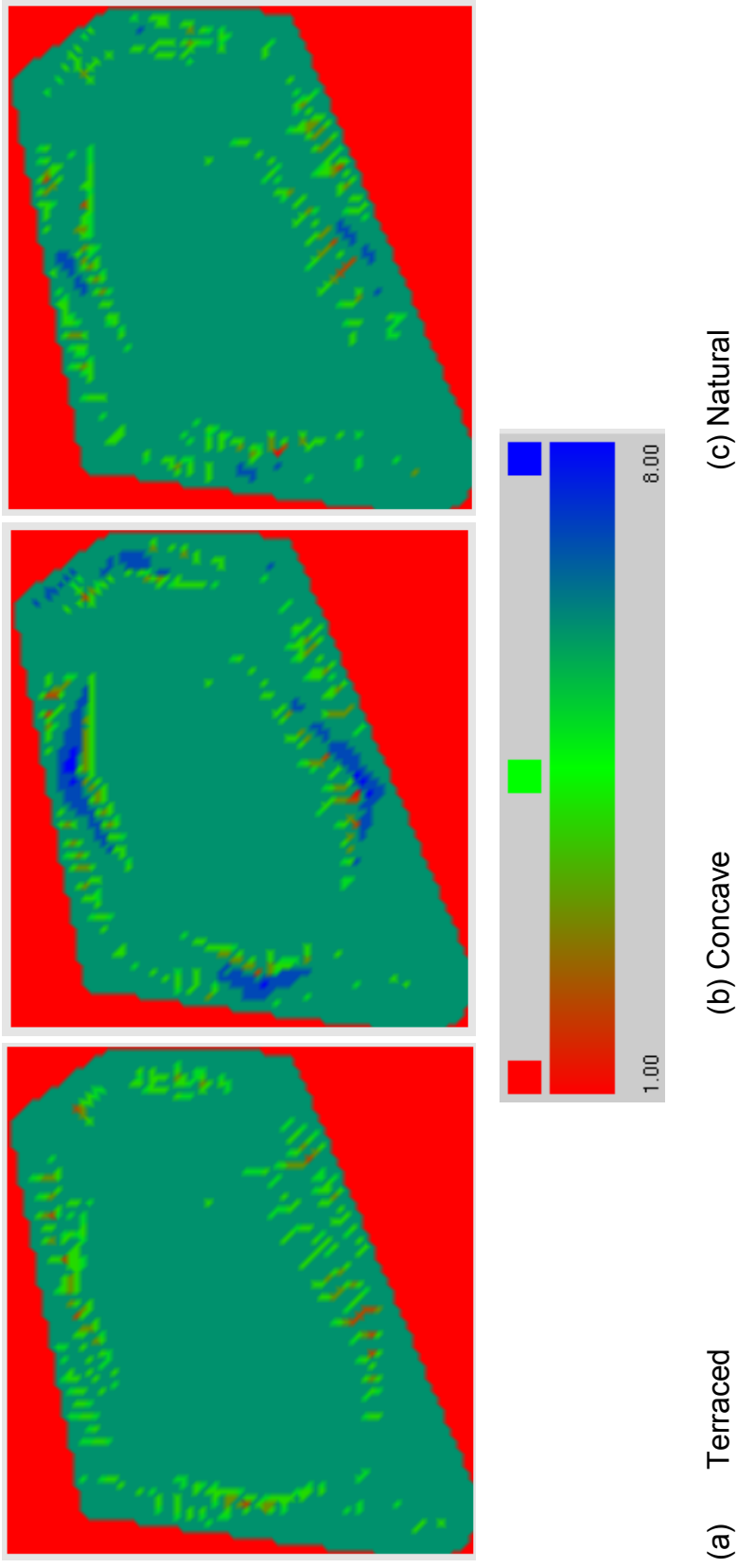


Fig. 4.19. Number of layers intact after 1000 years in a humid climate predicted by SIBERIA for a resistive barrier with a gravel admixture surface: (a) terraced side slopes, (b) concave side slopes (deep), and (c) natural side slopes.

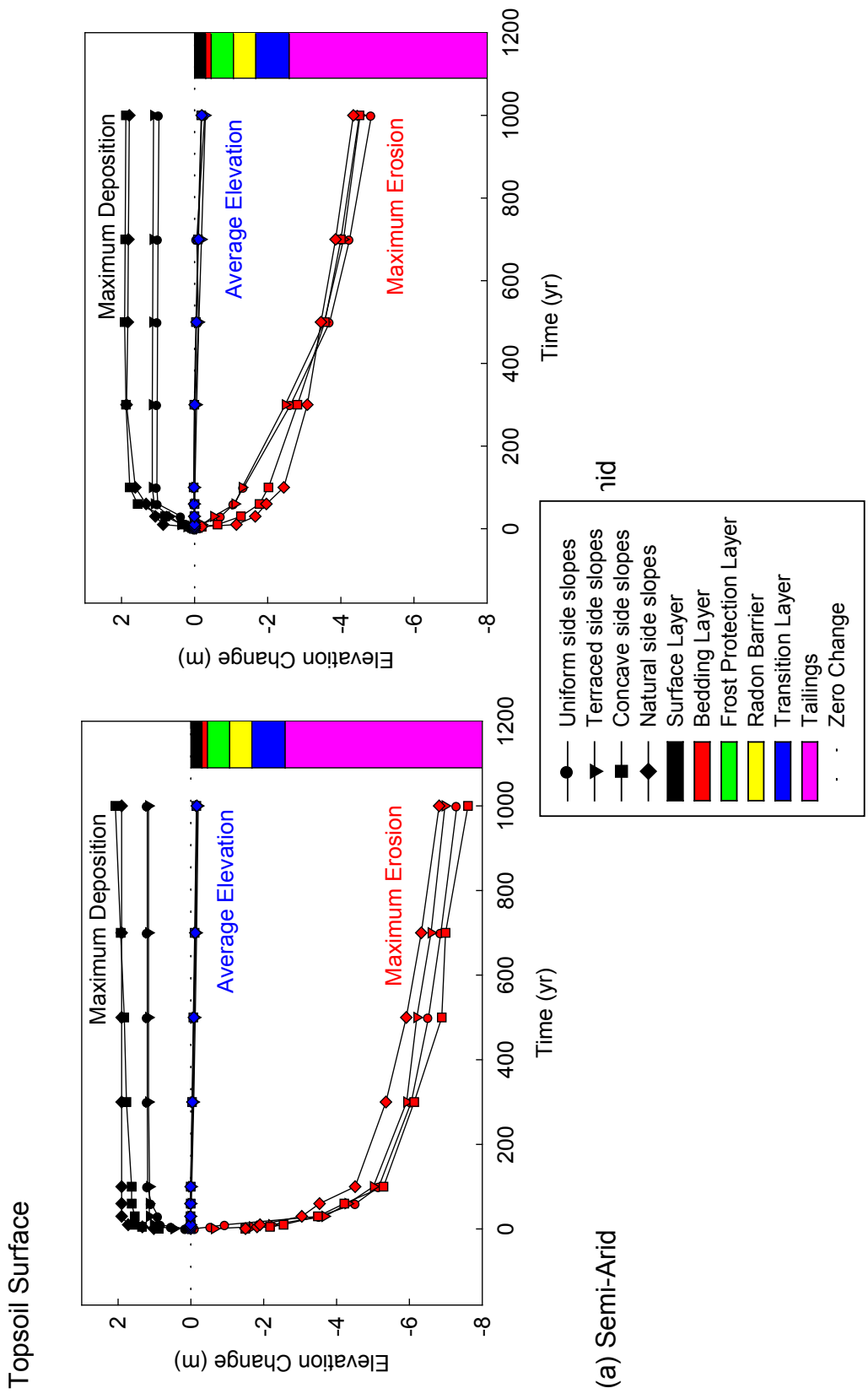


Fig. 4.20. Maximum erosion, maximum deposition, and average elevation change predicted by SIBERIA for resistive barriers with a topsoil surface and uniform, terraced, concave (semi-arid: shallow, humid: deep), or natural side slopes: (a) semi-arid climate and (b) humid climate.

Topsoil Surface (Semi-Arid Climate)

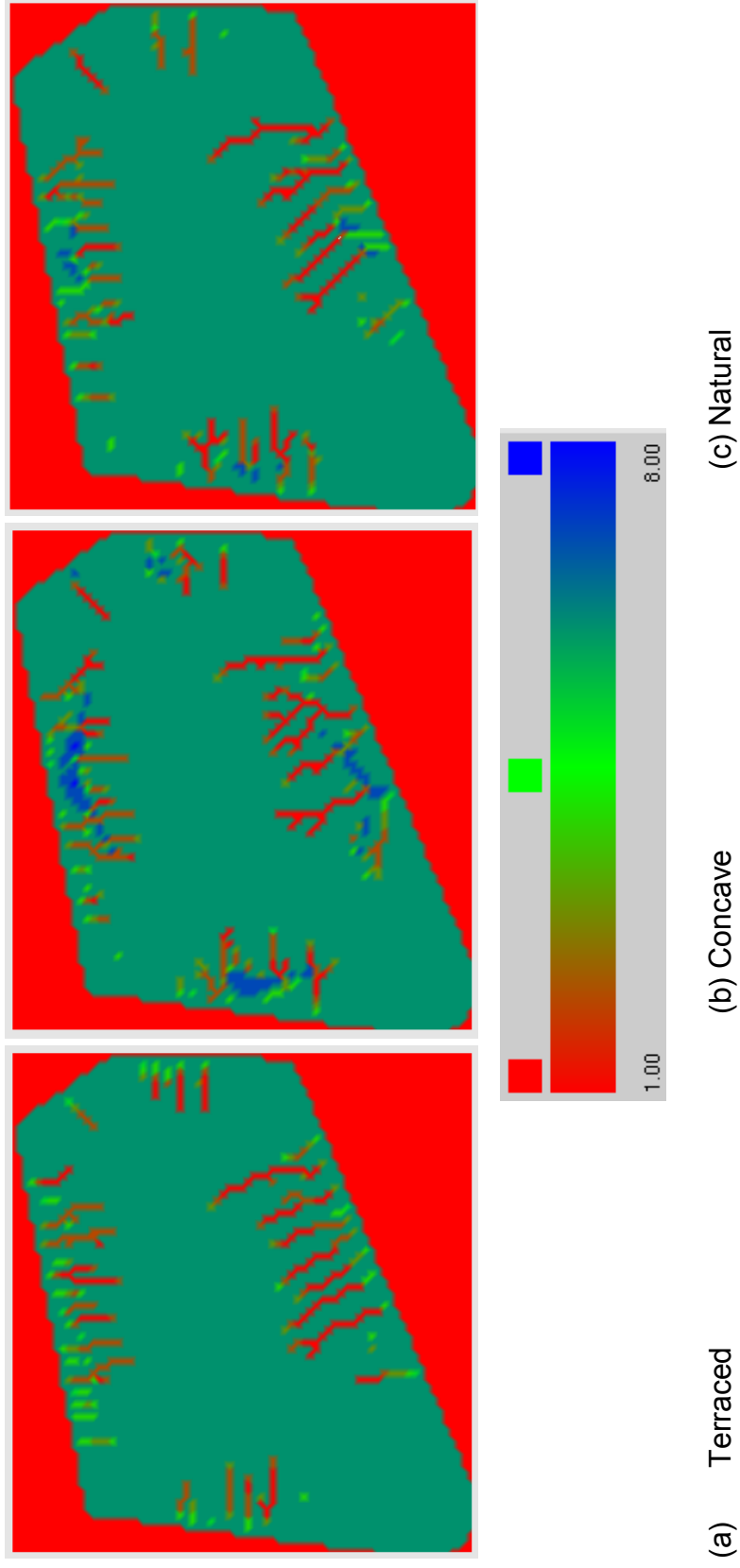


Fig. 4.21. Number of layers intact after 1000 years in a semi-arid climate predicted by SIBERIA for a resistive barrier with a topsoil surface: (a) terraced side slopes, (b) concave side slopes (shallow), and (c) natural side slopes.

Predictions of maximum erosion and average erosion depths for a topsoil surface in a humid climate are shown in Fig. 4.20 (b). After 1000 years, the concave and natural slopes have about 1 m more deposition than terraced slopes. Sediment is deposited at the base of the concave slope (blue shading) shown in Fig. 4.22. This increased deposition does have a small effect on maximum erosion depth, with concave and natural slopes having less maximum erosion than terraced slopes (Fig. 4.20 (b)). The topsoil in the humid climate behaves similarly to rip-rap and gravel admixture in the semi-arid climate because erosion is more widespread for a topsoil surface in a humid climate due to the smaller particle size of topsoil. The three surfaces in the humid climate can be compared by the following figures: rip-rap, Fig. 4.16; gravel admixture, Fig. 4.19; topsoil, Fig. 4.22. Additional figures showing the elevation and surface views of the scenarios producing the least erosion are in Appendix G.

Topsoil Surface (Humid Climate)

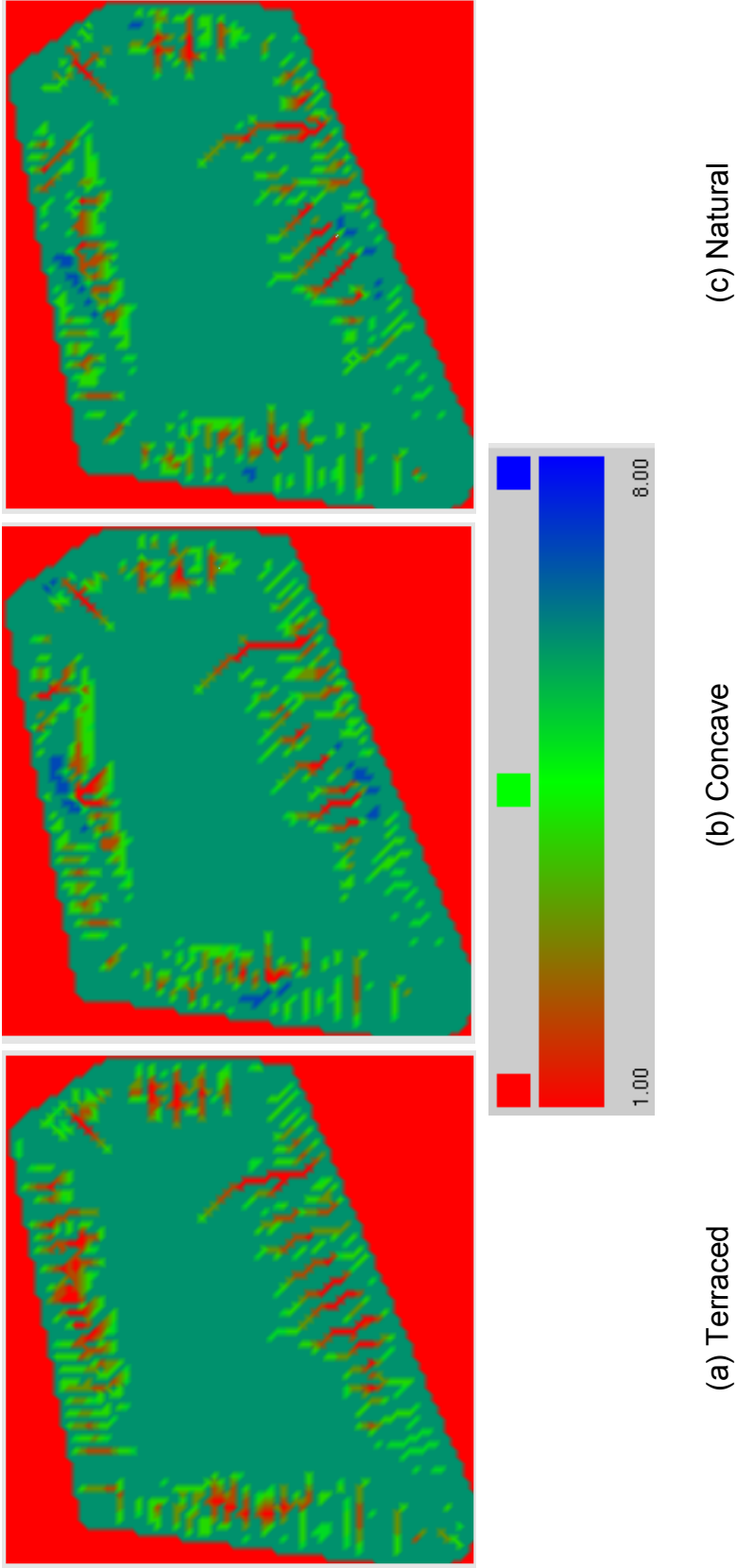


Fig. 4.22. Number of layers intact after 1000 years in a humid climate predicted by SIBERIA for a resistive barrier with a topsoil surface: (a) terraced side slopes, (b) concave side slopes (deep), and (c) natural side slopes.

5 SUMMARY AND PRACTICAL IMPLICATIONS

The objective of this study was to evaluate strategies to control erosion and percolation through barriers used for LLRW disposal sites. Two models were used to evaluate strategies; the SIBERIA landform evolution model was used to predict erosion and the SVFLUX hydrologic model was used to predict percolation into the stored waste (tailings in this study). Predictions from these two models were used to assess barrier design strategies in semi-arid and humid climates in terms of ability to limit erosion and percolation into the tailings. Type of barrier, type of surface layer, presence of vegetation, and type of side slope topography were evaluated for their effects on erosion and hydrology.

Three surface layers were evaluated: topsoil, rip-rap, and gravel admixture. Armored surfaces such as rip-rap and gravel admixture had less erosion than finer textured surfaces, such as topsoil. However, armoring a barrier with rip-rap transmits more percolation than any other surface layer in either climate due to water trapping induced by the textural contrast between the rip-rap and underlying finer layers. In contrast, a gravel admixture surface layer erodes more than a rip-rap surface, but transmits less percolation in either climate.

Incorporating vegetation reduces erosion and promotes evapotranspiration, decreasing percolation. For the examples that were evaluated, vegetation reduced erosion by 1.5 m in the semi-arid climate and 4 m in the humid climate over 1000 years. Barriers that employ a surface layer employing a gravel admixture and planted with native vegetation are expected to provide a good balance between effective control of erosion and percolation. Rip-rap could be used on side slopes outside the limits of waste to control erosion in areas where erosive effects are more significant and percolation is not important.

Slope length and grade difference at the nickpoint affect erosion. Erosion is greater for longer slopes and slopes with a large-grade difference at the nickpoint between the top and side slopes. Grade difference may be more important than slope length; therefore reducing changes in grade at the nickpoint will reduce erosion. Creating a smoother nickpoint, as in natural side slopes, will slow the erosion process and yield less deep erosion in upslope regions. Slope lengths should be kept as short as practical and grade differences as small as practical to reduce erosion.

Slope shape affects both erosion and deposition of sediment. In areas where larger amounts of erosion occur (i.e. semi-arid climates), erosion can be mitigated through the use of concave or natural slopes that deposit eroded sediment on site. Terraced slopes with an armored surface prevent the most erosion in a humid climate. Terraces cause a smaller erosion rate due to the use of many short slope lengths.

Use of “bands” of rip-rap on side slopes (alternating rip-rap with other material), humps at the end of each terrace to aide on-site deposition, and chemicals to limit

both erosion and percolation (i.e. bentonite, sodium nitrate, gypsum) should be evaluated in future studies. Other future work should expand the use of native vegetation to include more varieties and the strategic placement of various varieties so they may have the greatest effect on controlling erosion and percolation.

6 REFERENCES

- Allen, Z. (2010, April 13). *Fire Weather Operating Plan*, Retrieved April 25, 2011, from National Weather Service: http://www.erh.noaa.gov/pbz/fwxw/ops_plan_10.htm
- Anderson, C., and Stormont, J. (1997). *Prediction of long-term erosion from landfill covers in the southwest*, Conference Proceedings, International Containment Technology Conference, February 9-12, 1997, St. Petersburg, FL. USA, 389-395.
- Anderson, C., and Stormont, J. (2005). Gravel Admixtures for Erosion Protection in Semi-Arid Climates. In J. Briaud, and S. Bhatia (Ed.), *Geo-Frontiers 2005 Congress Geotechnical Special Publication No. 135 Erosion of Soils and Scour of Foundations*, American Society of Civil Engineers, Austin, TX, USA.
- Benson, C. (2001). Waste Containment: Strategies and Performance, *Australian Geomechanics*, 36 (4).
- Benson, C. (2011, April 18). *Water Balance Modeling*, University of Wisconsin-Madison, Madison, WI, USA.
- Benson, C., Lee, S., Wang, X., Albright, W., and Waugh, W. (2008). *Hydraulic Properties and Geomorphology of the Earthen Component of the Final Cover at the Monticello Uranium Mill Tailings Repository*, Geo Engineering Report No. 08-04, University of Wisconsin-Madison, Desert Research Institute, and US Department of Energy Environmental Sciences Laboratory.
- Benson, C., Sawangsuriya, A., Trzebiatowski, B., and Albright, W. (2007). Postconstruction Changes in the Hydraulic Properties of Water Balance Cover Soils, *Journal of Geotechnical and Geoenvironmental Engineering*, 133 (4), 349-359.
- Benson, C., Waugh, W., Albright, W., and Smith, G. (2010). *The RECAP Test Sections at the Grand Junction Disposal Site: Construction Documentation and Instrument Calibration*, Geological Engineering, University of Wisconsin-Madison, Madison, WI, USA.
- Benson, C. and Gurdal, T. (2013), Hydrologic Properties of Final Cover Soils, Foundation Engineering in the Face of Uncertainty, *GSP No. 229*, J. Withiam et al., Eds., ASCE, Reston VA, 283-297.
- Benson, C., Albright, W., Fratta, D., Tinjum, J., Kucukkirca, E., Lee, S., Scalia, J., Schlicht, P., Wang, X. (2011), Engineered Covers for Waste Containment: Changes in Engineering Properties & Implications for Long-Term Performance Assessment, NUREG/CR-7028, Office of Research, U.S. Nuclear Regulatory Commission, Washington.

Bohnhoff, G., Ogorzalek, A., Benson, C., Shackelford, C., and Apiwantragoon, P. (2009), Field Data and Water-Balance Predictions for a Monolithic Cover in a Semiarid Climate, *J. Geotech. and Geoenvironmental Eng.*, 135(3), 333-348.

Braun, J., and Sambridge, M. (1997). Modelling landscape evolution on geological time scales: a new method based on irregular spatial discretization, *Basin Research*, 9, 27-52.

Coulthard, T. (2001). Landscape evolution models: a software review, *Hydrological Processes*, 15, 165-173.

Coulthard, T., and Macklin, M. (2000). How sensitive are river systems to climate and land-use changes? A model based evaluation, *Journal of Quaternary Science*.

Coulthard, T., Maklin, M., and Kirkby, M. (2002). A cellular model of Holocene upland river basin and alluvial fan evolution, *Earth Surface Processes and Landforms*, 27, 269-288.

Coulthard, T., Hicks, D., and Van De Wiel, M. (2007). Cellular Modelling of river catchments and reaches: Advantages, limitations and prospects, *Geomorphology* 90, 192-207.

Coulthard, T. , Kirkby, M., and Macklin, M. (1998). Non-linearity and spatial resolution in a cellular automaton model of a small upland basin, *Hydrology and Earth System Sciences*, 2, 257-264.

Coulthard, T., Kirkby, M., and Macklin, M. (2000). Modelling geomorphic response to environmental change in an upland catchment, *Hydrological Processes*, 14, 2031-2045.

Coulthard, T., Kirkby, M., and Macklin, M. (1999). Modelling the impacts of Holocene environmental change on the fluvial and hillslope morphology of an upland landscape, using a cellular automaton approach, *Fluvial Processes and Environmental Change*, 31-47.

Dinwiddie, C., and Walter, G. (2008). *Software validation test plan and report for EAMS Version 2.09 and SIBERIA Version 8.33*, Center for Nuclear Waste Regulatory Analyses. U.S. Nuclear Regulatory Commission.

DOE Office of Legacy Management. (2009, May 5). Grand Junction, Colorado, Processing Site and Disposal Site, U.S. Department of Energy Office of Legacy Management, Grand Junction, CO, United States of America.

USEPA. (1983). Standards for the Disposal of Uranium Mill Tailings, *40 CFR 192*, Washington, D.C., USA.

Evans, K., and Willgoose, G. (2000). Post-mining landform evolution modelling: 2. Effects of vegetation and surface ripping, *Earth Surface Processes and Landforms*, 25, 803-823.

Fangmeier, R., Elliot, W., Workman, S., Huffman, R., and Schwab, G. (2006). *Soil and Water Conservation Engineering* (5th ed.), Thomson Delmar Learning, Clifton Park, NY, USA.

Flanagan, D., and Meyer, C. (2010, December 8). *WEPP: Spilling the Secrets of Water Erosion*, Retrieved December 9, 2010 from <http://www.ars.usda.gov/is/AR/archive/apr97/wepp0497.htm?pf=1>

Flanagan, D., and Nearing, M. (1995). *NSERL Report No. 10 USDA - Water Erosion Prediction Project Hillslope Profile and Watershed Model Documentation*, USDA-ARS National Soil Erosion Research Laboratory, West Lafayette, IN, USA.

Foster, G., Flanagan, D., Nearing, M., Lane, L., Risse, L., and Finkner, S. (1995). *NSERL Report No. 10 Technical Documentation: USDA-Water Erosion Prediction Project (WEPP)*, National Soil Erosion Research Laboratory USDA-ARS-MWA, West Lafayette, IN, USA.

Grand Valley Project. (2011, May 10). Retrieved May 13, 2011, from United States Department of the Interior, Bureau of Reclamation: http://www.usbr.gov/projects/Project.jsp?proj_Name=Grand%20Valley%20Project&dpagetype=ProjectDataPage

Gurdal, T., Benson, C., and Albright, W. (2003). *Hydrologic properties of final cover soils from the alternative cover assessment program*, Geo-Engineering Report No. 03-02, Geo-Engineering Program, University of Wisconsin – Madison, Madison, WI, USA.

Hancock, G. (2004). The use of landscape evolution models in mining rehabilitation design, *Environmental Geology*, 46, 562-573.

Hancock, G., and Turley, E. (2006). Evaluation of proposed waste rock dump designs using the SIBERIA erosion model, *Environmental Geology*, 49, 765-779.

Hancock, G., and Willgoose, G. (2001). Use of a landscape simulator in the validation of the SIBERIA catchment evolution model: Declining equilibrium landforms, *American Geophysical Union*, 37 (7), 1981-1992.

Hancock, G., Evans, K., Willgoose, G., Moliere, D., Saynor, M., and Loch, R. (2000). Medium-term erosion simulation of an abandoned mine site using the SIBERIA landscape evolution model, *Australian Journal of Soil Research*, 38, 249-263.

Hancock, G., Loch, R., and Willgoose, G. (2003). The design of post-mining landscapes using geomorphic principles, *Earth Surface Processes and Landforms*, 28, 1097-1110.

Hancock, G., Lowry, J., Coulthard, T., Evans, K., and Moliere, D. (2010). A catchment scale evaluation of the SIBERIA and CAESAR landscape evolution models, *Earth Surface Processes and Landforms*, 35, 863-875.

Hancock, G., Lowry, J., Moliere, D., and Evans, K. (2008). An evaluation of an enhanced soil erosion and landscape evolution model: a case study assessment of the former Nabarlek uranium mine, Northern Territory, Australia, *Earth Surface Processes and Landforms*, 33, 2045-2063.

Holtz, R. and Kovacs, W. (1981). *An Introduction to Geotechnical Engineering*. Prentice Hall, Upper Saddle River, NJ, USA.

Hudson, N. (1987). *Soil and water conservation in semi-arid areas*, Food and Agriculture Organization of the United Nations, Amptill, Bedford, U.K.

Kirkby, M. (1971). Hillslope process-response models based on the continuity equation, *Slopes Form and Process*, 15-30.

Kirkham, M. (2005). *Principles of Soil and Plant Water Relations*, Elsevier Inc., Burlington, MA, USA.

Klett, J., Fahey, B., and Cox, R. (2010, May 12). *Native Shrubs for Colorado Landscapes*, Retrieved April 21, 2011, from Colorado State University Extension: <http://www.ext.colostate.edu/pubs/garden/07422.html>

McFadden, L., Wells, S., and Jercinovich, M. (1987). Influences of eolian and pedogenic processes on the origin and evolution of desert pavements, *Geology*, 15, 504-508.

Morgan, R. (1995). *Soil Erosion and Conservation*, Longman Group Limited, Essex, England.

Nearing, M. (2004). Capabilities and limitations of erosion models and data, *13th International Soil Conservation Organisation Conference*, Brisbane: Conserving Soil and Water for Society: Sharing Solutions, 1-6.

Penman, H. (1948). Natural evapotranspiration from open water, bare soil and grass, *Proceedings of the Royal Society A*, London, 120-145.

Richardson, G. and Waugh, W.J. (1996). *The design of final covers systems for arid and semi-arid regions of the west*, 3rd International Symposium on Environmental Geotechnology, June 10-12, 1996.

Sackschewsky, M., Kemp, C., Link, S., and Waugh, W. J. (1995). Soil water balance changes in engineered soil surfaces, *Journal of Environmental Quality*, 24, 352-359.

Sharmeen, S. (2000). *Modelling the long-term evolution of mine spoils, soil erosion and soil development*, PhD Thesis, University of Newcastle, Australia, Department of Civil, Surveying, and Environmental Engineering.

SoilVision Systems Ltd. (2004-2010). *SVOFFICE Overview*, Retrieved March 22, 2011 from <http://www.soilvision.com/subdomains/svoffice.com/index.shtml>

Stormont, J., and Anderson, C. (2003). *Erosional stability of the proposed Lee Acres cover*, Report to Cheney – Walters – Echols, University of New Mexico, Albuquerque, NM, USA.

Toy, T., Foster, G., and Galetovic, J. (1998). *Guidelines for the Use of the Revised Universal Soil Loss Equation (RUSLE) Version 1.06 on Mined Lands, Construction Sites, and Reclaimed Lands*, The Office of Technology Transfer, Western Regional Coordinating Center, Office of Surface Mining, Denver, CO, USA.

Toy, T., Foster, G., and Renard, K. (2002). *Soil Erosion: Processes, Prediction, Measurement, and Control*. John Wiley and Sons, Inc., New York, NY, USA.

Tucker, G., and Slingerland, R. (1994). Erosional dynamics, flexural isostasy, and long-lived escarpments: A numerical modeling study, *Journal of Geophysical Research*, 99 (B6), 12229-12243.

Tucker, G., Gasparini, N., Lancaster, S., and Bras, R. (1997). *An Integrated Hillslope and Channel Evolution Model as an Investigation and Prediction Tool*, Year 2 annual report DACA99-95-R-0020, Department of Civil and Environmental Engineering, Massachusetts Institute of Technology, Cambridge, MA, USA.

Tucker, G., Gasparini, N., Lancaster, S., and Gras, R. (1997). *An integrated hillslope and channel evolution model as an investigation and prediction tool*, Technical Report prepared for the U.S. Army Corps of Engineers.

Tucker, G., Lancaster, S., Gasparini, N., Bras, R., and Rybarczyk, S. (2001). An object-oriented framework for distributed hydrologic and geomorphic modeling using triangulated irregular networks, *Computers and Geosciences*, 27, 959-973.

USDA-ARS. (2008). *Draft User's Reference Guide Revised Universal Soil Loss Equation Version 2*, USDA-Agricultural Research Service, Washington, D.C., USA.

USDA-ARS. (2010). *Revised Universal Soil Loss Equation 2 - RUSLE2 Development*. Retrieved February 23, 2011 from <http://www.ars.usda.gov/Research/docs.htm?docid=6027>

USDA-ARS. (2010 (2)). *Revised Universal Soil Loss Equation 2 - How RUSLE2 Computes Rill and Interrill Erosion*, Retrieved February 23, 2011 from <http://www.ars.usda.gov/Research/docs.htm?docid=6014>

USDA-ARS. (1995). *WEPP User Summary*, USDA-ARS-MWA, National Soil Erosion Research Laboratory, West Lafayette, IN, USA.

Van De Wiel, M., Coulthard, T., Macklin, M., and Lewin, J. (2007). Embedding reach-scale fluvial dynamics within the CAESAR cellular automaton landscape evolution model, *Geomorphology* 90 , 283-301.

Walter, G., and Dubreuilh, P. (2007). *Evaluation of approaches to simulate engineered cover performance and degradation*, U.S. Nuclear Regulatory Commission. Center for Nuclear Waste Regulatory Analyses, San Antonio, TX, USA.

Waugh, W., Thiede, M., Bates, D., Cadwell, L., Gee, G., and Kemp, C. (1994). Plant cover and water balance in gravel admixtures at an arid waste-burial site, *Journal of Environmental Quality*, 23, 676-685.

Welsh, K., Dearing, J., Chiverrell, R., and Coulthard, T. (2009). Testing a cellular modelling approach to simulating late-Holocene sediment and water transfer from catchment to lake in the French Alps since 1826, *The Holocene*, 19 (5), 785-798.

White, R. (2010). *Fire Weather Operating Plan*, Retrieved May 13, 2011, from National Weather Service, Pittsburgh, PA:
http://www.erh.noaa.gov/pbz/fxwx/ops_plan_10.htm

Willgoose, G. (2010, December 6). Personal interview, C. L. Smith, Interviewer.

Willgoose, G. (2005b). Mathematical Modeling of Whole Landscape Evolution, *Annual Review of Earth and Planetary Sciences*, 33, 443-459.

Willgoose, G. (2005a). *User Manual for SIBERIA*, Retrieved March 1, 2010, from Telluric Research: <http://www.telluricresearch.com/index.html>

Willgoose, G., and Riley, S. (1998). Application of a catchment evolution model to the prediction of long-term erosion on the spoil heap at Ranger uranium mine: Initial analysis, *Supervising Scientist Report 132, Supervising Scientist, Canberra* .

Willgoose, G., and Sharmeen, S. (2006). A One-dimensional model for simulating armouring and erosion on hillslopes: 1. Model development and event-scale dynamics, *Earth Surface Processes and Landforms*, 31, 970-991.

Willgoose, G., Bras, R., and Rodriguez-Iturbe, I. (1991a). A coupled channel network growth and hillslope evolution model: 1. Theory, *Water Resources Research*, 27 (7), 1671-1684.

Willgoose, G., Bras, R., and Rodriguez-Iturbe, I. (1991b). A physically based coupled network growth and hillslope evolution model: 2 Applications, *Water Resources Research*, 27 (7), 1685-1696.

Willgoose, G., Bras, R., and Rodriguez-Iturbe, I. (1991c). Results from a new model of river basin evolution, *Earth Surface Processes and Landforms*, 16, 237-254.

Wilson, G., Fredlund, D., and Barbour, S. (1994). Coupled soil-atmosphere modeling for soil evaporation, *Canadian Geotechnical Journal*, 31, 151-161.

Wischmeier, W., and Smith, D. (1978). *Predicting rainfall-erosion losses: A guide to conservation planning*, Agriculture Handbook 537, U.S. Department of Agriculture, Washington, D.C., USA.

APPENDIX A

WEPP Sensitivity Analysis to Initial Soil Water Content and Albedo

Appendix A: WEPP Sensitivity Analysis to Initial Soil Water Content and Albedo

A sensitivity analysis was performed to determine if the initial soil water content and the soil albedo had an effect on sediment loss within WEPP. The following tables represent these sensitivity analyses. The figures and tables in this appendix coincide with Section 3.2.1.

Table A.1. Effects of initial soil water content on discharge and sediment loss in WEPP. All other factors held constant.

Initial Soil Water Content	Discharge, q	Sediment Loss, q_s
%	mm/yr	kg/m ²
17	0.43	0.004
16	0.43	0.004
15	0.43	0.004
10	0.43	0.004
20	0.43	0.004
80	0.43	0.004
0	0.43	0.004

Table A.2. Effects of soil albedo on discharge and sediment loss in WEPP.
All other factors held constant.

Soil Albedo	Discharge, q	Sediment Loss, q_s
-	mm/yr	kg/m ²
0.25	0.43	0.004
0.35	0.43	0.004
0.5	0.43	0.004
0.9	0.53	0.005
0.75	0.44	0.005
0.6	0.44	0.005
0.1	0.43	0.004

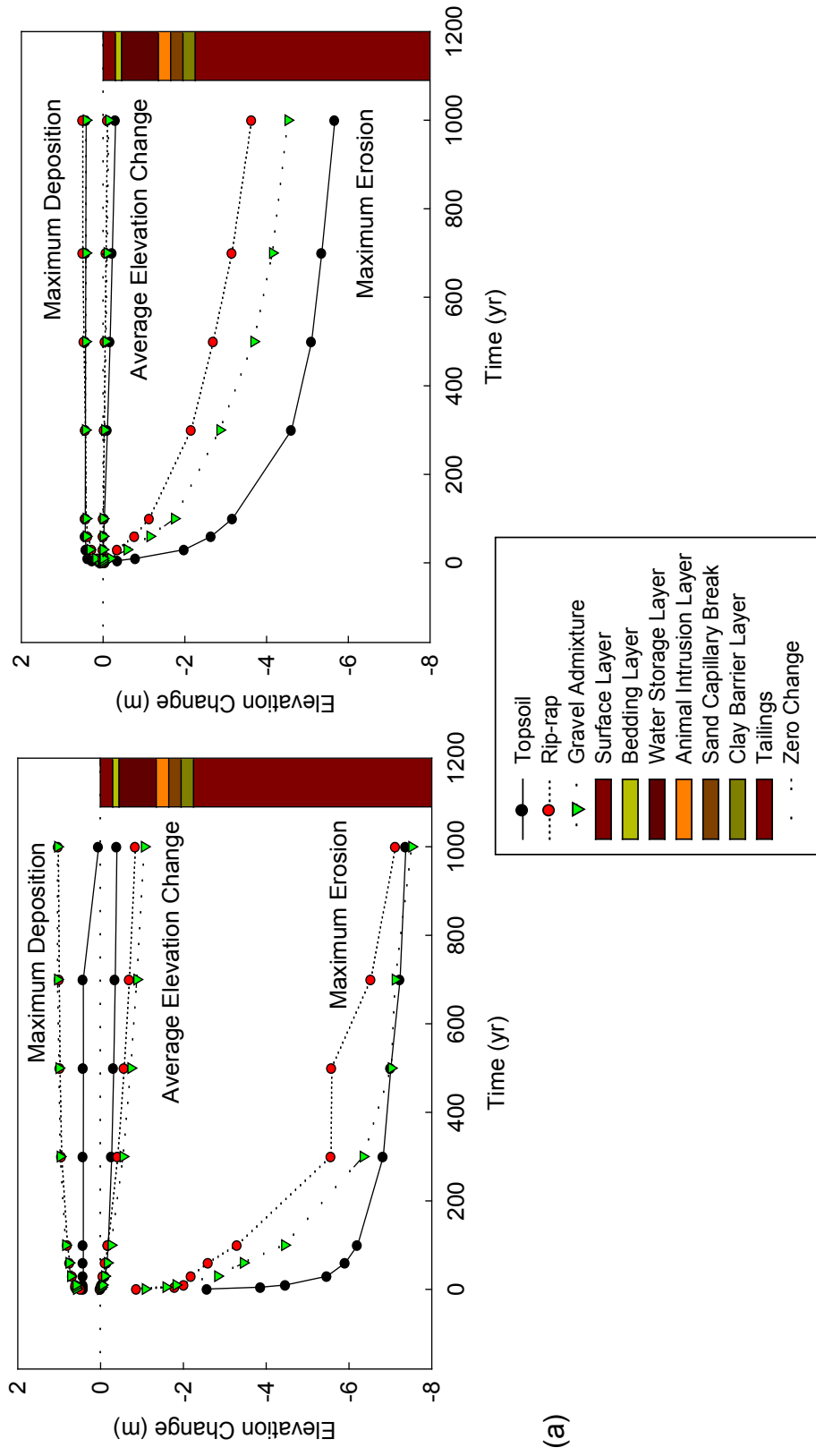
APPENDIX B

SIBERIA Predictions for Covers with Water Balance Barriers

Appendix B: SIBERIA Predictions for Covers with Water Balance Barriers

Erosion predicted by SIBERIA is shown for rip-rap, gravel admixture, and topsoil surface layers with a water balance barrier for the semi-arid and humid climate. The site topography used is the reference site, shown in Figure 3.1. The figures in this appendix coincide with Section 4.1.2.

Water Balance Barrier – Representative Site Topography



(a)

Figure B.1. Maximum erosion, maximum deposition, and average elevation change predicted by SIBERIA for rip-rap, topsoil, and gravel admixture surface layer for a water balance barrier using the representative site topography: (a) semi-arid climate and (b) humid climate.

Water Balance Barrier – Rip-rap Surface – Semi-Arid Climate

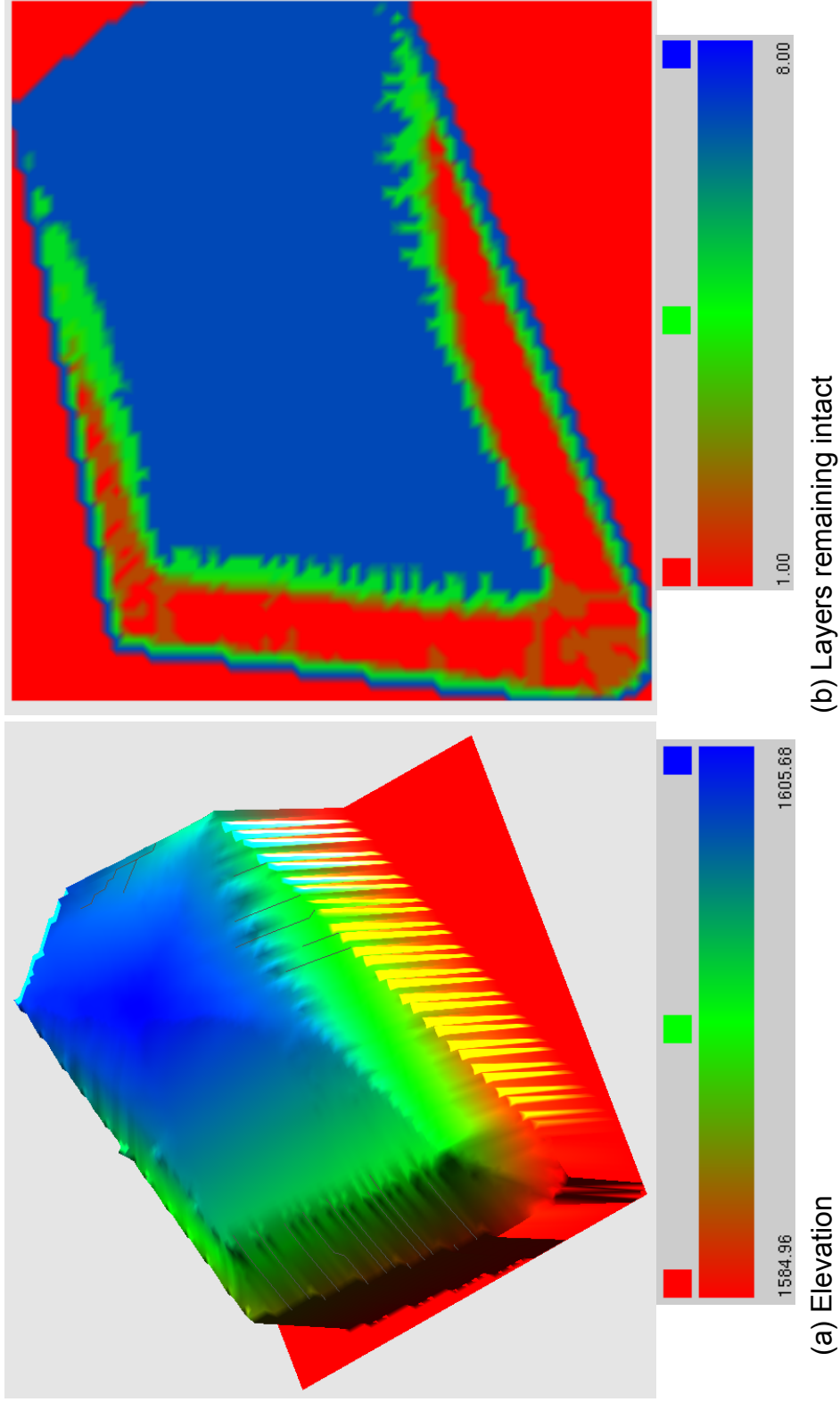


Figure B.2. Erosion predicted by SIBERIA for a rip-rap surface with a water balance barrier in a semi-arid climate using the representative site topography: a) elevation predictions of the surface after 1000 years of erosion and, b) number of layers remaining intact after 1000 years of erosion, plan view.

Water Balance Barrier – Gravel Admixture Surface – Semi-Arid Climate

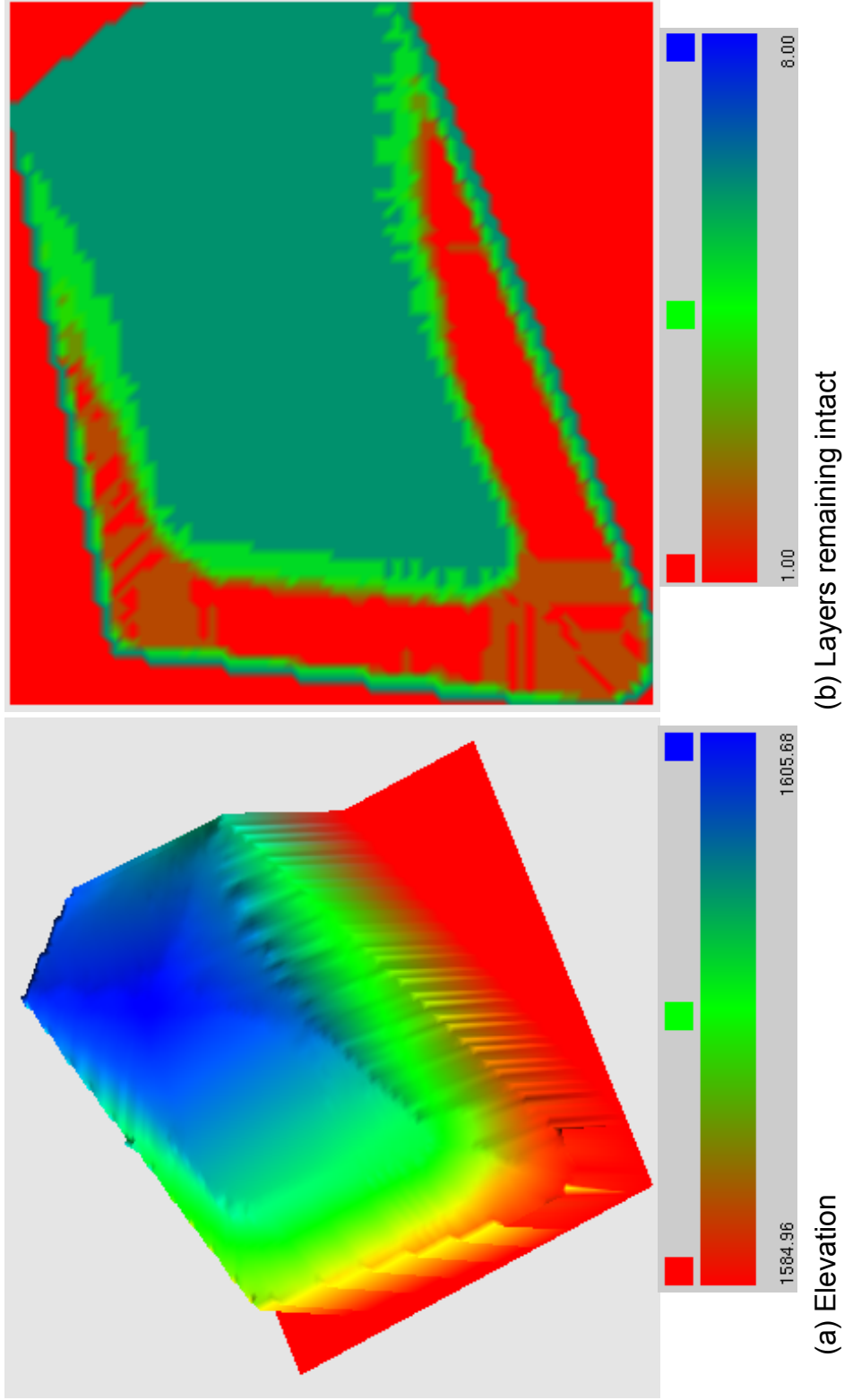


Figure B.3. Erosion predicted by SIBERIA for a gravel admixture surface with a water balance barrier in a semi-arid climate using the representative site topography: a) elevation predictions of the surface after 1000 years of erosion and, b) number of layers remaining intact after 1000 years of erosion, plan view.

Water Balance Barrier – Topsoil Surface – Semi-Arid Climate

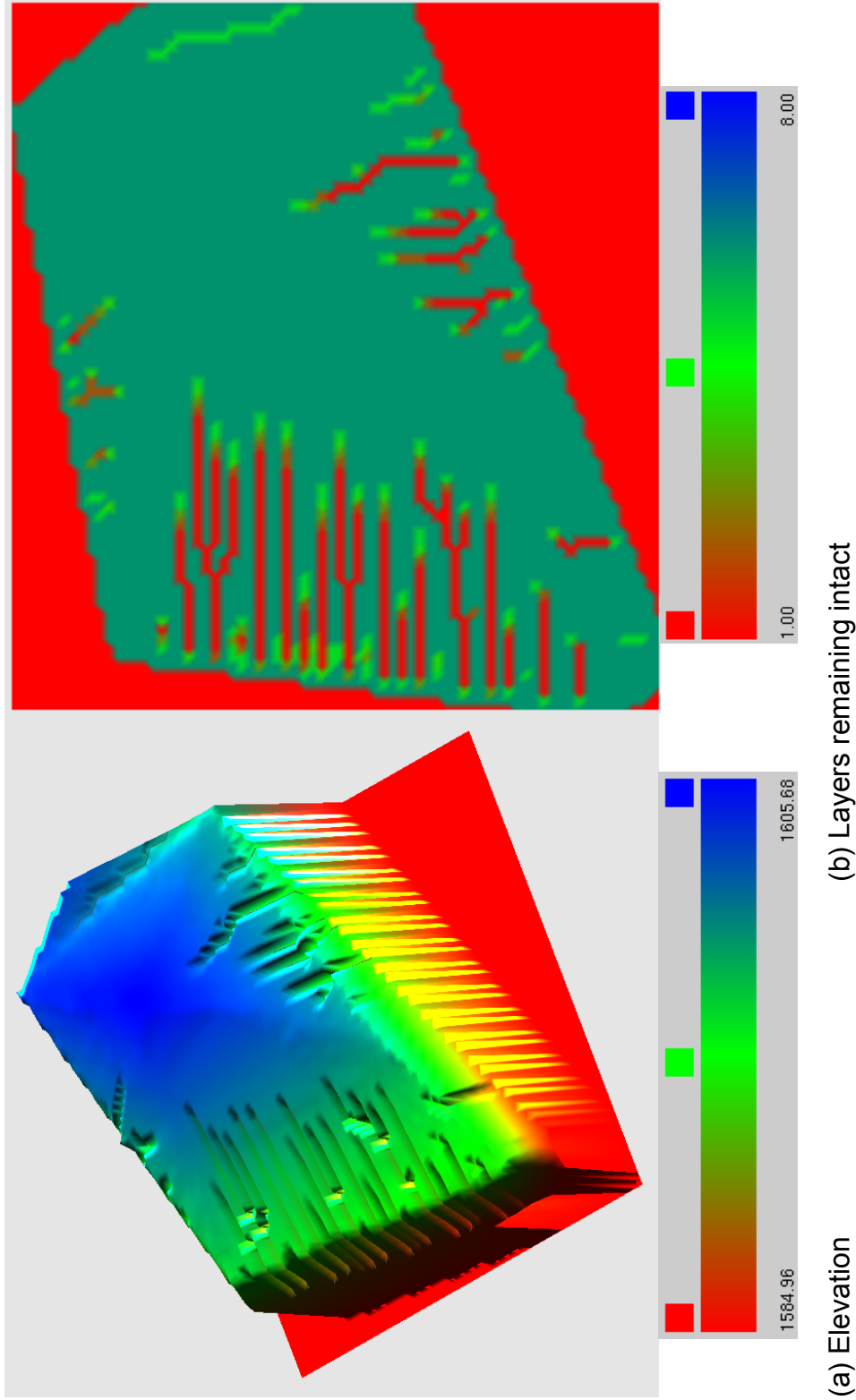


Figure B.4. Erosion predicted by SIBERIA for a topsoil surface with a water balance barrier in a semi-arid climate using the representative site topography: a) elevation predictions of the surface after 1000 years of erosion and, b) number of layers remaining intact after 1000 years of erosion, plan view.

Water Balance Barrier – Rip-rap Surface – Humid Climate

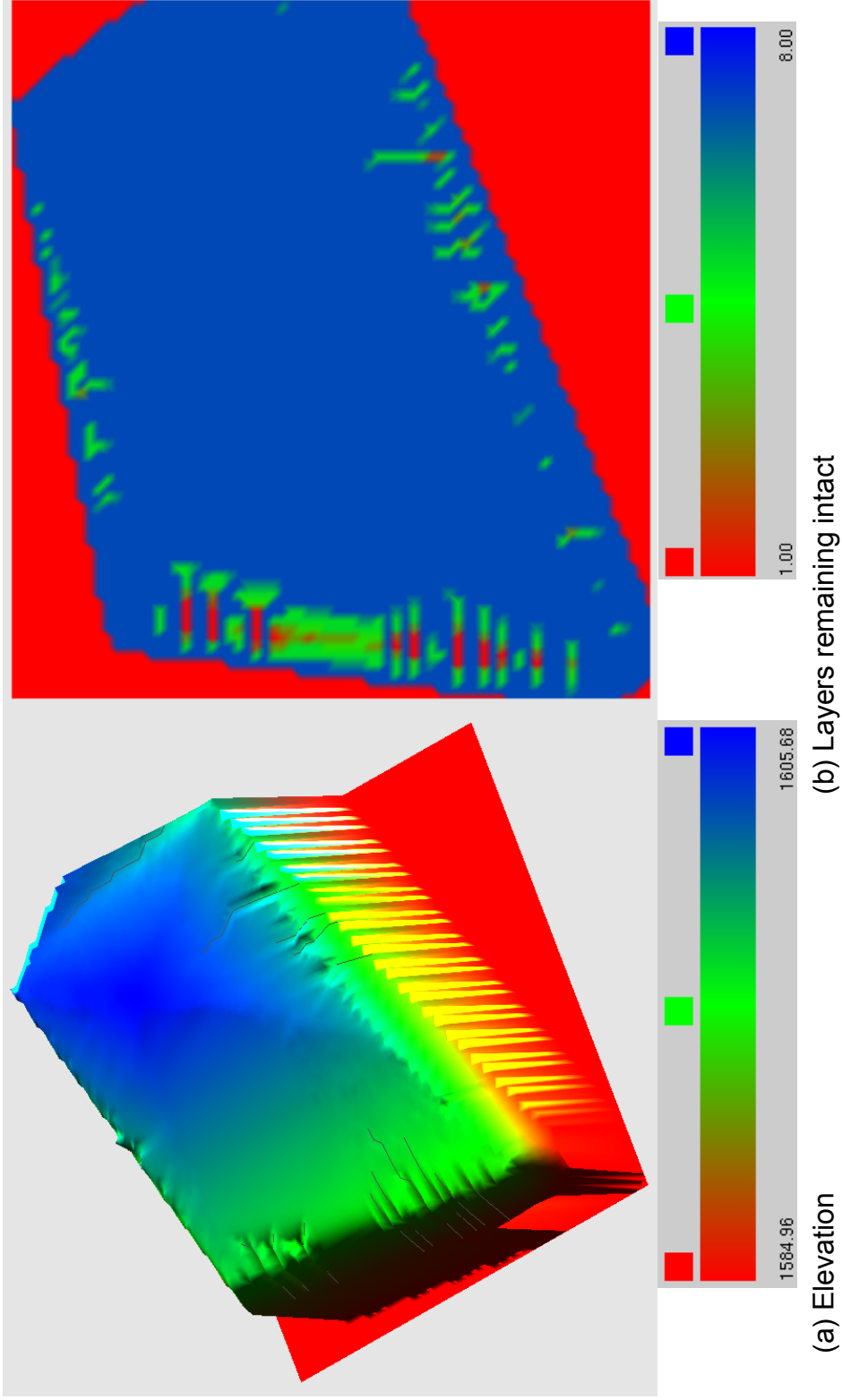


Figure B.5. Erosion predicted by SIBERIA for a rip-rap surface on a water balance barrier in a humid climate using the representative site topography: a) elevation predictions of the surface after 1000 years of erosion and b) number of layers remaining intact after 1000 years of erosion, plan view.

Water Balance Barrier – Gravel Admixture Surface – Humid Climate

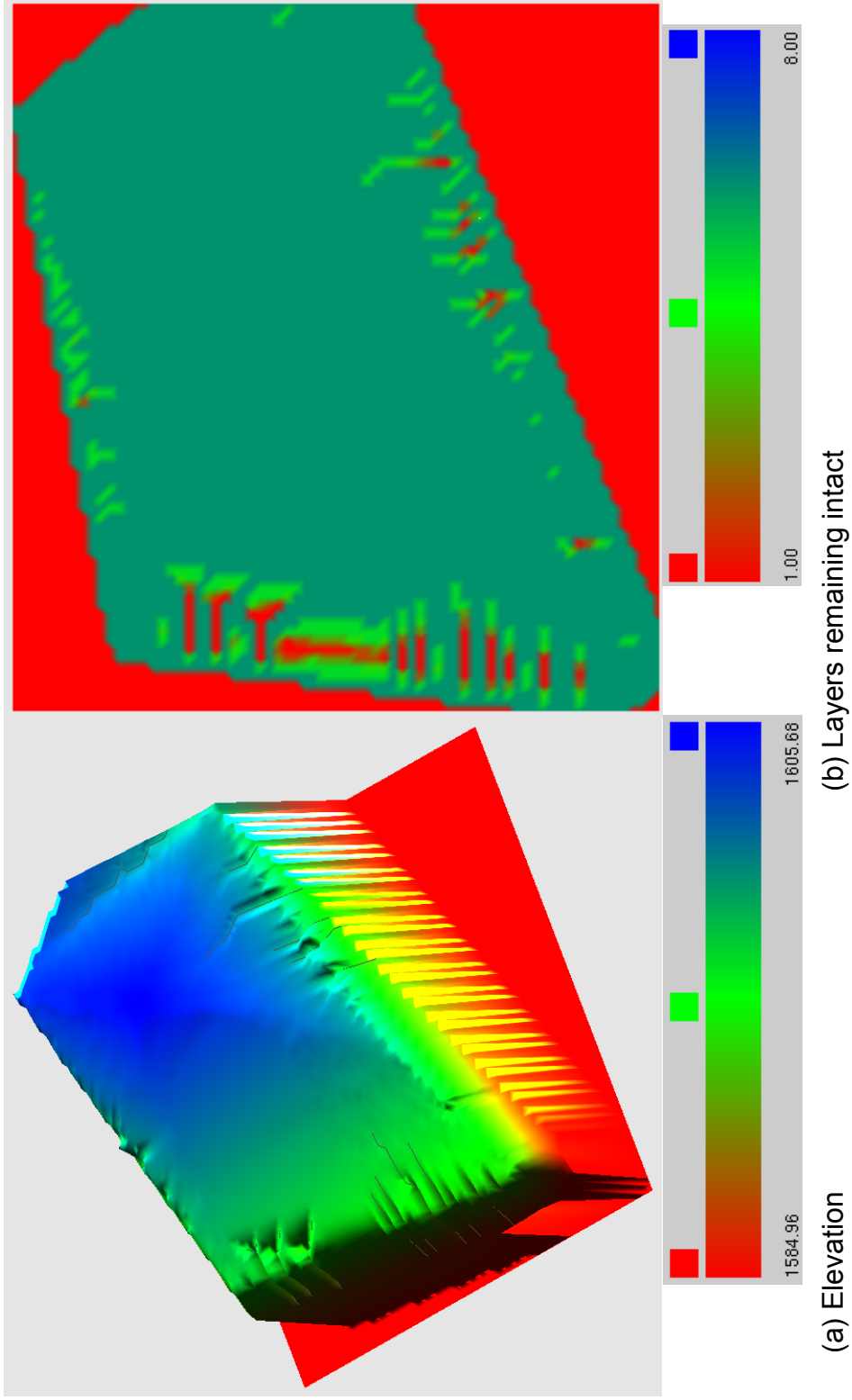


Figure B.6. Erosion predicted by SIBERIA for a gravel admixture surface on a water balance barrier in a humid climate using the representative site topography: a) elevation predictions of the surface after 1000 years of erosion and b) number of layers remaining intact after 1000 years of erosion, plan view.

Water Balance Barrier – Topsoil Surface – Humid Climate

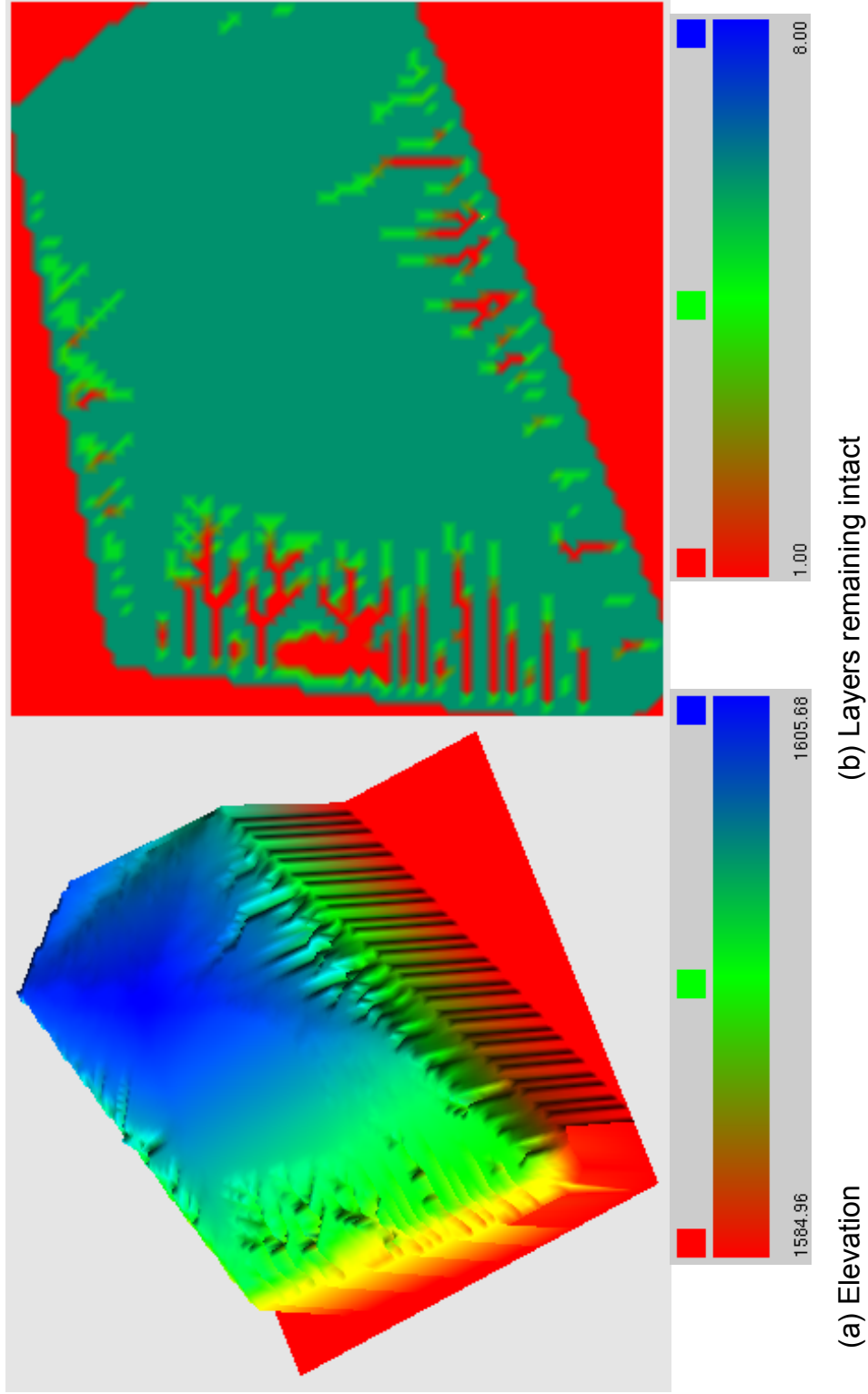


Figure B.7. Erosion predicted by SIBERIA for a topsoil surface on a water balance barrier in a humid climate using the representative site topography: a) elevation predictions of the surface after 1000 years of erosion and b) number of layers remaining intact after 1000 years of erosion, plan view.

APPENDIX C

SVFLUX Predictions for Resistive and Water Balance Covers

Appendix C: SVFLUX Predictions for Resistive and Water Balance Covers

The following figures show precipitation, evapotranspiration, soil-water storage, and cumulative percolation for resistive and water balance barriers for both resistive and water balance covers. Predictions are shown by climate. The figures in this appendix coincide with Section 4.1.3.

SVFLUX Predictions – Semi-Arid Climate

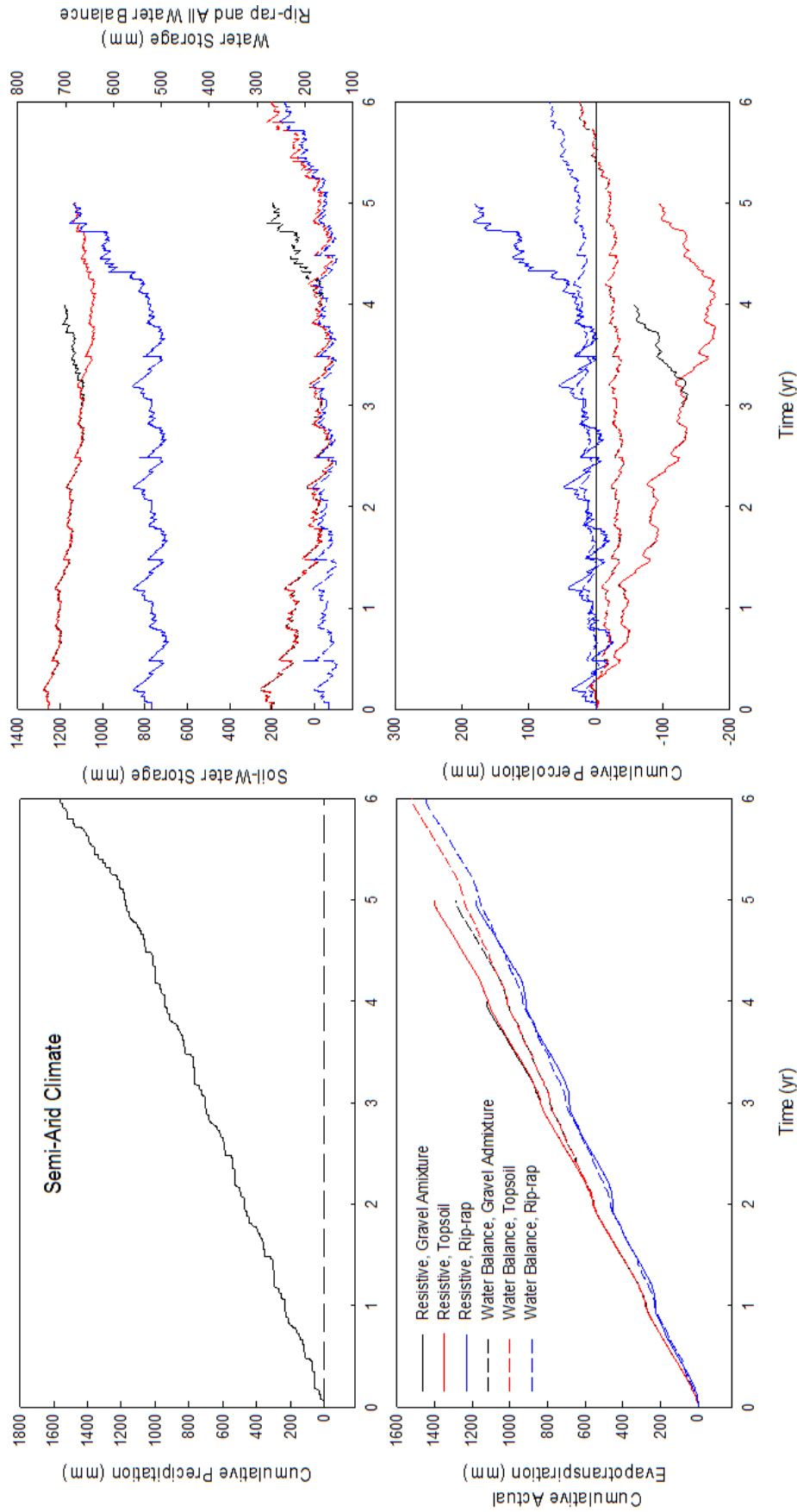


Figure C.1. Predictions from SVFLUX of precipitation, evapotranspiration, soil-water storage, and cumulative percolation for resistive and water balance barriers in a semi-arid climate. Some simulations required less years than others to stabilize. The last year of each simulation is the wettest year. Positive percolation is into the tailings, negative is out.

SVFLUX Predictions – Humid Climate

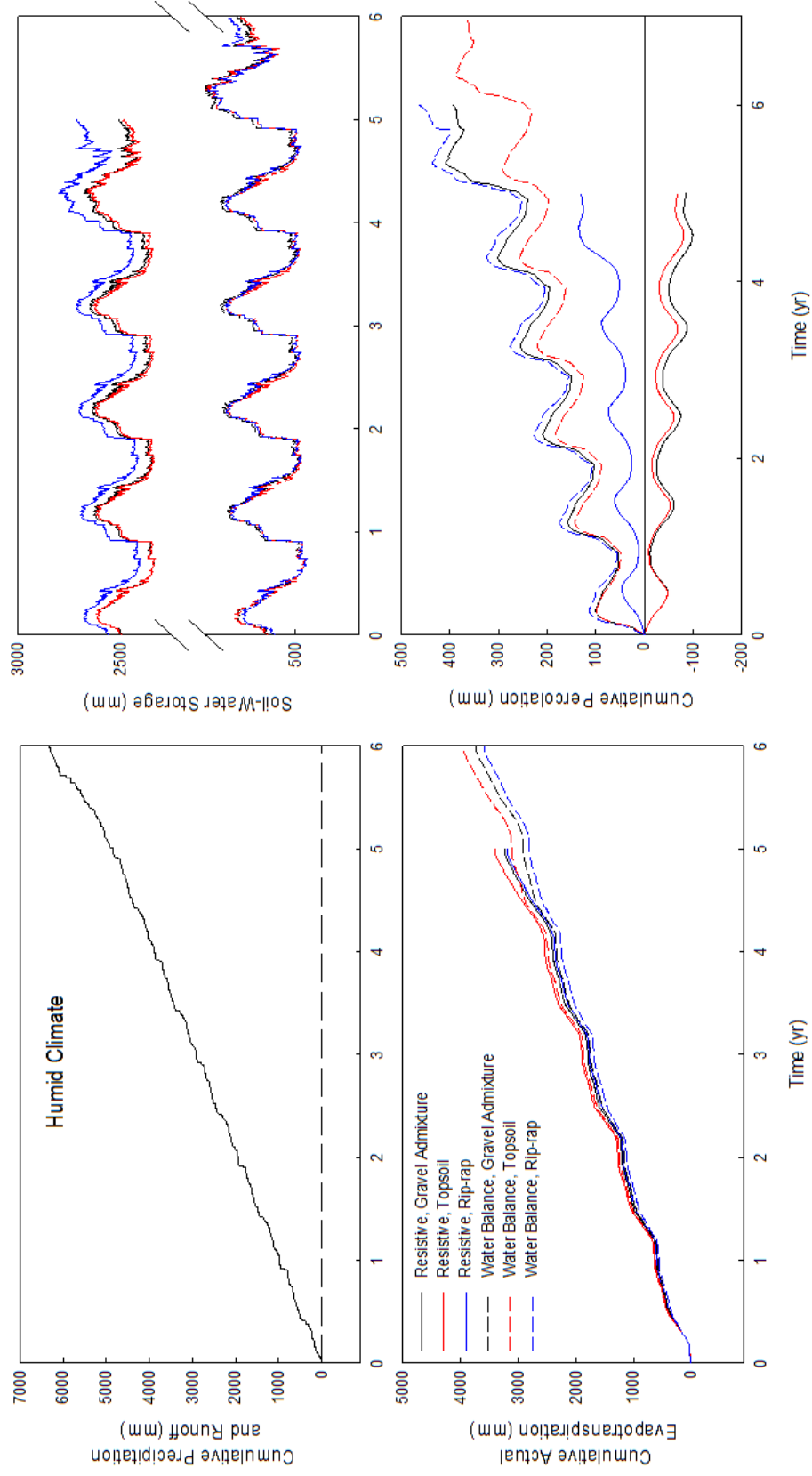


Figure C.2. Predictions from SVFLUX of precipitation, evapotranspiration, soil-water storage, and cumulative percolation for resistive and water balance barriers in a humid climate. Some simulations required less years than others to stabilize. The last year of each simulation is the wettest year. Positive percolation is into the tailings, negative is out.

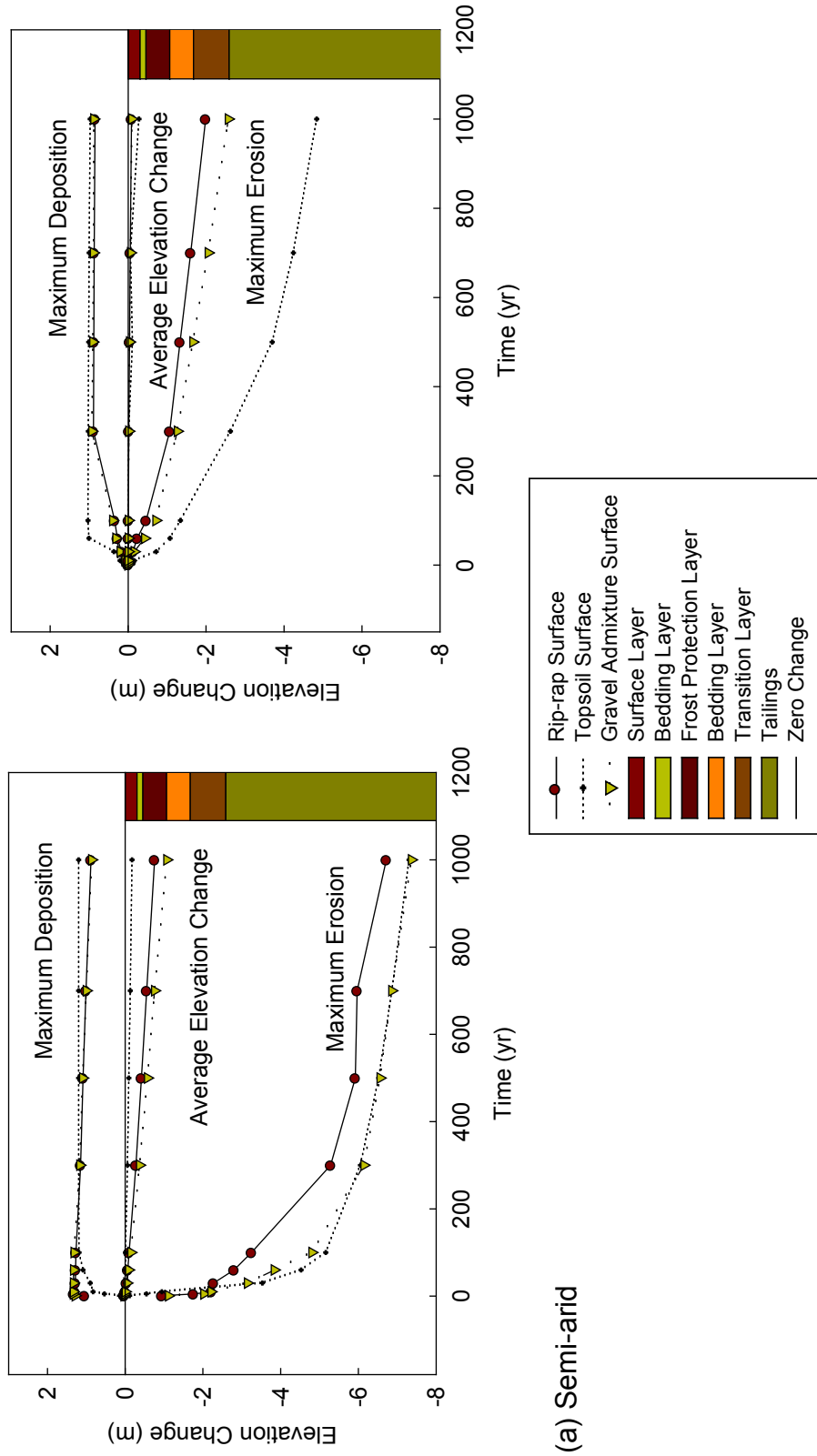
APPENDIX D

SIBERIA Predictions for Uniform Side Slope Topography

Appendix D: SIBERIA Predictions for Uniform Side Slope Topography

The following figures contain erosion predictions by SIBERIA for uniform side slope topography. These figures were used to evaluate different slope lengths and angles for uniform side slopes. The figures in this appendix coincide with Section 4.2.

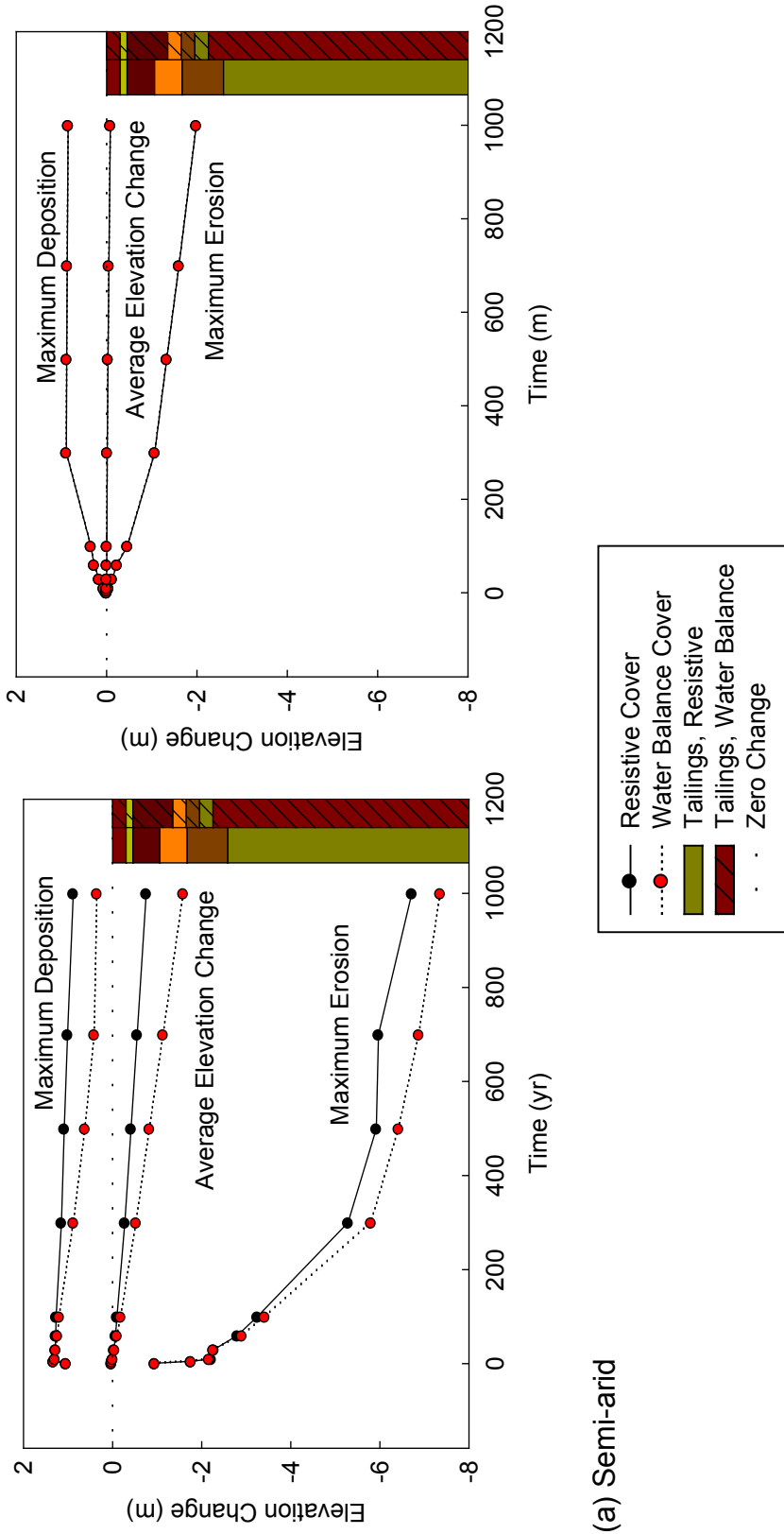
Uniform Side Slope Topography



(a) Semi-arid

Figure D.1. Maximum erosion, maximum deposition, and average elevation change predicted by SIBERIA for rip-rap, topsoil, and gravel admixture surfaces with 41 m side slopes and a resistive barrier: (a) semi-arid climate and (b) humid climate.

Resistive vs. Water Balance Covers – Uniform Side Slopes



(a) Semi-arid

Figure D.2. Maximum erosion, maximum deposition, and average elevation change in resistive and water balance barriers predicted by SIBERIA with 41 m side slopes and a rip-rap surface layer: (a) semi-arid climate and (b) humid climate.

Semi-Arid Climate

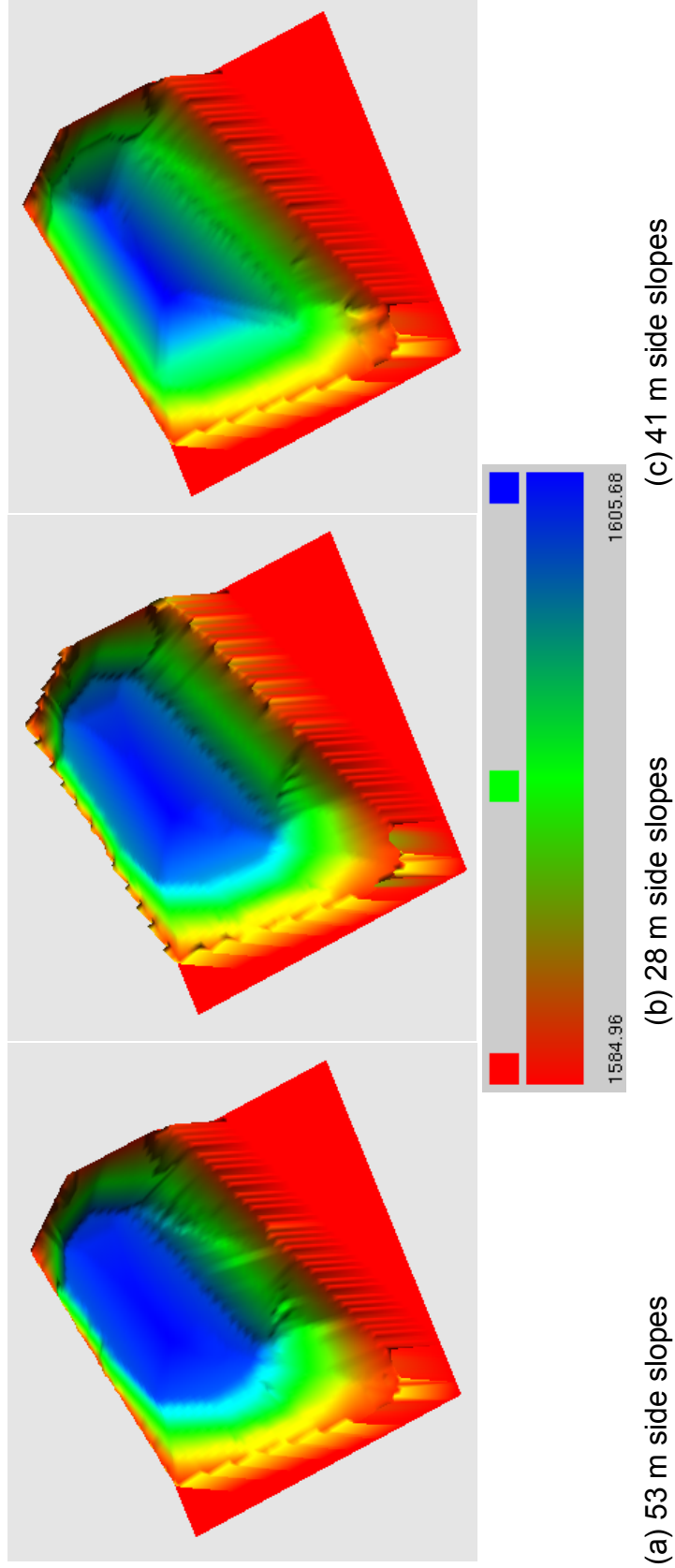


Figure D.3. Elevation predicted for a rip-rap surface with various slope lengths and angles in a semi-arid climate: (a) 53 m side slopes, 15.3% side slopes, 2% top slope, (b) 28 m side slopes, 18.5% side slopes, 3% top slope, and (c) 41 m side slopes, 20% side slopes, 5.3% top slope. Elevation is shown in m and denoted by the color scale above.

Semi-Arid Climate

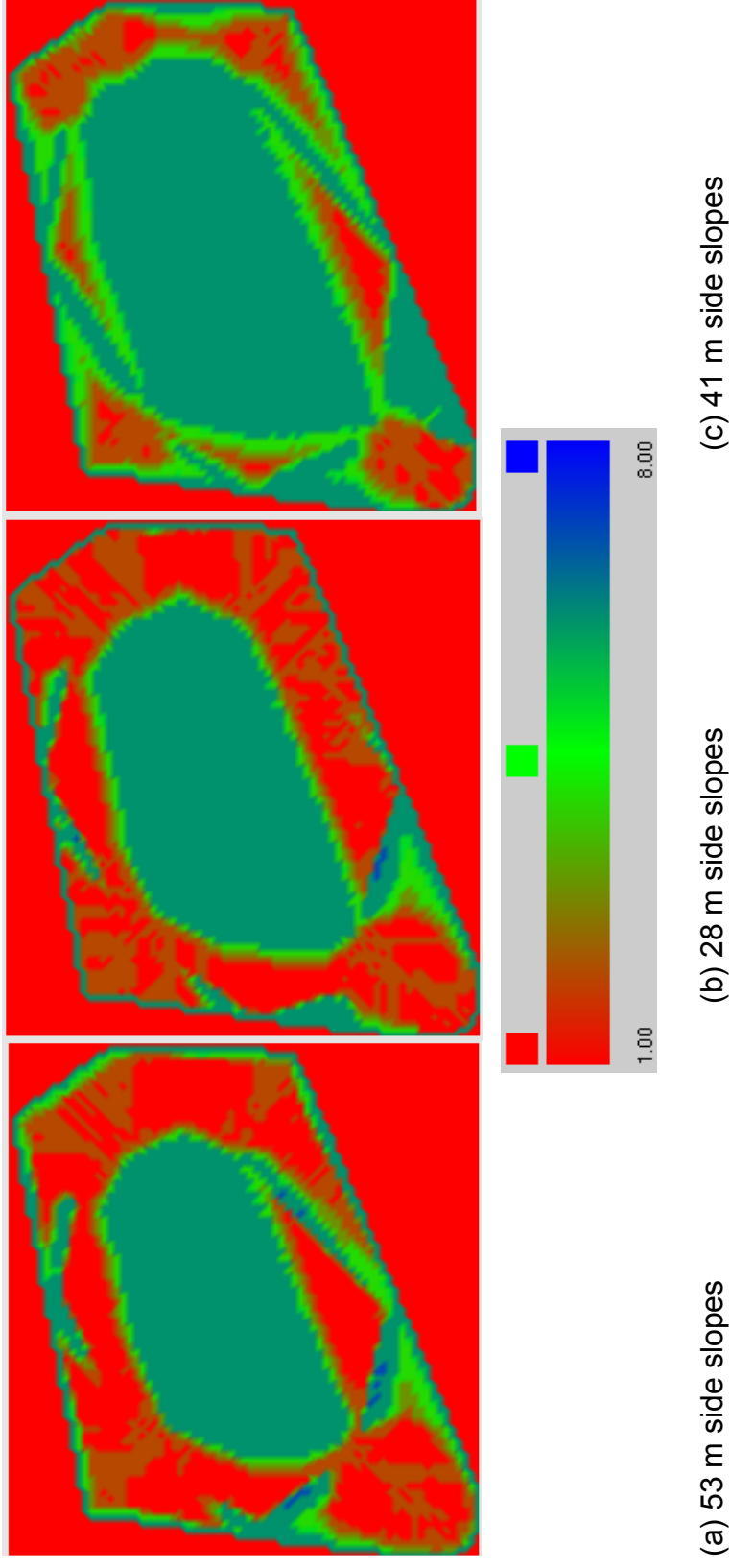
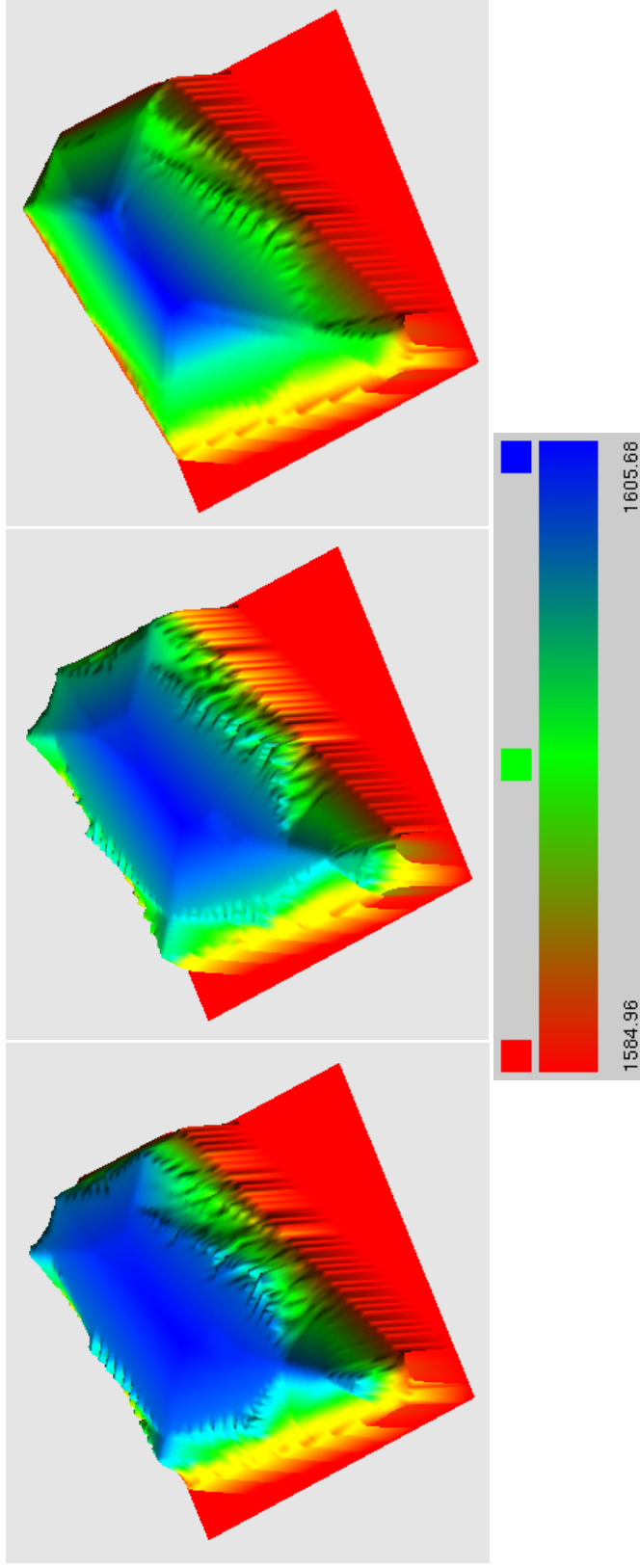


Figure D.4. Plan view predicted for a rip-rap surface with various slope lengths and angles in a semi-arid climate: (a) 53 m side slopes, 15.3% side slopes, 2% top slope, (b) 28 m side slopes, 18.5% side slopes, 3% top slope, and (c) 41 m side slopes, 20% side slopes, 5.3% top slope.

Humid Climate



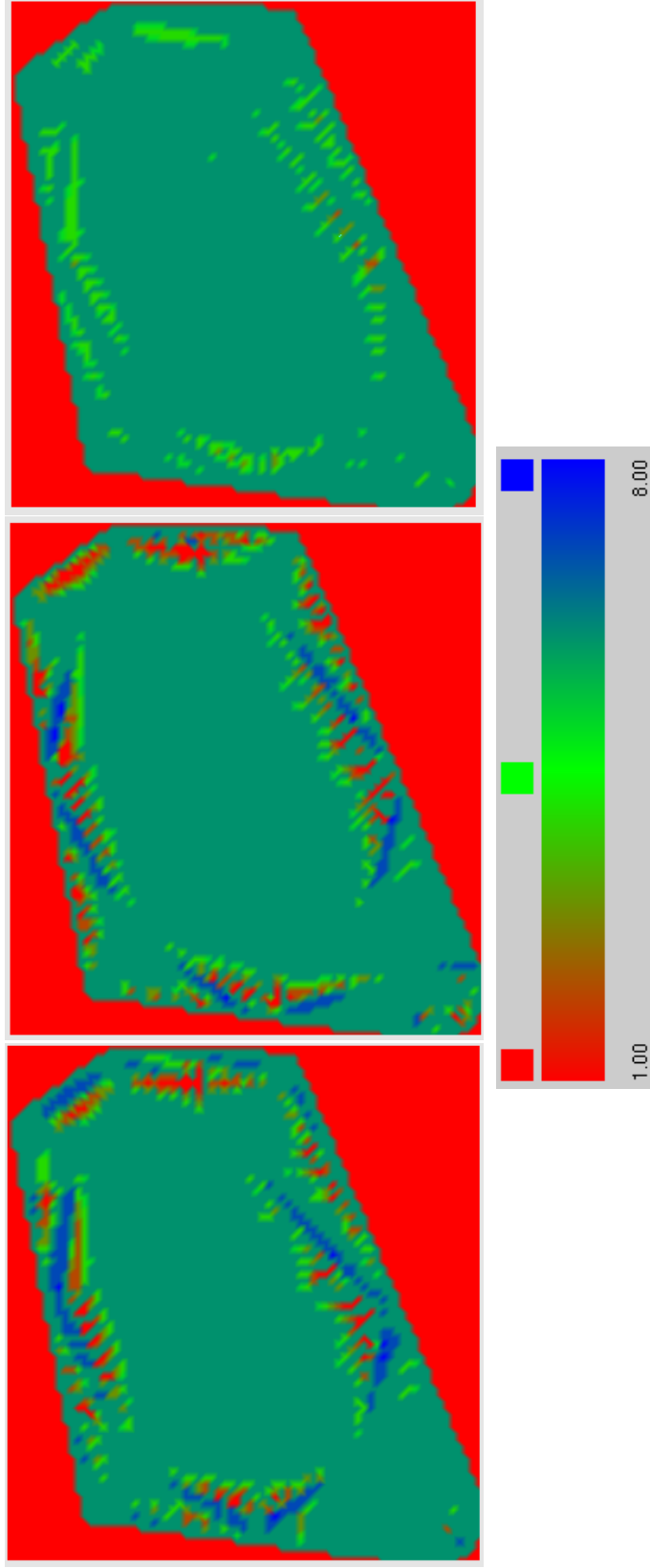
(a) 53 m side slopes

(b) 28 m side slopes

(c) 41 m side slopes

Figure D.5. Elevation predicted for a rip-rap surface with various slope lengths and angles in a humid climate: (a) 53 m side slopes, 15.3% side slopes, 2% top slope, (b) 28 m side slopes, 18.5% side slopes, 3% top slope, and (c) 41 m side slopes, 20% side slopes, 5.3% top slope. Elevation is shown in m and denoted by the color scale above.

Humid Climate



(a) 53 m side slopes

(b) 28 m side slopes

(c) 41 m side slopes

Figure D.6. Plan view predicted for a rip-rap surface with various slope lengths and angles in a humid climate: (a) 53 m side slopes, 15.3% side slopes, 2% top slope, (b) 28 m side slopes, 18.5% side slopes, 3% top slope, and (c) 41 m side slopes, 20% side slopes, 5.3% top slope.

APPENDIX E

Topographic Maps Used in SIBERIA

Appendix E: Topographic Maps Used in SIBERIA

Topography used in this study was changed to show the effects of slope length and angle and the effects of slope shape on erosion. The following figures show the topography used in this study in creating the DTMs for input into SIBERIA. The figures in this appendix coincide with Section 4.2.

Representative Site Topography

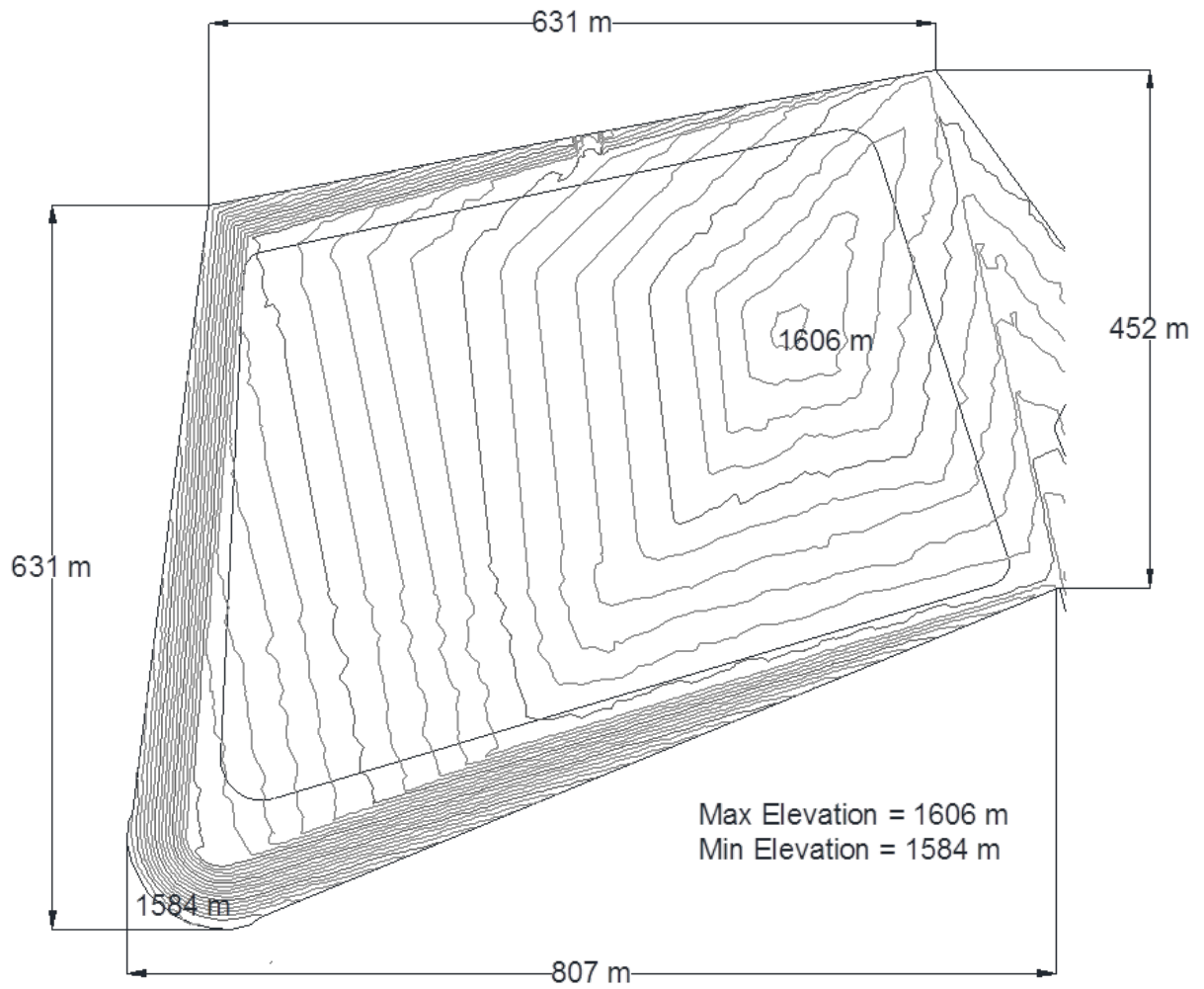


Figure E.1. Topographic map of the representative site.

Modified, Uniform Site Topography

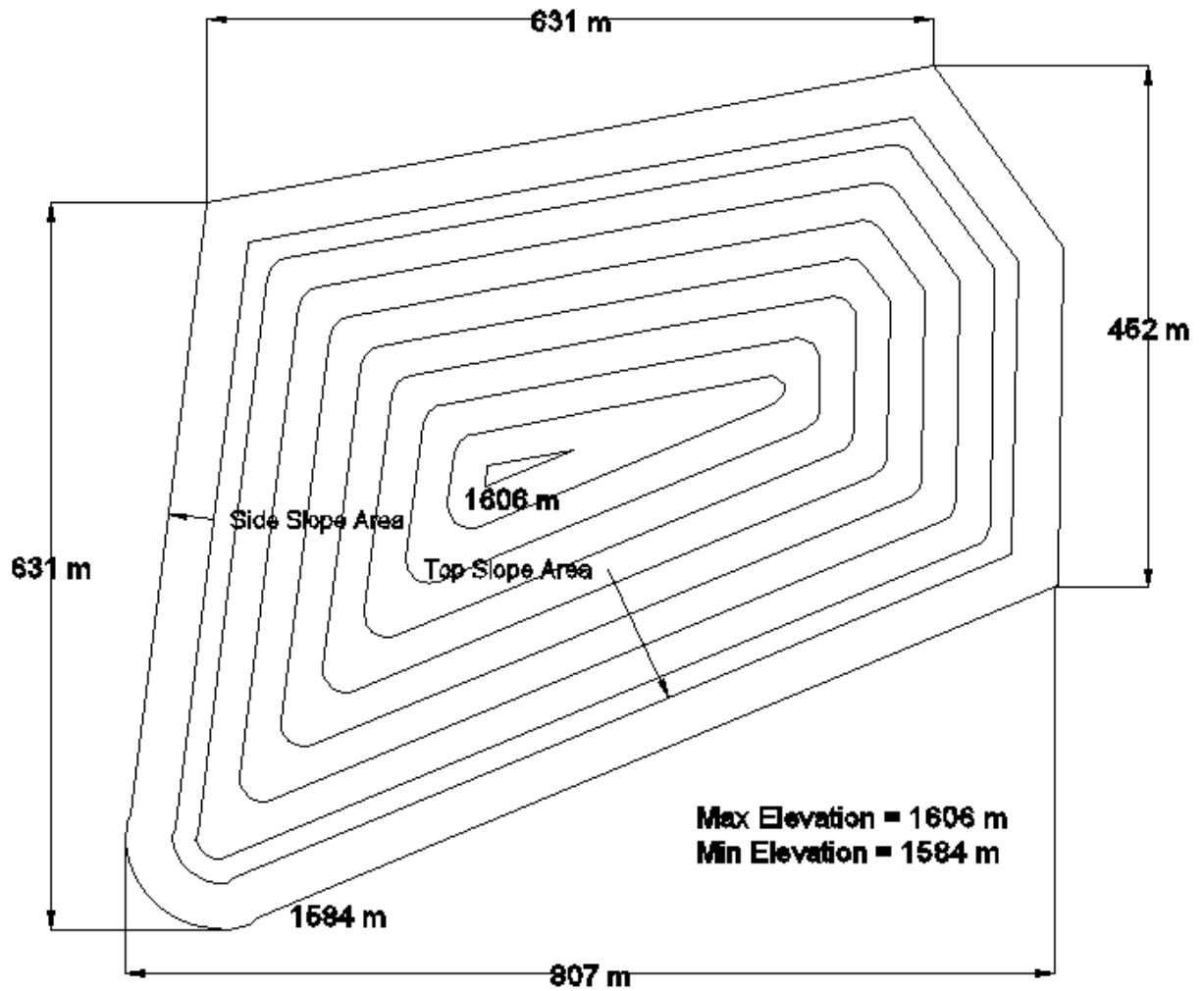


Figure E.2. Modified site topography used to create uniform, terraced, concave, and natural side slopes. See Fig. 4.13 for side slope views with top and side slope grades

APPENDIX F

SIBERIA Predictions for Shallow and Deep Concave Side Slopes

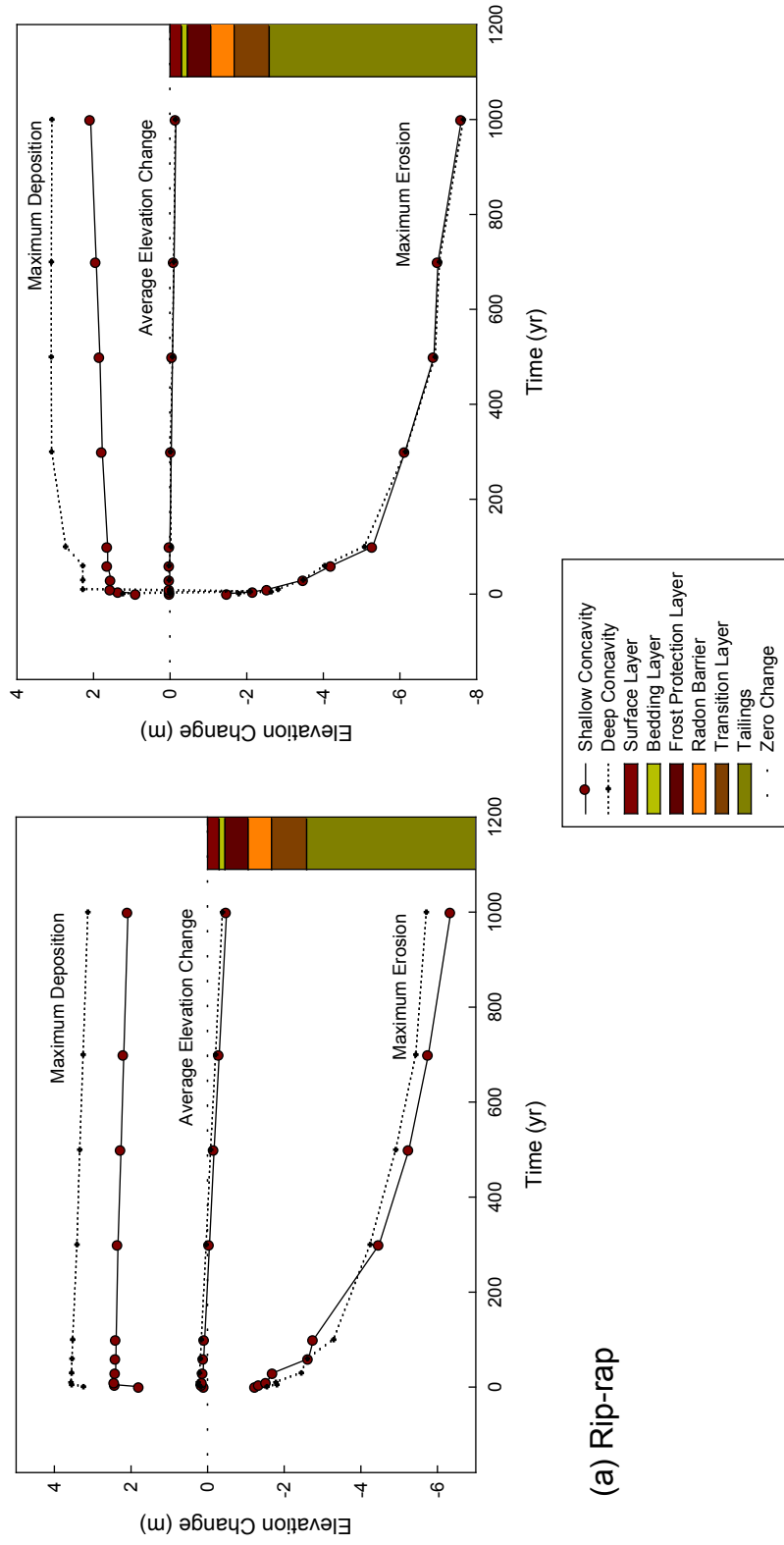
Appendix F: SIBERIA Predictions for Shallow and Deep Concave Side Slopes

The following tables and figures pertain to the evaluation of shallow and deep concave side slopes for use with various surface layer soil types and both the semi-arid and humid climate. The figures and tables in this appendix coincide with Section 4.3.

Table F.1. Best case scenario for concave side slopes based on climate and surface material.

Climate	Surface Material	Best Case Concavity Scenario
Humid	Rip-rap	Shallow
	Gravel Admixture	Shallow
Semi-Arid	Rip-rap	Deep
	Topsoil	Shallow

Shallow vs. Deep Concavity – Semi-Arid Climate



(a) Rip-rap

Figure F.1. Maximum erosion, maximum deposition, and average elevation change for resistive barrier in a semi-arid climate: a comparison of shallow and deep concavity for (a) a rip-rap surface, and (b) a topsoil surface.

Shallow vs. Deep Concavity – Humid Climate

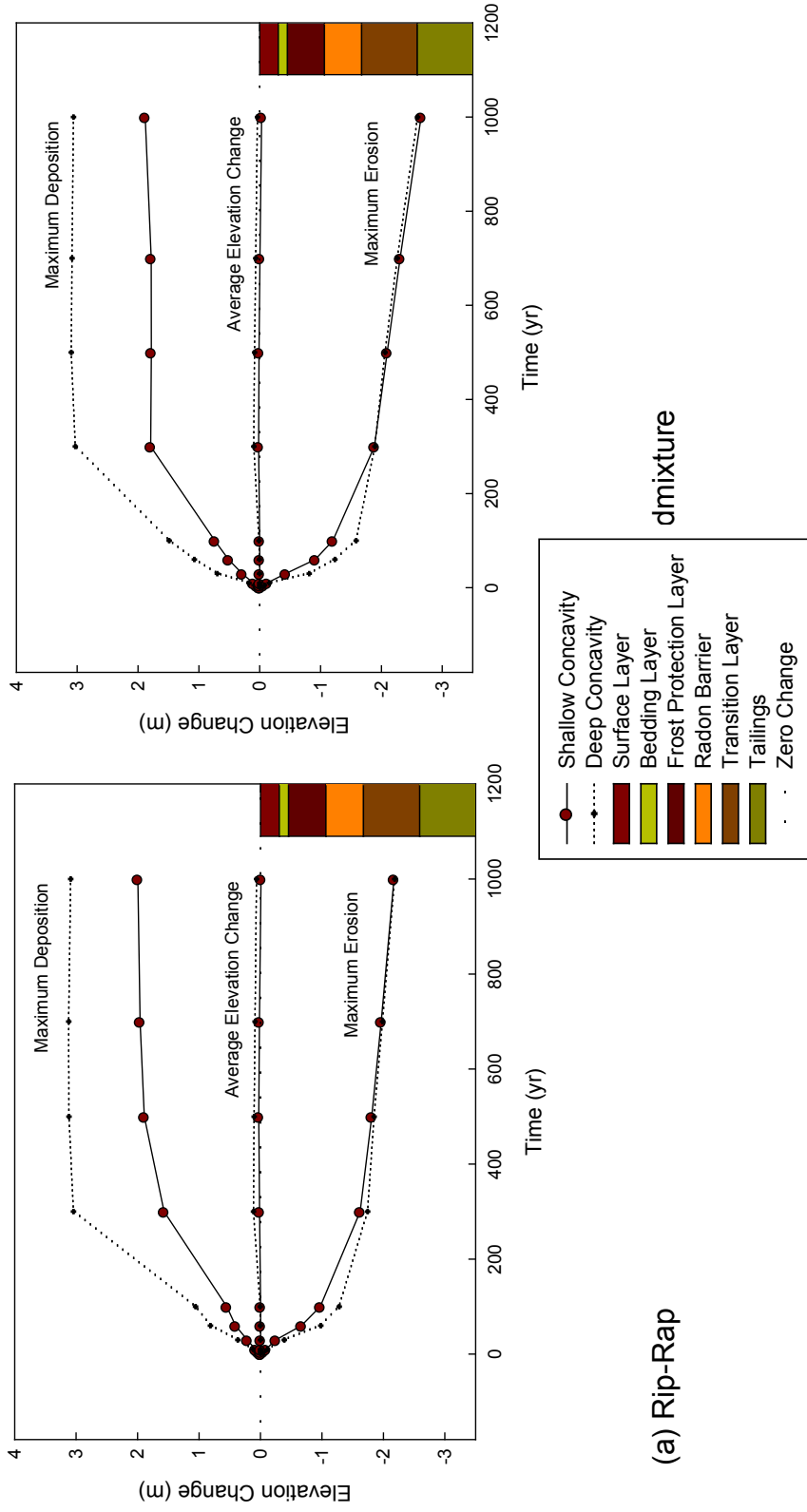


Figure F.2. Maximum erosion, maximum deposition, and average elevation change for resistive barrier in a humid climate: a comparison of shallow and deep concavity for (a) a rip-rap surface, and (b) a gravel admixture surface.

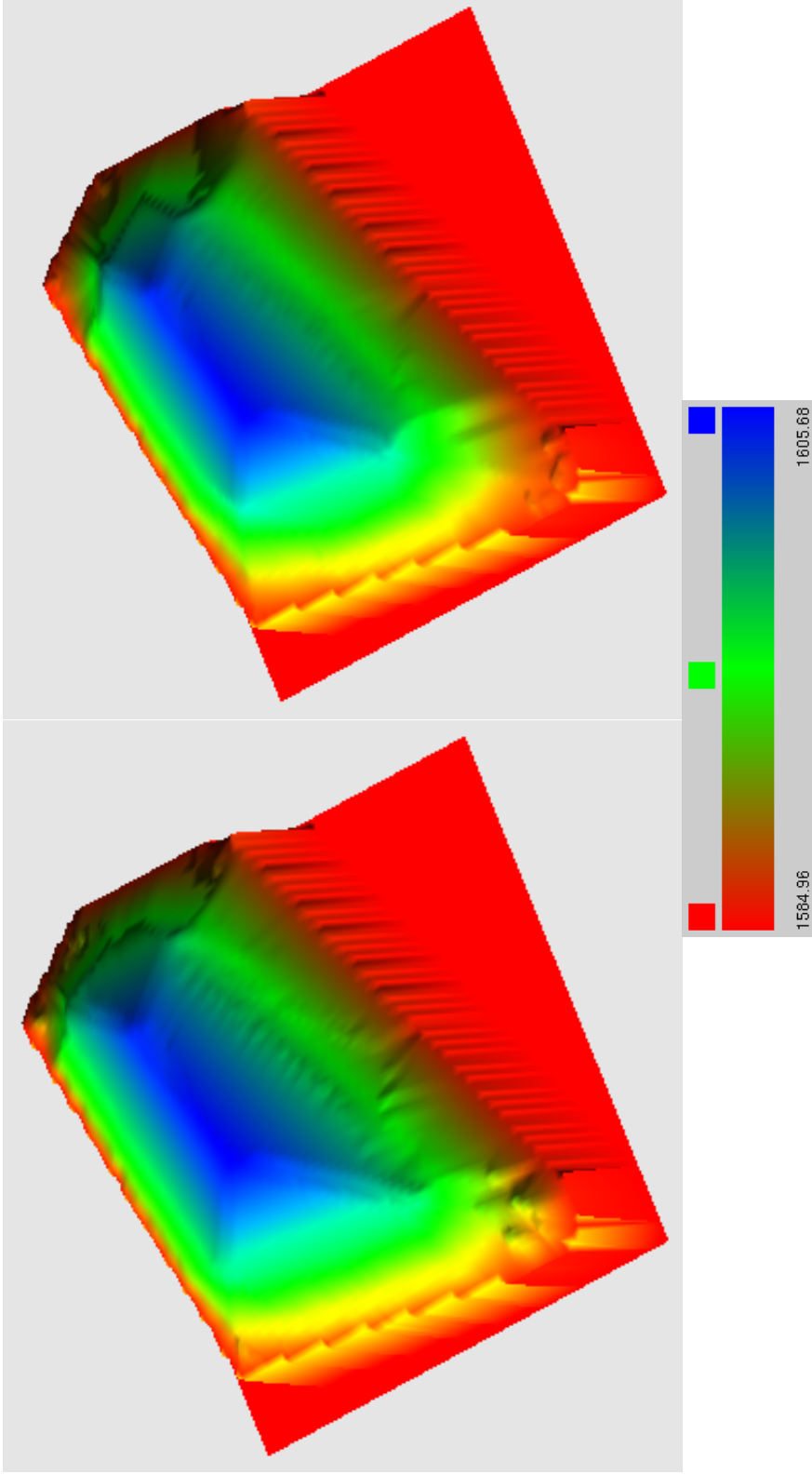
APPENDIX G

SIBERIA Predictions for Least Eroded Surfaces

Appendix G: SIBERIA Predictions for Least Eroded Surfaces

The following figures show SIBERIA predictions showing the best case erosion scenario based on surface layer type, climate, and slope shape. The figures show 3D and plan views of erosion over the surface. The figures in this appendix coincide with Section 4.3.

Best Case Scenario – Semi-Arid Climate

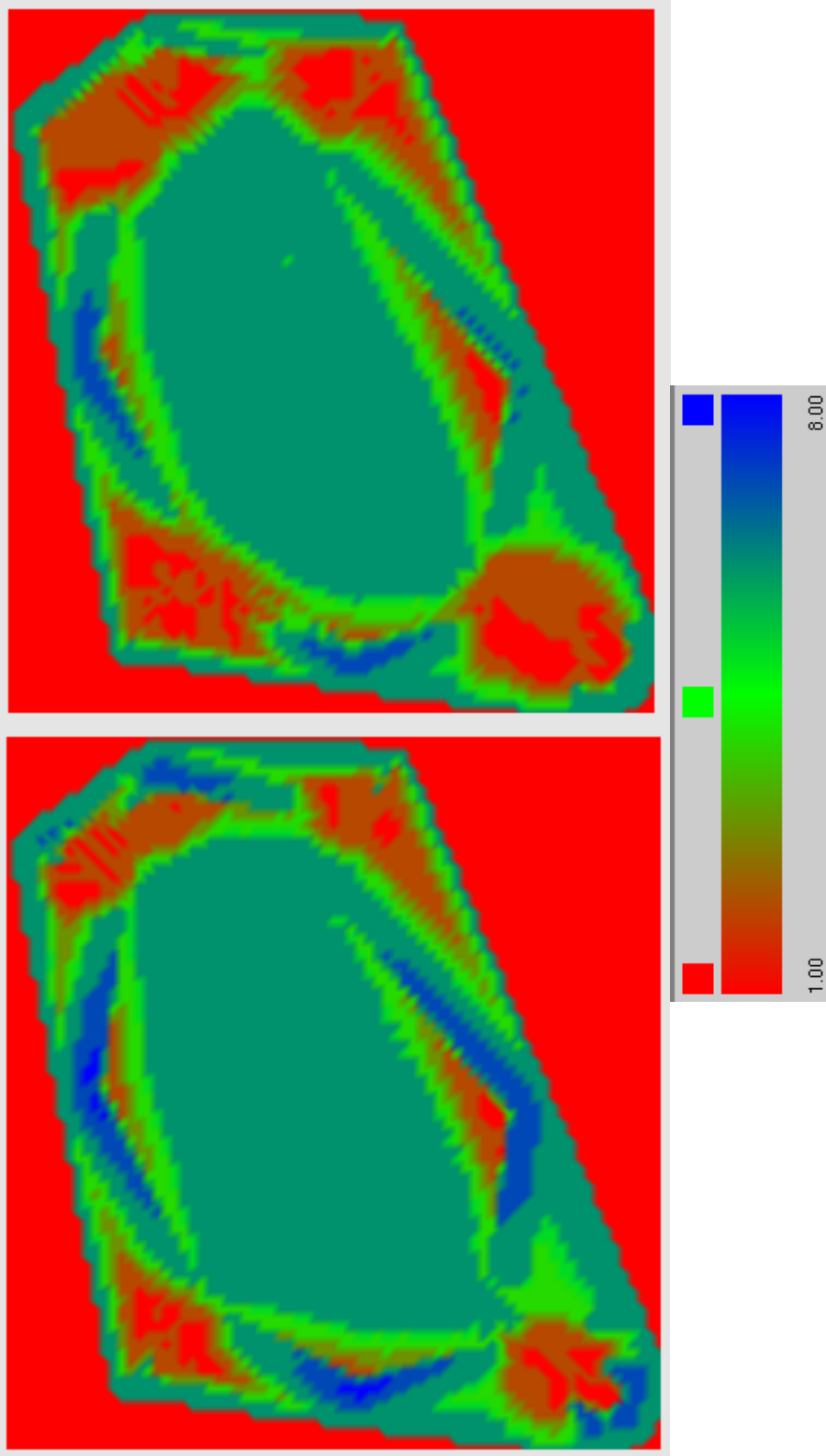


(a) Rip-rap

(b) Gravel admixture

Figure G.1. Elevation predictions from SIBERIA of the topography producing the least erosion with a resistive barrier in a semi-arid climate: (a) rip-rap surface layer with deep concavity and (b) gravel admixture surface layer with shallow concavity.

Best Case Scenario – Semi-Arid Climate



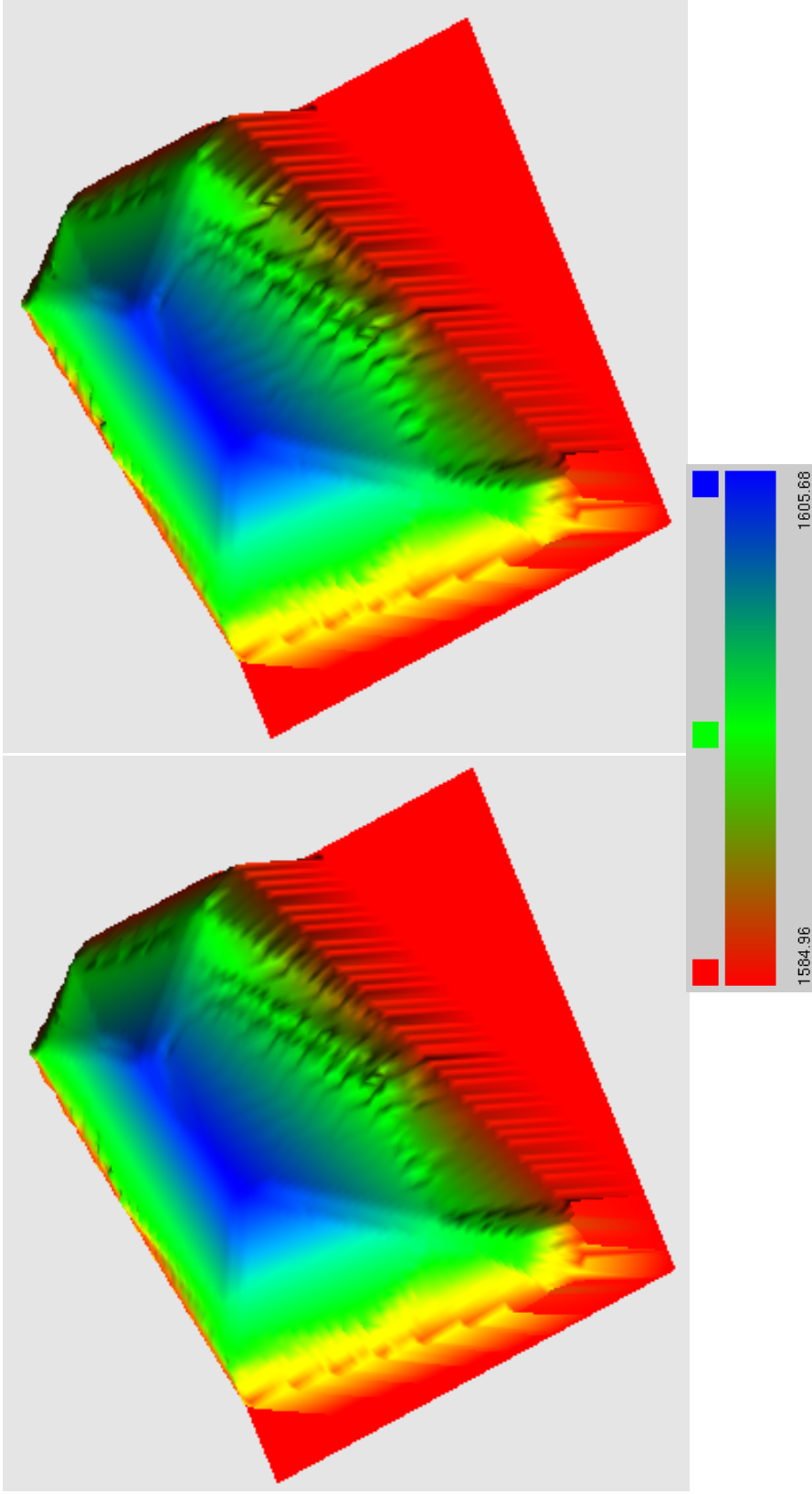
G-3

(a) Rip-rap

(b) Gravel admixture

Figure G.2. Plan view SIBERIA predictions of the topography producing the least erosion with a resistive barrier in a semi-arid climate: (a) rip-rap surface layer with deep concavity and (b) gravel admixture surface layer with shallow concavity.

Best Case Scenario – Humid Climate

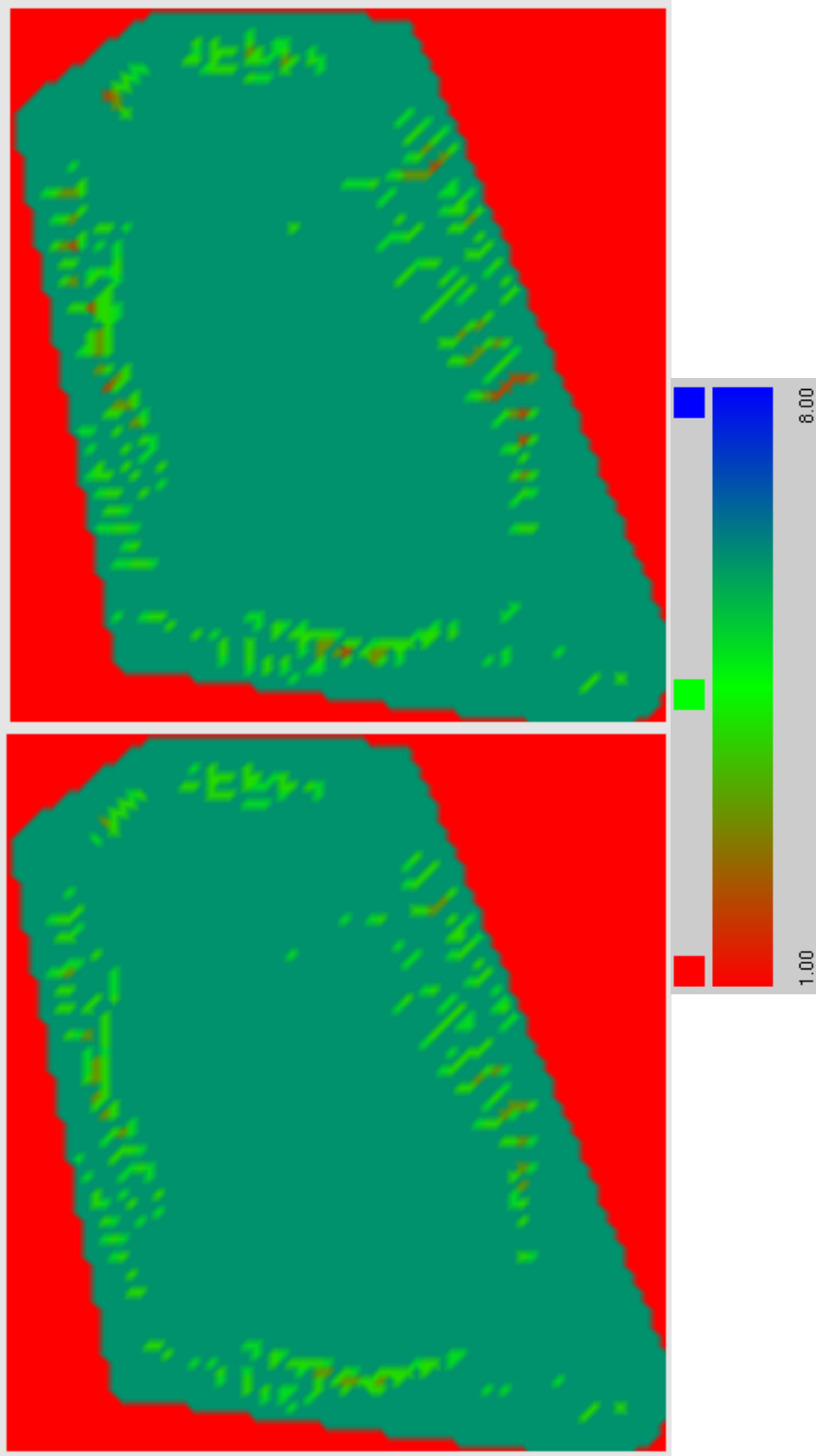


(a) Rip-rap

(b) Gravel admixture

Figure G.3. Elevation predictions from SIBERIA of the topography producing the least erosion with a resistive barrier in a humid climate: (a) rip-rap surface layer with terraces and (b) gravel admixture surface layer with terraces.

Best Case Scenario – Humid Climate



(a) Rip-rap

(b) Gravel admixture

Figure G.4. Plan view SIBERIA predictions of the topography producing the least erosion with a resistive barrier in a humid climate: (a) rip-rap surface layer with terraces and (b) gravel admixture surface layer with terraces.

APPENDIX H

Steps for Running SIBERIA Landform Evolution Model Using a Digital Terrain Model and Viewing Model Output

Appendix H: Steps for Running SIBERIA Landform Evolution Model Using a Digital Terrain Model and Viewing Model Output

To begin modeling with SIBERIA, an AutoCAD drawing of the existing site topography from the Grand Junction, CO reference site was first obtained to be used to create the digital terrain model. The gridding suite in EAMS had trouble reading files with several layers and hidden lines and would not grid the drawing. The unnecessary lines of the AutoCAD drawing were removed so only the contour lines of the area to be modeled remained. After these edits, the drawing was saved as a .dxf file.

Using EAMS, the .dxf file was imported for the gridding process. To grid everything in the .dxf file, the area of interest was kept as the default inputs, all four directions = -1. Grid spacing was selected as 10 m. The .dxf gridding resulted in two additional files, one .raw file and one .grid.raw file. The .grid.raw file stores coordinate and elevation information of the DTM and is used as the site input in SIBERIA.

After gridding the DTM, layers of the barrier, output file types, and output data were specified. The layer.model file located with the program files was modified to include layers of soil that constitute the barrier. This file can be opened and modified in a text editor program such as Notepad or WordPad. The individual layers of the barrier were specified using the layer capping command which places layers of a specified thickness and erodibility (β_1) above the DTM elevations. This keeps the shape of the site true, but adds the thickness of the barrier to the elevation of the true land surface. The layer.model file must be specified in the erosion parameters portion of SIBERIA. An example of the layer.model file used is shown in Appendix C.

The siberia.setup file was modified in a text editor program and is where outputs recorded and reported are selected. The siberia.setup file is explained both within the file itself and in the SIBERIA User Manual (Willgoose 2005a). Critical output selections included: showing the model screen, the maximum, minimum, and mean change in elevation at a point from the start of the simulation, the erosion loss in units of weight per area, the sediment flux, the minimum and average amount of soil layers completely intact, and the output of the grid coordinates as time progresses in the form of a .xyz file. The siberia.setup file used in this study is in Appendix D.

Once the DTM was gridded, the layer.model file has been modified, and the siberia.setup file has been modified SIBERIA can be set up to run. Under the SIBERIA menu Input from Gridded RAW was selected. This brought up a window with output file type, start time, number of outputs and where a unique file name were be specified. The output file type was selected as .rst2 for ease of use in the EAMS Viewer. The start time was set to zero. The number of outputs was set to 10, at times 1, 5, 10, 30, 60, 100, 300, 500, 700, and 1000, to view erosion as in occurs

and relative erosion rates at different times. Next, EAMS opened a window to select a database file. The database file is used to store parameter information. Several database files including a default file were included in the siberia_parameters.sdb database. From this database, the default file was selected and edited to include the desired parameters. A new database file was created by selecting edit parameters, modifying the parameters, and saving the file within the database. This was beneficial for multiple runs using the same base parameters as when the sediment transport equation parameter calibration is taking place, or when only a few parameters were required to change. The parameters selected for the database file were that of the top layer, except the parameter β_1 . This parameter was the erodibility of the bottom layer. The top layers were included in the layer.model file. The parameters modified from default are in Table 3.4.

Control parameters to define the duration of the simulation, time period between outputs, erosion file output, time step, and modes for running the erosion, runoff, and sediment transport models. The time step was set sufficiently small (0.01 yr) so that erosion events could be captured. The output settings used in the siberia.setup file include having SIBERIA output elevation data at each output time in an .xyz format, the amount of sediment being transported, the elevation change (maximum erosion, maximum deposition, and average change in elevation), and the erosion loss in tons/hectare. Once the setup of the model was complete, SIBERIA was run by selecting "Prepare and Run SIBERIA".

Once SIBERIA had finished running the output was viewed with the viewer program in the EAMS suite. Open in the File menu was selected to find the file labeled with the file name specified followed by the year (i.e. 700). Only two files can be opened at one time. The outputs selected in the siberia.setup file were viewed by selecting Statistics in the File menu. The statistics were reported as a minimum, maximum, and mean for the entire DTM (i.e. the minimum Z Change is the greatest erosion depth found at any one point on the DTM).

Graphs of the DTM and corresponding changes were viewed by selecting Draw in the Surface menu. The graphs shown in this study were the Elevation and Layer_No selections. Modifications to the viewer graphs were made by right clicking and using the viewing, lighting, and rendering menus. Position was changed with the number pad on a computer keyboard. Vertical exaggeration was useful for smaller elevation changes. If desired another program can be used for graphing by using the .xyz file that contains the coordinates of each point on the grid at the specified time.

APPENDIX I

A Sample layer.model File Used in SIBERIA

Appendix I: A Sample layer.model File Used in SIBERIA

```
sa_vrr_gj_layer
SIBERIA EXTERNAL
This is a siberia models input file. The first line of the file
above is fixed and should not be edited. The next three lines (i.e these lines
are for file description data and can be modified by the user
#
#
=====
===
==
# This file contains the extnded models information for SIBERIA
# (including regional variations in runoff, erosion and tectonics, layering)
#
=====
===
==
#
# The format of this file is as a series of example commands giving the
# general format of the commands. The commands can be in any order and there
# are no limits on the number of commands in the file. Each command is a
# single line of information.
#
# We suggest that you copy the appropriate command line examples and edit copies
# so that you always have copies of the original correct form of the command.
#
# NB 1. All commands are independent of each other so that runoff and erosion
# commands can be entered independently. However, the runoff commands are
# dependent
# on each other with subsequent runoff commands working on the result of
# previous
# runoff commands if the regions over which they apply are overlapping. The same
# is true of the erosion commands, tectonics, layers, etc.
#
# In particular, if you have regions
# of different material you may change the runoff for that region and not the
# erosion
# model if that is appropriate (and vice versa) or you may change both if
# appropriate, or you may change one 'absolute' and one 'relative' if desired.
#
# 2. These commands assume that the erosion model and the runoff model are
# initially
# everywhere uniform and determined by the b1, m1, n1, b3, n3 parameters
# specified in
# the RST2 file.
#
# Compatible with SIBERIA V8.29
# =====
# UPDATE HISTORY
# -----
# 1/12/2003 Additions to for region based uplift and aggradation (V8.20)
```

```

# 7/ 4/2004 Additions to support new LAYERS module (V8.25)
# 11/2004 Further modifications for LAYERS module (V8.28)
#
#
=====
===
==
# EROSION commands
#
=====
===
==
#
# These commands are read in SIBERIA when the parameter ModeErode=3 and
# the EROSION file parameter=-1 is set to this file.
#
# The EROSION commands come in two forms:
# -----
# GENERAL EROSION MODEL
# -----
# The most general form of the erosion commands from left to right is
# - 'EROSION' indicating this is an erosion command (starts in column 1)
# - one of either 'ABSOLUTE' or 'RELATIVE' indicating
# ABSOLUTE: the erosion parameters are as given
# RELATIVE: the erosion parameters given are multiplied with
# the erosion parameters at that point previously
# given .... ie. this changes the parameters by a relative amount
# - the parameters b1, m1, n1. For RELATIVE these are interpreted as
# multipliers
# - the region file for applying those parameters (it must inside '')
#
# The command below replaces the erosion model over the region defined by
test1.rgn
# with an erosion model with b1(new)=0.01, m1(new)=0.6, n1(new)=0.7
#
#EROSION ABSOLUTE 0.01 0.6 0.7 'control\test1.rgn'
#
# The command below replaces the erosion model over the region defined by
test2.rgn
# with an erosion model with b1(new)=0.05, m1(new)=0.2, n1(new)=0.3
# NB. Because this command after the test1.rgn command where
# test1.rgn and test2.rgn overlap test2.rgn overwrites test1.rgn
#
#EROSION ABSOLUTE 0.05 0.2 0.3 'control\test2.rgn'
#
# The command below modifies the erosion model over the region defined by
test3.rgn
# with an erosion model with b1(new)=b1(old)*0.1
# m1(new)=m1(old)*0.7
# n1(new)=n1(old)*1.2
# NB. Because this command after the test1.rgn and test2.rgn commands where
# test1.rgn, test2.rgn and test3.rgn overlap test3.rgn overwrites the other
files

```

```

#
#EROSION RELATIVE 0.1 0.7 1.2 'control\test.rgn'
#
#
# ERODIBILITY ONLY EROSION MODEL
# -----
#
# A more specific form of the erosion command only modifies the erodibility
# and is of the form
# - 'ERODIBILITY' indicating this is an erosion command (starts in column 1)
# - one of either 'ABSOLUTE' or 'RELATIVE' indicating
# ABSOLUTE: the erosion parameters are as given
# RELATIVE: the erosion parameters given are multiplied with
# the erosion parameters at that point previously
# given .... ie. this changes the parameters by a relative amount
# - the parameter b1. For RELATIVE these are interpreted as multipliers
# - the region file for applying those parameters (it must inside ")
#
# The command below modifies the erosion model over the region defined by
test3.rgn
# with an erosion model with  $b1(new)=b1(old)*0.1$ 
#
#ERODIBILITY RELATIVE 0.1 'control\test.rgn'
#
#
#
#
=====
===
==
# RUNOFF commands
#
=====
===
==
#
# These commands are read in SIBERIA when the parameter ModeRunoff=3 and
# the RUNOFF file parameter=-2 is set to this file.
#
# The general form of the erosion commands from left to right is
# - 'RUNOFF' indicating this is a runoff command (starts in column 1)
# - one of either 'ABSOLUTE' or 'RELATIVE' indicating
# ABSOLUTE: the runoff parameters are as given
# RELATIVE: the runoff parameters given are multiplied with
# the runoff parameters at that point previously
# given .... ie. this changes the parameters by a relative amount
# - the parameters b3, m3. For RELATIVE these are interpreted as multipliers
# - the region file for applying those parameters (it must inside ")
#
#
# The command below replaces the runoff model over the region defined by test0.rgn
# with a runoff model with  $b3(new)=1.0$ ,  $m3(new)=0.8$ 
#

```

```

#RUNOFF ABSOLUTE 1.0 1.0 'test1.rgn'
#
#
# The command below updates the runoff model over the region defined by
test1_2.rgn
# with a runoff model with b3(new)=b3(old)*2.0, m3(new)=m3(old)*0.9
#
#RUNOFF RELATIVE 2.0 0.9 'control\test1_2.rgn'
#
#
# The command below updates the runoff model over the region defined by test0.rgn
# with a runoff model with b3(new)=b3(old)*0.5, m3(new)=m3(old)*1.0
#
#RUNOFF RELATIVE 0.5 1.0 'control\test.rgn'
#
#
#
=====
===
==
# CHANNEL commands
#
=====
===
==
#
#
# These commands are read in SIBERIA when the parameter ModeChannel=3 and
# the CHANNEL file parameter=-6 is set to this file.
#
# The general form of the erosion commands from left to right is
# - 'CHANNEL' indicating this is an runoff command (starts in column 1)
# - one of either 'ABSOLUTE' or 'RELATIVE' indicating
# ABSOLUTE: the runoff parameters are as given
# RELATIVE: the runoff parameters given are multiplied with
# the runoff parameters at that point previously
# given .... ie. this changes the parameters by a relative amount
# - the parameters b5, m5, n5. For RELATIVE these are interpreted as
multipliers
# - the region file for applying those parameters (it must inside ")
#
#CHANNEL RELATIVE 0.5 1.0 1.0 'control\test.rgn'
#
#
#
=====
===
==
# UPLIFT commands
#
=====
===
==

```

```

#
#
# These commands are read in SIBERIA when the parameter ModeChannel=4 and
# the UPLIFT file parameter=-3 is set to this file.
#
# The general form of the erosion commands from left to right is
# - 'UPLIFT' indicating this is an runoff command (starts in column 1)
# - one of either 'ABSOLUTE' or 'RELATIVE' indicating
# ABSOLUTE: the uplift parameters are as given
# RELATIVE: this mode is ignored in the current version (NB. RELATIVE or
# ABSOLUTE must still be input).
# - one parameter: the uplift rate/timestep.
# - the region file for applying this parameters (it must inside ")
#
#UPLIFT ABSOLUTE 0.5 1.0 1.0 'control\test.rgn'
#
#
#
=====
===
==
# KNOWN AGGRADATION/DEGRADATION rate commands
#
=====
===
==
#
#
# These commands are read in SIBERIA when the parameter ModeChannel=4 and
# the UPLIFT file parameter=-3 is set to this file.
#
# The general form of the erosion commands from left to right is
# - 'UPLIFT' indicating this is an runoff command (starts in column 1)
# - one parameter: the known aggradation/timestep. Note is a positive number is
input
# this is interpreted as aggradation, whereas if a negative number if input
this
# is interpreted as a degradation
# - the region file for applying this parameters (it must inside ")
#
#AGGRADATION 0.5 'control\test.rgn'
#
#
#
#
#
#
#
#
#
#
#
=====
===
==
# LAYERS MODULE commands

```

```

#
=====
===
==
#
# Whenever a LAYERS file and ModeErode=4 is specified the file is read for all
# commands that start with LAYERS.
#
# ALL lines starting with other commands (e.g. RUNOFF, UPLIFT) are ignored. Note
# that RUNOFF and EROSION and ERODIBILITY commands conflict with LAYERS and errors
# may occur if ModeErode=3 or ModeRunoff=3 is set in addition to a LAYER file.
#
# LAYER commands can be divided into four kinds.
#
# - LAYER CONTROL. These commands allow the user to control the internal
# computational behaviour of the LAYER model (e.g. maximum thickness of
layers)
# - LAYER PARAMETERS. These commands provide information about the erosion/runoff
# model parameters that are to be used for subsequent LAYER commands (or
until
# they are superseded by a new LAYER parameter command).
# - LAYER ELEVATION. These commands input the elevation properties of
# the layer being created. The properties of the LAYER being created are
those
# input by the most recent LAYER PARAMETER commands.
# - LAYER MASKING. These commands input information on the spatial extent of
# the LAYER currently being created. These commands allow you to create a
LAYER
# that is restricted in spatial extent so that it doesn't have to barrier the
# entire computational domain.
# - LAYER DETACHMENT. These commands input information of the detachment
limitation
# of the material in that layer.
#
#
# LAYER CONTROL COMMANDS
# -----
#
# - the maximum thickness of a layer created by SIBERIA during deposition. This
does
# not preclude the user from inputting a thicker layer but all layers generated
by
# the computations will have a maximum thickness as below. NB thin layers can
# significantly increase the memory consumption of the code and this increase
# may be superlinear (i.e. halving the layer thickness may increase memory
# consumption by more than a factor of 2).
#
#LAYER THICKNESS 0.1
#
#
# LAYER PARAMETER COMMANDS
# -----
#

```

```

# - the general format of these commands is as for the EROSION/RUNOFF models
# for region input at the top of this file, except that a region file is not
# input as part of the command line. For instance for EROSION parameters input
# is:
# - 'EROSION' indicating this is an erosion command (starts in column 1)
# - one of either 'ABSOLUTE' or 'RELATIVE' indicating
# ABSOLUTE: the erosion parameters are as given
# RELATIVE: the erosion parameters given are multiplied with
# the erosion parameters at that point previously
# given .... ie. this changes the parameters by a relative amount
# (initially the parameters are those set in the parameters input
# at the start)
# DEFAULT: sets the parameters back to the default values (those
# input in the parameters input at the start). This can be handy
# for resetting parameters when you have input lots of layers
with
# RELATIVE parameters.
# - the parameters. For RELATIVE these are interpreted as multipliers
# on the last value for the parameters.
# - there are parameters for the layer detachment limitation model are grouped
# at the end of the layer section
#
#
# - Erosion model parameters 'b1,m1,n1'
#
#LAYER EROSION RELATIVE 0.1 0.2 0.3
#LAYER EROSION ABSOLUTE 1.0 2.0 3.0
#LAYER EROSION DEFAULT
#
# - Erodibility parameter 'b1'
#
#LAYER ERODIBILITY RELATIVE 0.1
#LAYER ERODIBILITY ABSOLUTE 0.3
#LAYER ERODIBILITY DEFAULT
#
#
# - Runoff model parameters 'b3,m3'
#
#LAYER RUNOFF RELATIVE 0.5 0.95
#LAYER RUNOFF ABSOLUTE 0.1 0.5
#LAYER RUNOFF DEFAULT
#
# - Maximum slope parameter 's0max'
#
#LAYER ANGLE_OF_REPOSE RELATIVE 0.5
#LAYER ANGLE_OF_REPOSE ABSOLUTE 0.2
#LAYER ANGLE_OF_REPOSE DEFAULT
#
# - Creep parameter 'dZ'
#
#LAYER CREEP RELATIVE 0.6
#LAYER CREEP ABSOLUTE 0.01
#LAYER CREEP DEFAULT

```

```

#
#
# LAYER ELEVATION COMMANDS
# -----
#
# - the commands for input of the elevations for the layers. NB the input
# elevations
# are for the base of the layer unless otherwise noted (i.e. the layer extends
# upwards from the elevations input.
#
# - a layer barriering the surface of thickness given. The top of the capping layer
# is the landform surface and the bottom of the capping is 'thickness' below
# that
# surface
#
LAYER ERODIBILITY ABSOLUTE 2.10
LAYER CAPPING 2.590
LAYER ERODIBILITY ABSOLUTE 7.30
LAYER CAPPING 1.675
LAYER ERODIBILITY ABSOLUTE 1.84
LAYER CAPPING 1.065
LAYER ERODIBILITY ABSOLUTE 2.10
LAYER CAPPING 0.455
LAYER ERODIBILITY ABSOLUTE 0.002
LAYER CAPPING 0.305
#
# - a layer with base horizontal and with the layer's base at the elevation given
#LAYER Z 25.2
#
# - a layer that is a bilinear spline. the 1st 4 values are the coordinates of the
# four corners of the rectangular
# region (in node coordinates), and the 2nd four values are the elevations at
# the
# four corners in the order SW, SE, NW, NE corners.
# NB. the spline extends over the
# whole domain and the corner coordinates are ONLY used to determine the
# elevations
# of the interpolated/extrapolated surface not the spatial extent of the surface
# NB: BILINEAR_CLAMPED restricts the layer to the box specified.
#
#LAYER BILINEAR 1 20 1 30 10.0 20.0 22.0 35.0
#LAYER BILINEAR_CLAMPED 1 20 1 30 10.0 20.0 22.0 35.0
#
# - a layer that has as its base the elevations as read from the rst2 file,
# with the elevations offset by
# the specified value (i.e. a negative offset is a lower elevation). NB the
# areal
# extent of the RST2 file must match the RST2 file of the landform DEM.
#
#LAYER DEM -2.1 'TEST.RST2'
#
#
# LAYER MASKING COMMANDS

```

```

# -----
#
# - these commands specify over what part of the domain the layer will be created.
If a
# mask is input and active then the layer will be created for the region
specified
# by the mask and will not be created outside the mask. For all other cases the
# layer will barrier the entire region.
#
# - the mask is that part of the domain specified by the region file. The mask
# is automatically activated after input of the region file.
#
#LAYER REGION_MASK 'TEST.RGN'
#
# - the mask is that a rectangle defined by the coordinates. The coordinates
# are in the order LOWX,HIGHX,LOWY,HIGHY where the rectangle coordinates
# are (LOWX,LOWY) and (HIGHX,HIGHY). The mask
# is automatically activated after input of the region file.
#
#LAYER REGION_CLIP 0 10 5 35
#
# - Any mask that has been input can be inactivated (i.e. turned off). In the
event
# that the is needed again then it can activated by setting REGION_ACTIVE ON.
NB.
# This command does not delete the mask ... it only turns it off ... it can
always be
# turned back on again later (unless the mask is overwritten with another RGN
file in
# the meantime by a #LAYER REGION_FILE command).
#
#LAYER REGION_ACTIVE OFF
#
# - If a mask has been input from a region file then this activates it (i.e. turns
it
# on). If no region file has been input then the command is ignored.
#
#LAYER REGION_ACTIVE ON
#
#
# LAYER DETACHMENT MODEL COMMANDS
# -----
#
# - Relative Detachment Rate (Default is 1.0)
# To turn detachment limitation ON (once ON it cannot be turned off)
#
#LAYER DETACHMENT ON
#
# - Set the Relative detachment rate for that layer's material
#
#LAYER DETACHMENT RELATIVE 0.6
#LAYER DETACHMENT ABSOLUTE 0.01
#LAYER DETACHMENT DEFAULT

```


APPENDIX J

The siberia.setup File Used in SIBERIA

APPENDIX J: The siberia.setup File Used in SIBERIA

```
siberia
#
#
# =====|
# |
# SIBERIA LICENSE AGREEMENT |
# ----- |
# |
# Please read the following licence information carefully. This |
# computer program ("SIBERIA") is licensed, not sold, to you for use|
# only under the terms of this license, and the copyright owner |
# reserves any rights not expressly granted to you. You own the |
# computer media on which SIBERIA is originally and subsequently |
# recorded or fixed, but the copyright owner retains ownership |
# of all copies of SIBERIA itself |
# |
# Unless otherwise stated this licence entitles you to |
# (a) copy this code onto a single computer, |
# (b) make backup copies of this software, |
# |
# You may not |
# (a) remove these license agreement, disclaimer, copyright, or |
# limitation of damages notices from this source code, |
# (b) distribute this software to others, |
# (c) rent, lease, resell, distribute, network, or create |
# derivative products works based upon this software, or |
# any part thereof. |
# (d) modify the software in this file without the written |
# permission of the copyright owner. |
# (e) disclose this source code and algorithms to |
# unlicensed users |
# |
# This Licence is effective until terminated. This Licence will |
# terminate automatically without notice from the copyright owner |
# If you fail to comply with any provision of this Licence. Upon |
# termination of this Licence you must destroy this software and |
# all copies thereof. You may terminate the Licence at any time |
# by destroying this software and any copies thereof. |
# |
# -----|
# |
# COPYRIGHT NOTICE |
# ----- |
# |
# The SIBERIA software is Copyright 1993-2004 by |
# |
# Professor Garry Raymond Willgoose, |
# Earth and Biosphere Institute |
# School of Geography |
# University of Leeds, UK, LS2 9JT |
# |
```

```

# SIBERIA and EAMS are distributed by: |
# |
# Telluric Research, |
# Scone, Australia |
# |
# g.r.willgoose@leeds.ac.uk, |
# |
# |
#-----|
# |
# DISCLAIMER |
# ----- |
# |
# SIBERIA is provided 'as is' without warranty of any kind |
# either express or implied, including without limitation any |
# warranty with respect to its merchantability, or its fitness for |
# any particular purpose. The entire risk as to the quality and |
# performance of SIBERIA is with you. Should SIBERIA |
# prove defective, you (and not the copyright owner), assume the |
# entire cost of all necessary servicing, repair or correction. |
# |
# The copyright owner does not warrant that the functions contained |
# in SIBERIA will meet your requirements or that the operation |
# of SIBERIA will be uninterrupted or error free or that defects |
# in SIBERIA will be corrected |
# |
#-----|
# |
# LIMITATION OF DAMAGES |
# ----- |
# |
# In no event will the copyright owner be liable (i) to you for any |
# incidental, consequential or indirect damages (including damages |
# for loss of business profits, business interruption, loss of |
# business information, and the like) arising out of the use of or |
# inability to use SIBERIA even if the copyright owner has been |
# advised of the possibility of such damages, or (ii) for any |
# claim by any other party. |
# |
# =====
#
#
# HOW TO USE THIS FILE
# -----
#
# This file controls the operation of SIBERIA. Its name should always be
'siberia.setup'
# (all in lower case on Unix or Mac OSX machines) and it should be situated in
the
# directory in which SIBERIA is being run.
# If the file exists in that directory then SIBERIA reads it automatically.
# If the file does not exist then SIBERIA simply continues on without it,
choosing default

```

```

# values where necessary.
#
# To make this file easier to use all of the allowable commands are listed below.
The commands
# are the lines all in UPPER CASE while the comments and explanations are the
lines in lower
# case.
#
# If a line starts in column 1 with either of # or ! character then that line is
treated
# as a comment and is ignored by SIBERIA. To make a command active all you have
to do
# is to uncomment the appropriate line (i.e. remove the # or ! from the first
column).
# To inactivate it you simply add the # or ! to the first column again.
Explanations
# for the commands are provided immediately above the commands.
#
# There are a number of commands that turn some mode in the model off or on.
There are always
# three options for these modes. ON = (turn that mode on), OFF = (turn that mode
off),
# DEFAULT = (do whatever the code decides is best in the circumstances). If you
do not
# enable one these three options then the code chooses DEFAULT automatically.
NOTE: the
# default action may not always be the same as it may vary with size of the
problem being
# solved, whether SIBERIA detects that is being run of a multiprocessor machine,
etc, so if
# you absolutely must have some form of behaviour then specify it otherwise
SIBERIA may run
# differently on different machines
#
# FILE REVISION HISTORY
# -----
# - updated for V8.28 5/ 4/2005 (GRW)
#
#
#
#
=====
===
==
# -- To echo whatever is output to the screen to a file called (in the example
command below
# it is 'junk.output') uncomment the line starting ECHO
# -- To NOT echo to a file uncomment the line starting NOECHO
# -- ECHO_INCR appends a unique number to the filename to ensure that it doesn't
overwrite
# the output file from previous runs of siberia
#

```

```

=====
===
==
#
#ECHO junk.output
#NOECHO
#ECHO_INCR siberia.output
#
ECHO_INCR siberia.output
#
#
=====
===
==
# -- To have the program halt at the end of the run without the window automatically
closing
# then uncomment the line PAUSE_AT_END ON.
# -- To have the window automatically close at the end of the run then uncomment the
line
# PAUSE_AT_END OFF
# -- To have the program do whatever its default behaviour is with the window at the
end
# of the run then uncomment line then uncomment PAUSE_AT_END DEFAULT.
#
=====
===
==
#
#PAUSE_AT_END ON
#PAUSE_AT_END OFF
#PAUSE_AT_END DEFAULT
#
PAUSE_AT_END OFF
#
#
=====
===
==
# -- To allow RST output files to be overwritten uncomment the line RST_OVERWRITE
ON.
# -- To stop RST output files from being overwritten uncomment the line
RST_OVERWRITE OFF
# -- To have the program do whatever its default behaviour (typically this is to NOT
# overwrite the RST files) uncomment RST_OVERWRITE DEFAULT.
#
=====
===
==
#
#RST_OVERWRITE ON
#RST_OVERWRITE OFF
RST_OVERWRITE DEFAULT
#

```

```

#
=====
===
==
# PARALLEL OPTIONS
# -----
# This option is to set the maximum no of threads that the parallel
implementation
# of SIBERIA can use. The code will use this number of threads and attempt to get
# that many number of processors from the computer. This option is ignored if
the
# standard serial version of code is being used. If this option is not used then
# the code grabs a default (typically small but > 1) number of processors. On
shared
# parallel supercomputers choosing a large number of threads may slow the
starting of
# the code until the requested number of processors become available.
#
=====
===
==
#
NO_THREADS 1
#
#
=====
===
==
# EAMS COMPATIBILITY OPTIONS
# -----
# Output the elevation data in an xyz format (identical to the format read by EAMS)
# in addition to the output in the .rst2 files. This option is also useful in EAMS
# for output back to mine management and CAD (e.g. AutoCad) packages.
#
=====
===
==
#
XYZ_FILE
#
#
=====
===
==
# OUTPUT OF SUPPLEMENTARY CALCULATION DATA
# -----
# The following OUTPUT commands provide supplementary information to what is
# in the RST file. The data below are output in a .RSU file. A maximum of 10
# datasets may be output.
#
# There are two forms of the OUTPUT command
# OUTPUT : This outputs the specified data set into an RSU file which is
# a text column format used by all of the software in the EAMS

```

```

suite
# and which is easily readable into data analysis programs (e.g.
EXCEL
# Kaleidograph, SigmaPlot).
# OUTPUT_BIN : In addition to the RSU file this form also outputs the dataset
into
# a binary file (the filename is name.abbrev.bin where 'name' is
the
# same as the RST and RSU files, 'abbrev' is a self evident
# abbreviation for the dataset requested) that can be streamed
into
# visualisation packages like IDL, EXPLORER etc.
# The format is 2 4byte integers (the x and y dimensions of the
grid)
# followed by the data in 4byte floating point (by the x
dimension first).
# Note is you request more than one dataset to be OUTPUT_BIN
then each
# dataset requested goes into a seperate file with the
appropriate
# name.
#
=====
===
==
#
# the amount of sediment being transported (cubic metres/timestep/m width)
analytically
# derived from the transport equation.
#
OUTPUT SED_FLUX
#
#
# the potential and actual sediment transport (cubic metres/timestep/m width) as
determined by
# the transport-detachment limited transport model (i.e. ModeSolver=8).
# They may not match SED_FLUX exactly due to time discretisation error.
#
#OUTPUT SED_FLUX_POTENTIAL
#OUTPUT SED_FLUX_ACTUAL
#
#
# the amount of sediment removed/timestep in units of height at any pt in the grid
at the
# the requested time.
#
OUTPUT YIELD
#
# the average amount of sediment removed/timestep in units of height averaged over
the
# total catchment draining through that node.
#
OUTPUT AVEYIELD

```

```

#
# the change in elevation at a point from the start of the simulation (+ve increase
# in elevation -ve decrease in elevation).
#
OUTPUT ZCHANGE
#
# the change in elevation from the start of the simulation averaged over the
catchment
# draining through that point at that point in time (ie. the catchment area used for
# calculating the average elevation for the initial conditions is NOT the catchment
# draining through that point at the beginning, but rather that catchment at the
simulation
# time for output)
#
OUTPUT AVEZCHANGE
#
# the channel initiation function at that point
#
#OUTPUT GULLYPOT
#
# the log of the channel initiation function at that point
#
#OUTPUT LOGGULLYPOT
#
# the suggested steady state elevation for area-slope equilibrium based on the
# erosion parameters used in the simulation) NOT YET IMPLEMENTED.
#
#OUTPUT ZSUGGEST
#
# the change in elevations required to modify the existing elevations so that
# the elevations would comply with the area-slope equilibrium based on the erosion
# parameters used in the simulation. (NOT YET IMPLEMENTED)
#
#OUTPUT DZSUGGEST
#
# the erosion loss in weight units at a point (simply the elevation loss divided
# by the bulk density). This assumes that the units of height are metres and the
# units of length for the grid spacing are also metres.
#
OUTPUT TONNESHECTARE
#
# the erosion loss in weight units averaged over the catchment draining through
# at that point (simply the elevation loss divided
# by the bulk density). This assumes that the units of height are metres and the
# units of length for the grid spacing are also metres.
#
OUTPUT AVETONNESHECTARE
#
# the stability number for every point in the domain for the last timestep
#
#OUTPUT STABILITY
#
# the area-slope number for every point in the domain. It is calculated as

```

```

# area*slope^((m1*m3-1)/n1) and for a landform with optimal shape in equilibrium
# with tectonic uplift should be constant everywhere in the domain
#
#OUTPUT AREASLOPE
#
# the area-slope-elevation number for every point in the domain. It is calculated
as
# area*slope^((m1*m3-1)/n1)/Zave^(1/n1) where Zave is the average elevation of the
# catchment draining though that point. For a landform with optimal shape
# with erosion down to a flat plain this should be constant everywhere
#
#OUTPUT AREASLOPEELEVATION
#
# The Mean annual discharge used in the erosion model
#
OUTPUT DISCHARGE_MEANANNUAL
#
#
# SOILS MODEL OUTPUTS
# -----
# The outputs that follow can only be output when the soils model is turned ON.
#
#OUTPUT SOILMOISTURE
#
# - Bedrock properties can only be output for ModeSoils=2
#
#OUTPUT BEDROCK_Z
#OUTPUT BEDROCK_SLOPE
#OUTPUT BEDROCK_AREA
#OUTPUT BEDROCK_DIRECTIONS
#
#
# LAYERS MODEL OUTPUTS
# -----
# The outputs that follow can only be output when the layering model is turned ON.
#
#
# The B1 of the surface Layer (equivalent to OUTPUT LAYER_1_B1 except SURFACE_B1
will
# give the surface B1 even if the layers model is used)
OUTPUT SURFACE_B1
# The B1 of the flow
#OUTPUT FLOW_B1
# Number of layers at that node
OUTPUT LAYER_NO
# Layer properties for the top 5 layers
# ... note if the layer doesn't exist then zeros are output
# ... OUTPUT LAYER_1_B1 is equivalent to OUTPUT SURFACE_B1 and is provided to
display
# B1 when layers is not used (SURFACE_B1 doesn't need the layers model while
# LAYER_1_B1 does).
#OUTPUT LAYER_1_B1

```

```

#OUTPUT LAYER_2_B1
#OUTPUT LAYER_3_B1
#OUTPUT LAYER_4_B1
#OUTPUT LAYER_5_B1
#
#OUTPUT LAYER_1_Z
#OUTPUT LAYER_2_Z
#OUTPUT LAYER_3_Z
#OUTPUT LAYER_4_Z
#OUTPUT LAYER_5_Z
#
#
# The Detachment-Limitation Model
# -----
# This model is only available in combination with the LAYERS module
# so the output commands are a subset of the LAYERS commands (and LAYERS
# model has to be activated to enable the detachment model)
#
# The detachment rate for the material in the flow
#OUTPUT LAYER_FLOW_DETACHMENT
#
# The detachment rate of the material for the various layers (note LAYER=1
# is equivalent to the detachment rate for the surface)
#OUTPUT LAYER_1_DETACHMENT
#OUTPUT LAYER_2_DETACHMENT
#OUTPUT LAYER_3_DETACHMENT
#OUTPUT LAYER_4_DETACHMENT
#OUTPUT LAYER_5_DETACHMENT
#
#
#
# INTERNAL MODEL STATES
# -----
# These commands provide diagnostic output of the internal model operations. They
# are primarily available to aid debugging of the code operation and provided here
# as a memory aid for the developer.
#
# States that control the stability/mass balance of the solver
#
# Elevation changes of predictor
#OUTPUT PREDICTOR_SED
#
# Elevation changes of corrector
#OUTPUT CORRECTOR_SED
#
# Difference between elevation changes of predictor and corrector
#OUTPUT PREDCORRECT_SED_DIFF
#
# Relative difference between elevation changes of predictor and corrector
#OUTPUT PREDCORRECT_SED_RATIO
#

```

```
#  
# The weights generated by the Dinfinity algorithm  
#  
#OUTPUT DINFWEIGHTS  
#  
# A domain mask 0=outside computational domain, 1=inside computational domain  
#OUTPUT DOMAIN
```


BIBLIOGRAPHIC DATA SHEET

(See instructions on the reverse)

NUREG/CR-7200

2. TITLE AND SUBTITLE

Influence of Coupling Erosion and Hydrology on the Long-Term Performance of Engineered Barriers

3. DATE REPORT PUBLISHED

MONTH

YEAR

May

2016

4. FIN OR GRANT NUMBER

N6724

5. AUTHOR(S)

C.L. Smith and C.H. Benson

6. TYPE OF REPORT

Technical

7. PERIOD COVERED (Inclusive Dates)

September 2008 - June 2014

8. PERFORMING ORGANIZATION - NAME AND ADDRESS (If NRC, provide Division, Office or Region, U. S. Nuclear Regulatory Commission, and mailing address; if contractor, provide name and mailing address.)

Geological Engineering
University of Wisconsin-Madison
1415 Engineering Drive
Madison, Wisconsin 53706

9. SPONSORING ORGANIZATION - NAME AND ADDRESS (If NRC, type "Same as above", if contractor, provide NRC Division, Office or Region, U. S. Nuclear Regulatory Commission, and mailing address.)

Division of Risk Analysis
Office of Nuclear Regulatory Research
U.S. Nuclear Regulatory Commission
Washington, DC 20555

10. SUPPLEMENTARY NOTES

11. ABSTRACT (200 words or less)

Design strategies were evaluated that couple erosion and hydrology for barriers over low level radioactive waste (LLW) disposal facilities by conducting long-term (1000 yr) parametric simulations with a landform evolution and hydrologic models. Topography of the Grand Junction Uranium Mill Tailings Disposal Site in Grand Junction, CO was used to define a realistic geometry. The most significant differences in maximum erosion depths were attributed to climate and vegetation. Approximately 4 m greater maximum erosion depth was estimated in semi-arid climates compared to humid climate for simulations with a rip-rap or gravel admixture surface. Vegetation decreased erosion in the semi-arid climate by 1.5 m, and by 4 m in the humid climate. Vegetation also increased the amount of evapotranspiration that occurred, decreasing percolation into the waste. Short slopes, slopes with a low grade, and slopes with small grade differences at the nickpoint decreased erosion. The humid climate had the least erosion when terraced slopes were utilized. Due to higher erosion rates in the semi-arid climate, natural and concave slopes that promote deposition produced the least erosion. Overall, a rip-rap surface layer prevented erosion most effectively for any type of topography, climate, or cover type. However, covers with a riprap surface had higher percolation rates. In contrast, a gravel admixture surface had slightly greater erosion, but was more effective in limited percolation.

12. KEY WORDS/DESCRIPTORS (List words or phrases that will assist researchers in locating the report.)

Empirical Soil Erosion Models
Landform Evolution Models
Engineered barriers for waste containment
long-term performance assessments
Influence of climate and vegetation to erosion
Influence of rip-rap to prevent erosion of soil covers
Waste containment

13. AVAILABILITY STATEMENT

unlimited

14. SECURITY CLASSIFICATION

(This Page)

unclassified

(This Report)

unclassified

15. NUMBER OF PAGES

16. PRICE



Federal Recycling Program



**UNITED STATES
NUCLEAR REGULATORY COMMISSION**
WASHINGTON, DC 20555-0001

OFFICIAL BUSINESS



NUREG/CR-7200

**Influence of Coupling Erosion and Hydrology on the Long-Term
Performance of Engineered Surface Barriers**

May 2016